



Stars

High-Resolution X-ray Spectroscopy

David Huenemoerder (MIT)



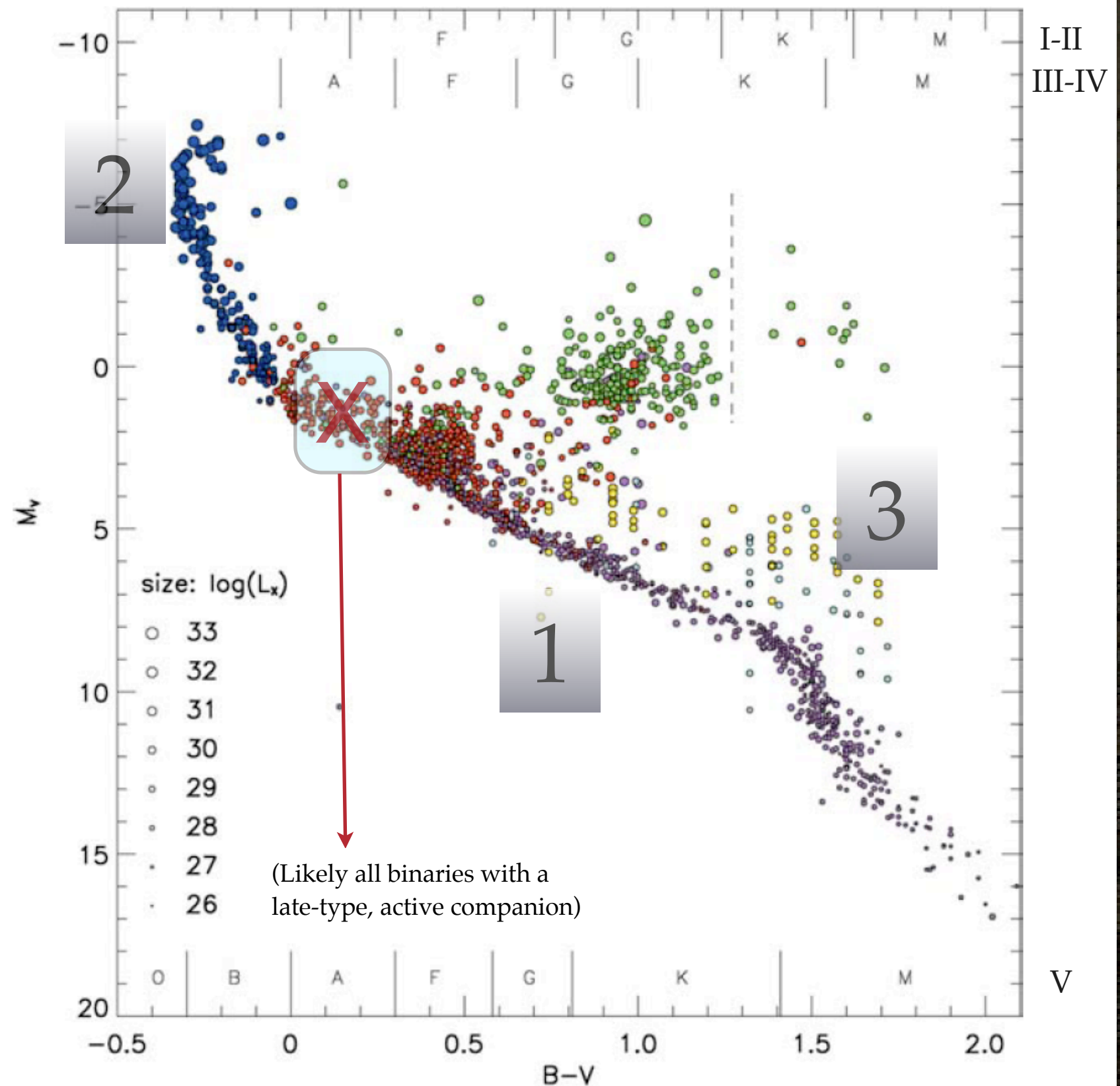
X-Rays from Normal Stars

Stars of nearly all spectral types are known to emit X-rays. Here we will look at a few classes which illustrate some of the basic physical processes and their signatures in high-resolution X-ray spectra:

- 1) Coronal emission from G-K-M giants and dwarfs
- 2) OB-star star winds
- 3) Pre-main sequence stars

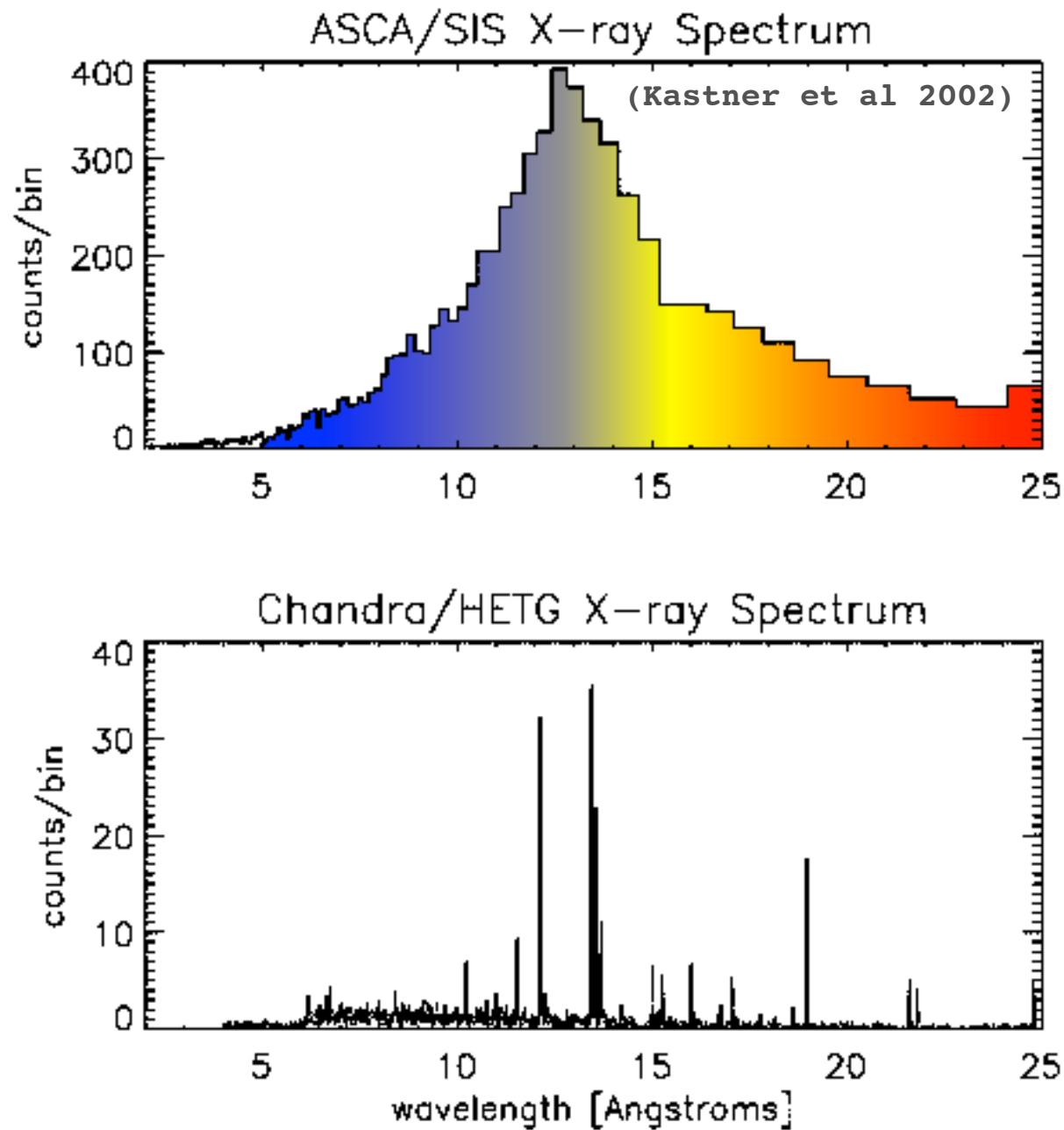
(we are ignoring degenerate objects: white dwarfs, neutron stars, and black holes, as well as exploding stars).

(Gudel 2004)



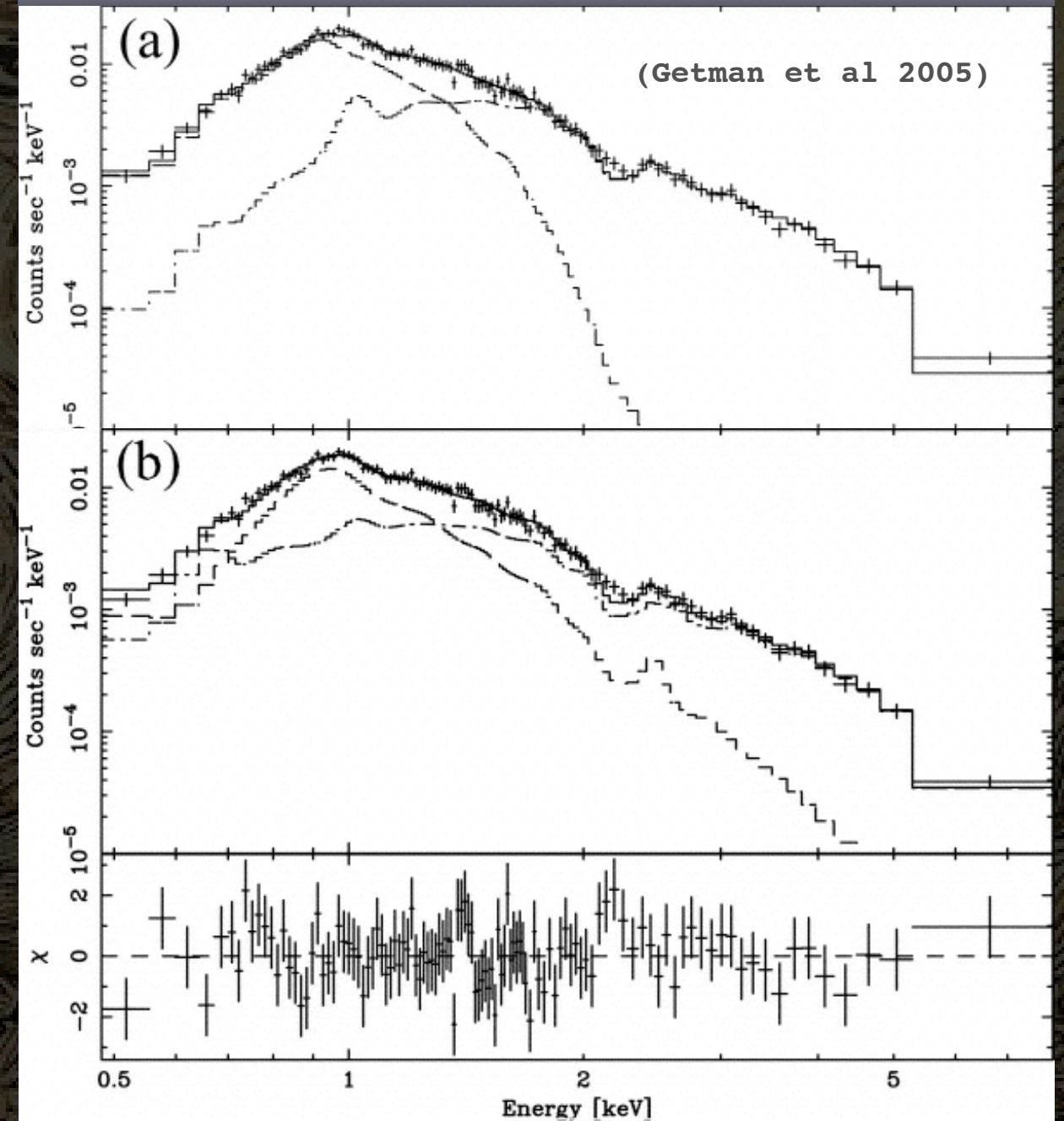
Why High-Resolution?

To obtain spectral line diagnostics



High resolution revealed strong neon, weak iron.

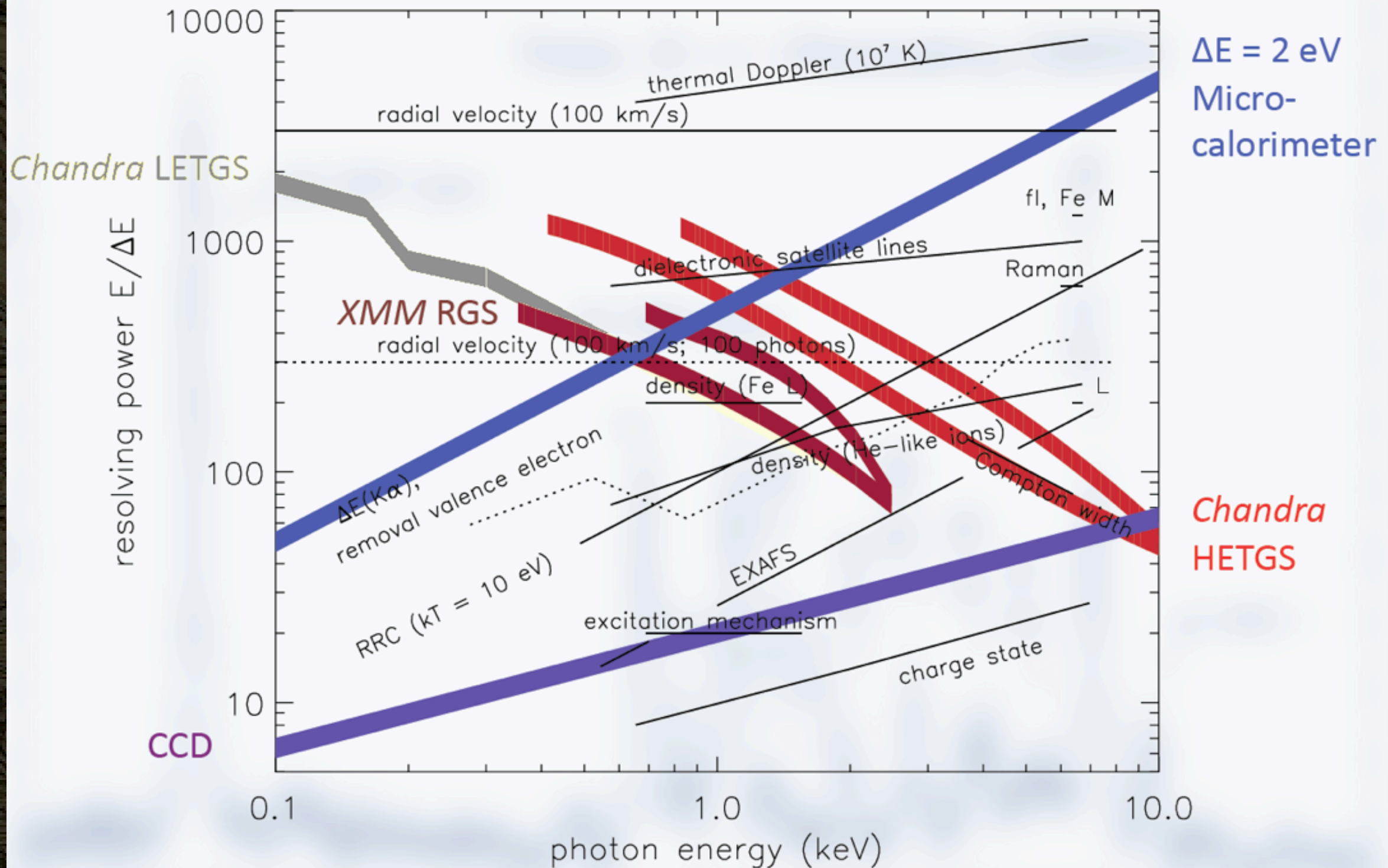
To obtain unique diagnostics



3 components, 5 parameters (NH, kT[2], norm[2]), two acceptable (but very different) models.

How High is High?

Resolving Power (from Paerels, 2009, MSSL Workshop #3)



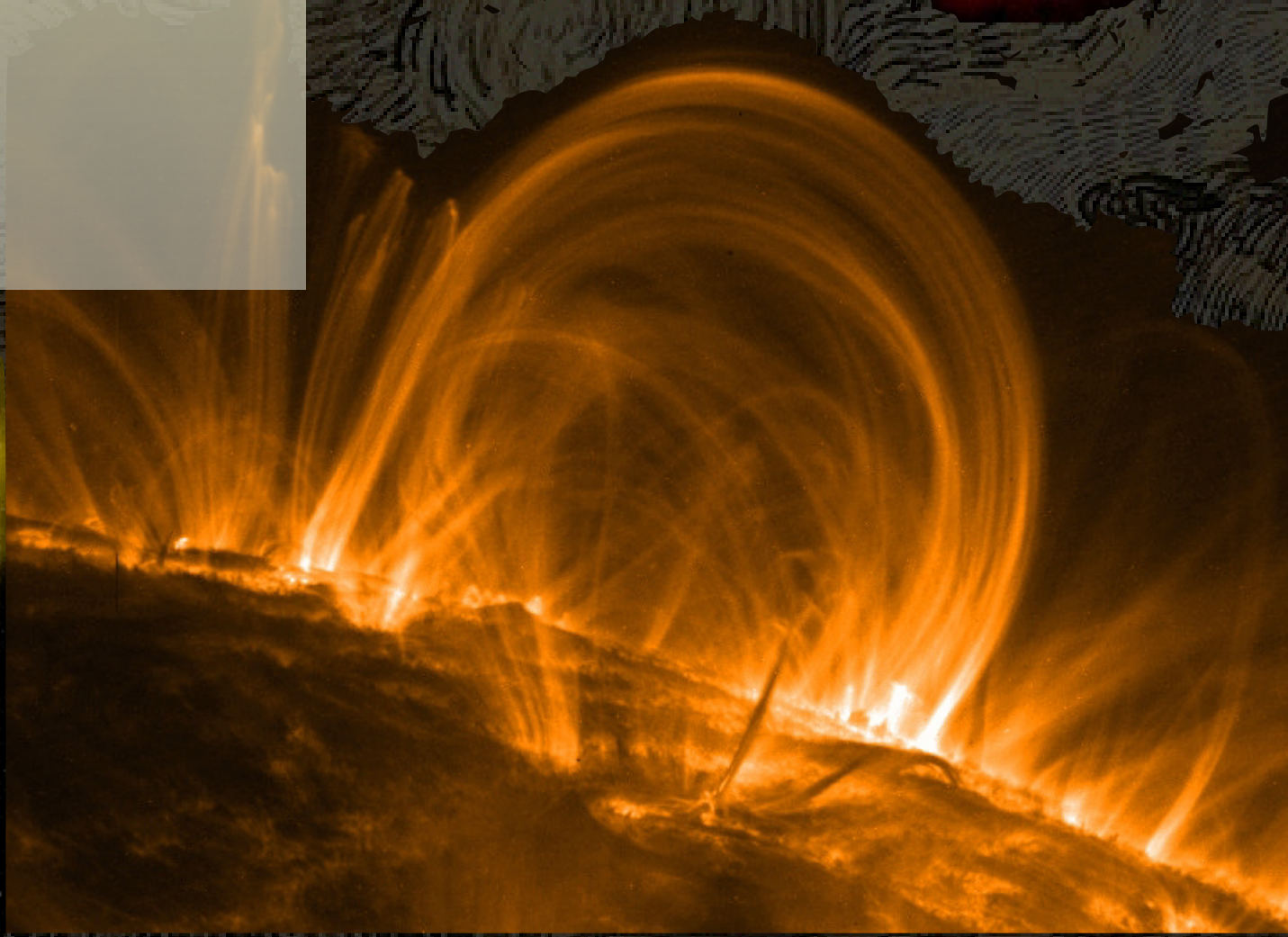
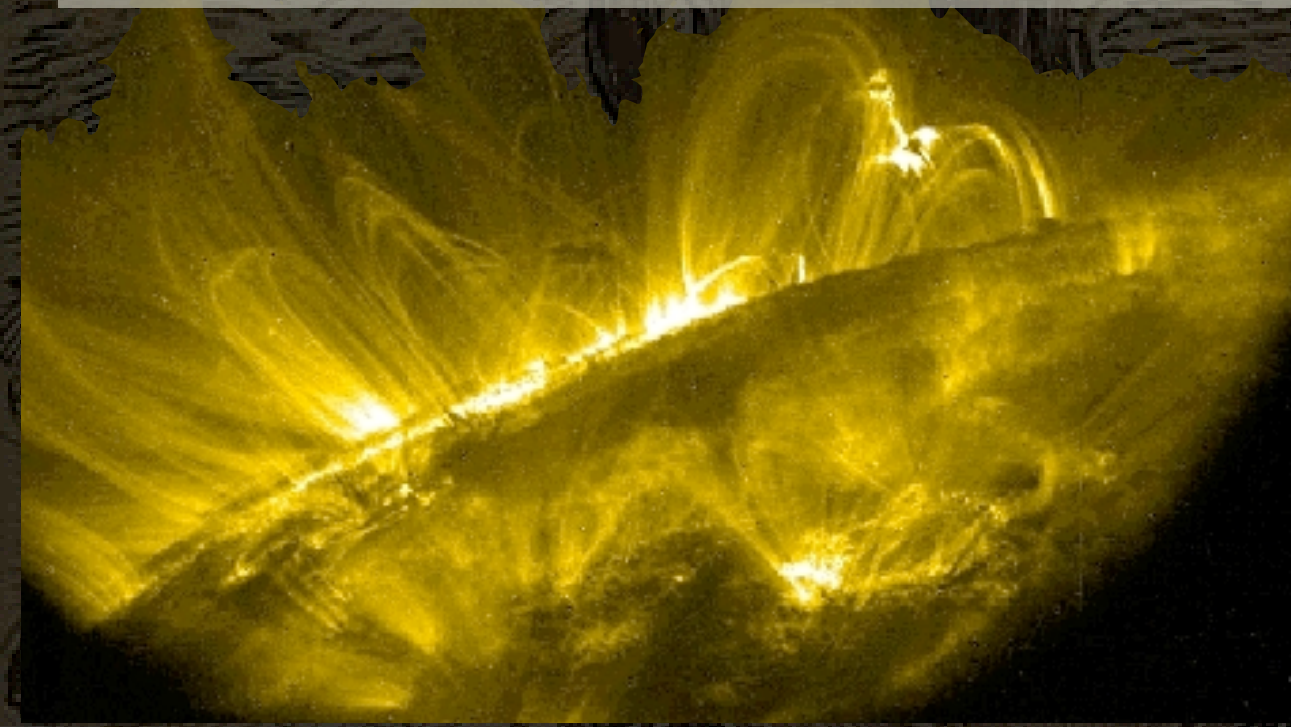
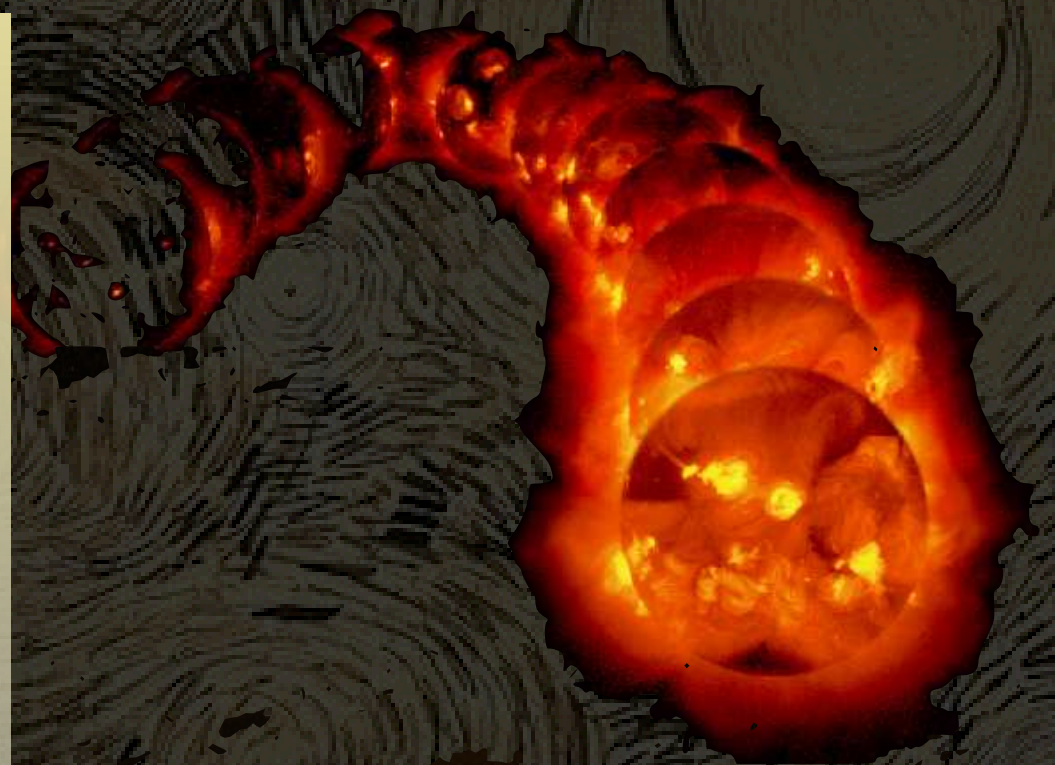
Solar Coronal Emission

Coronal Equilibrium: all ions are in the ground state; collisionally ionized, radiatively recombine.

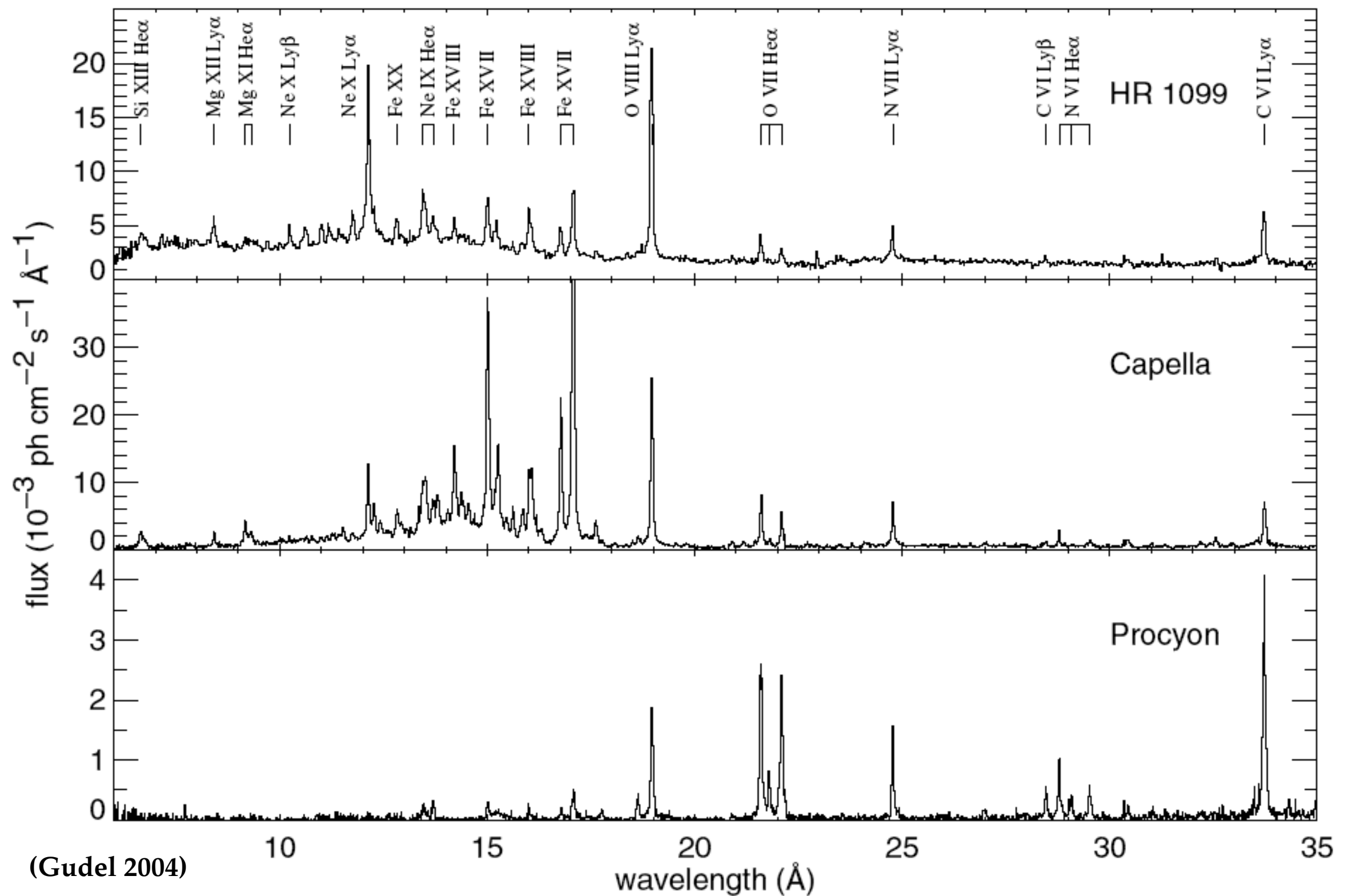
Optically thin plasma (relatively straightforward to model).

Solar coronal emission is controlled by magnetic fields. Very non-uniform and dynamic (flares, activity cycles).

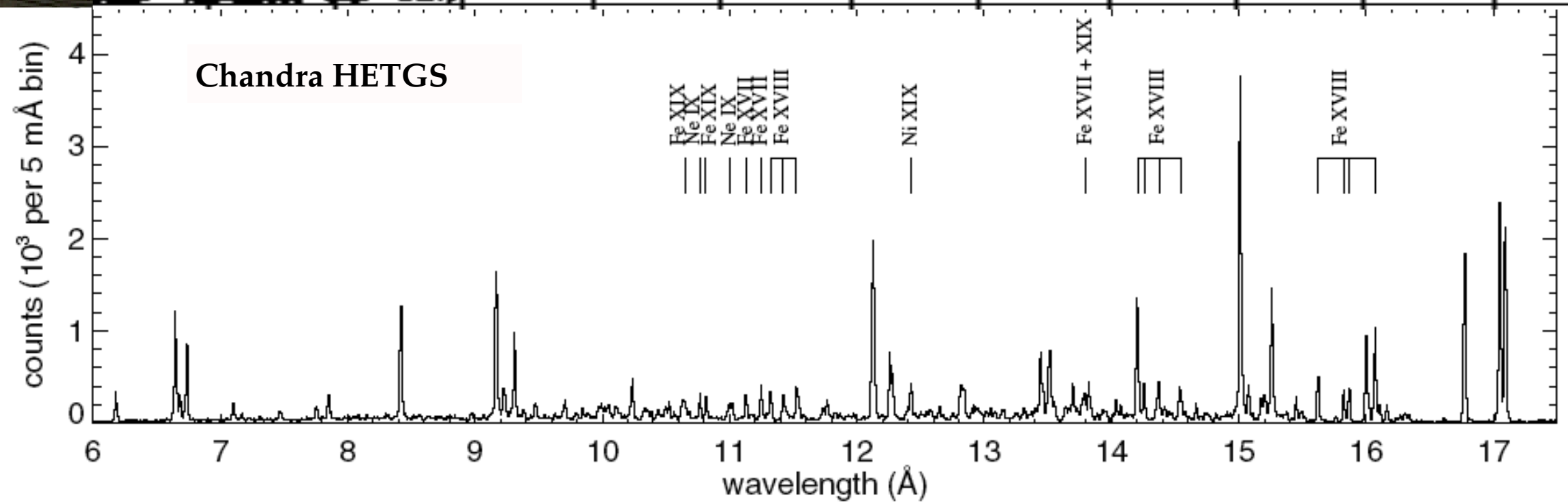
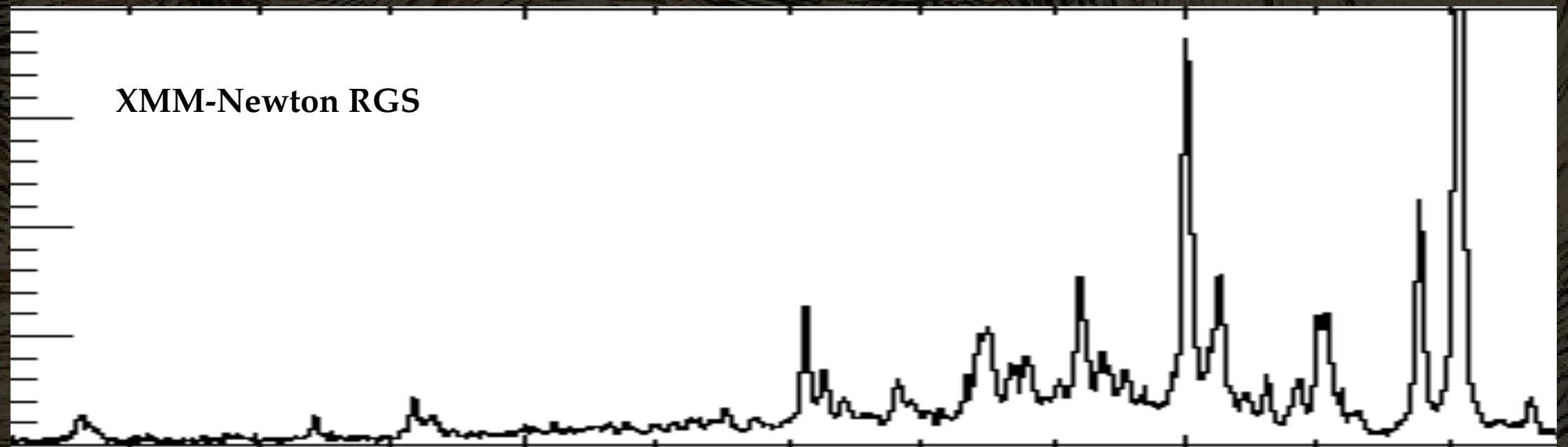
$L_x/L_{\text{bol}} \sim 10^{-6}$ (other stars: up to 10^{-3})



Representative Spectra



Representative Spectra: Capella



How do we know line IDs and strengths?

Lots and lots of atomic data, plus a physical plasma model. E.g., ATOMDB (APED, APEC), FAC, MEKAL, Chianti, ... (Note: high-resolution means: need relativistic calculations!)

Plasma models: Temperature, density, ion balance, level populations, abundances, velocities.

(Gu et al 2006)

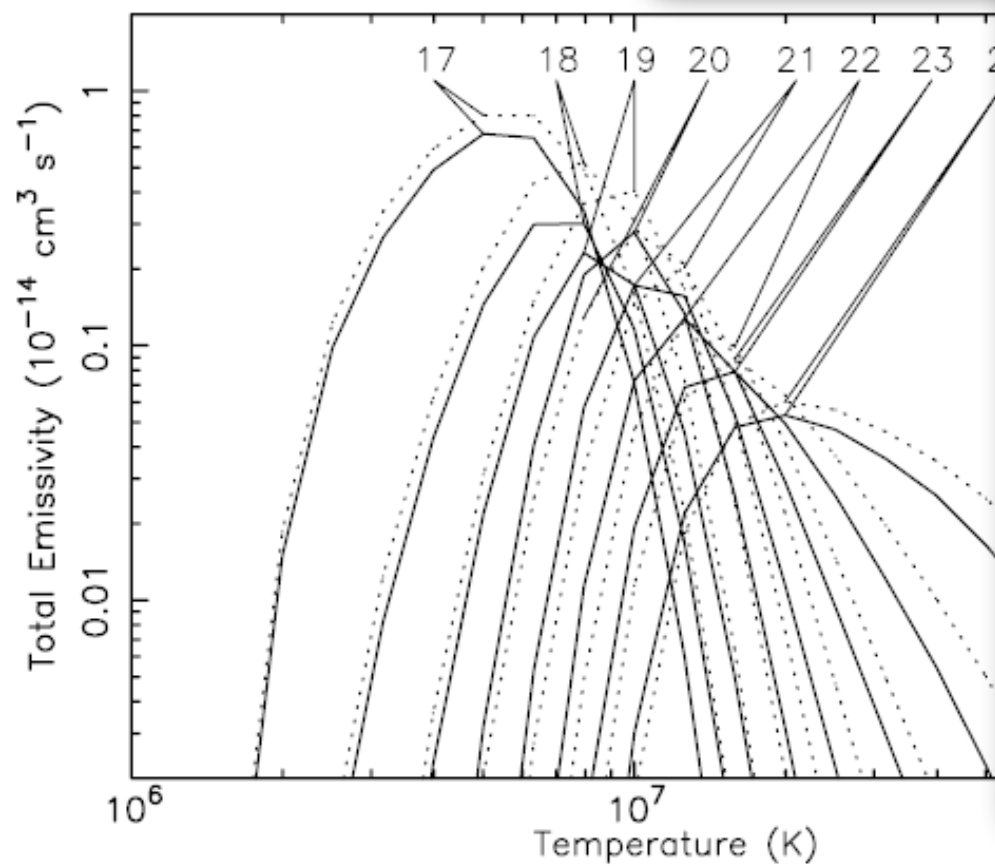
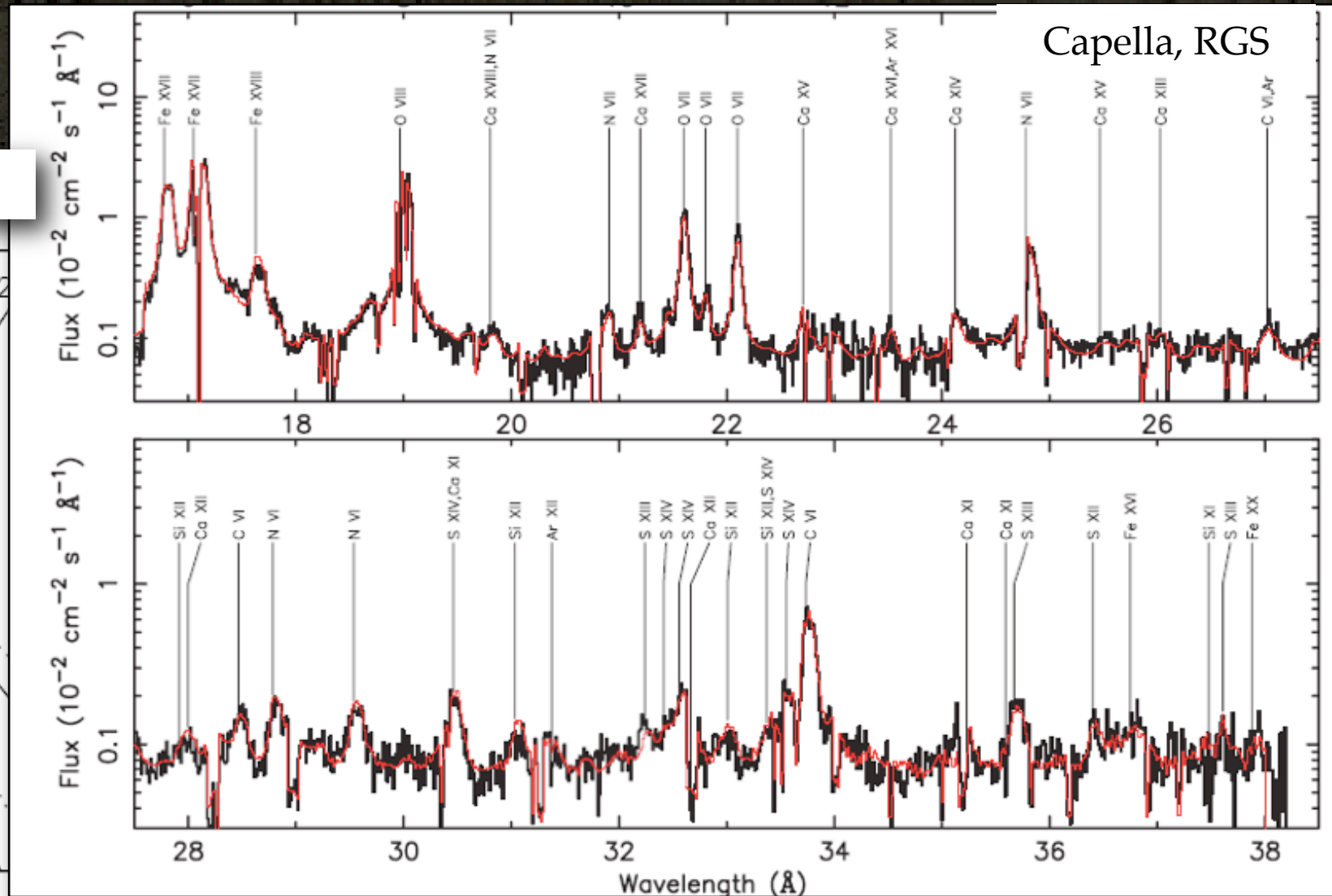


FIG. 1.—Total emissivities of Fe L-shell ions in the 5–20 Å region. The solid lines are from the original APED/APEC database; the dotted lines are from our new line list. The numbers label Fe charge states, 17 for Fe xvii, 18 for Fe xviii, and so on.

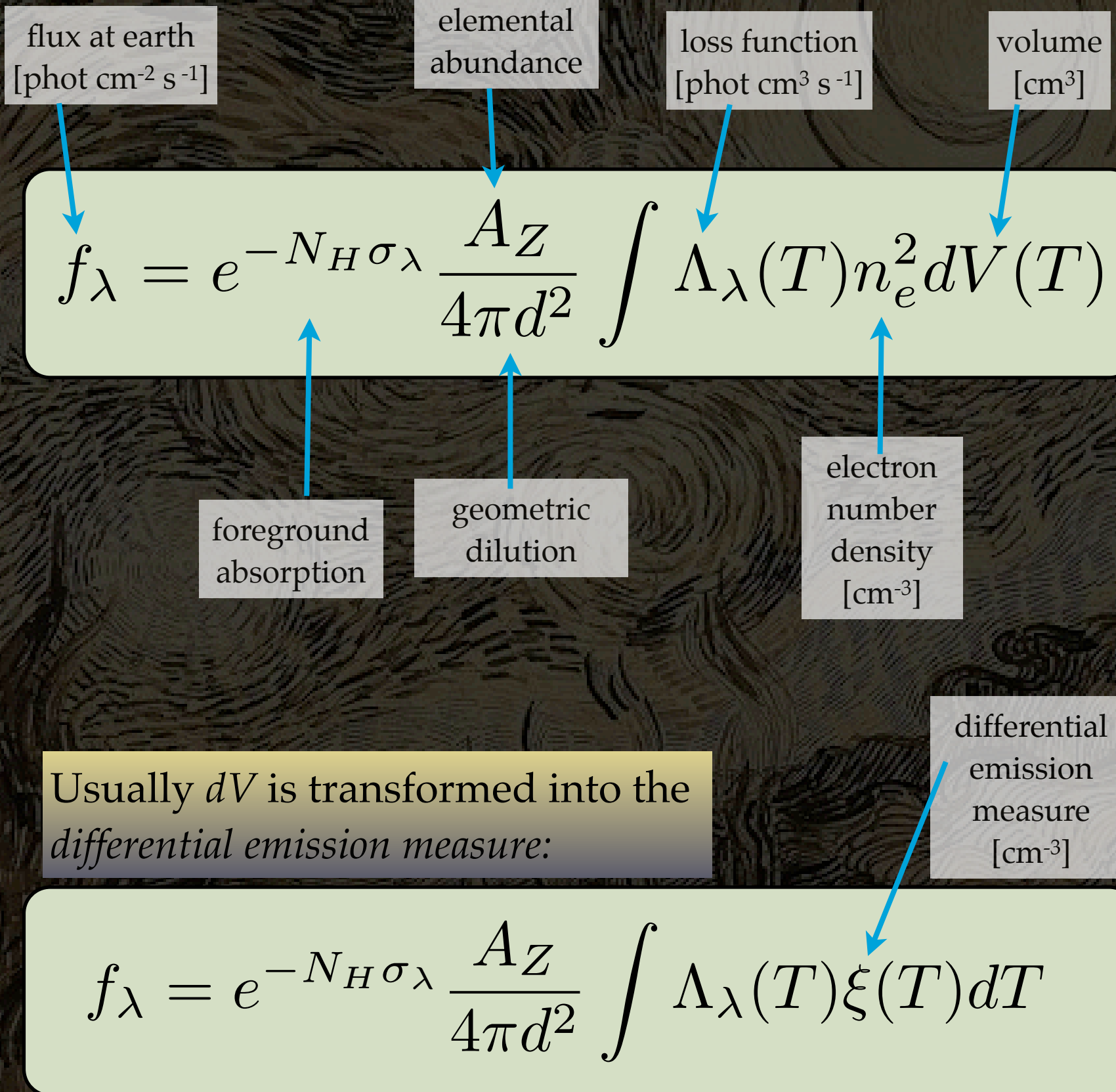


Coronal Equilibrium & Emission Line Flux

The loss function (Λ , also called emissivity, or cooling function; related to j_ν , or η_ν --- notation varies) includes both ionization fraction and level population terms (i.e., atomic data goes here).

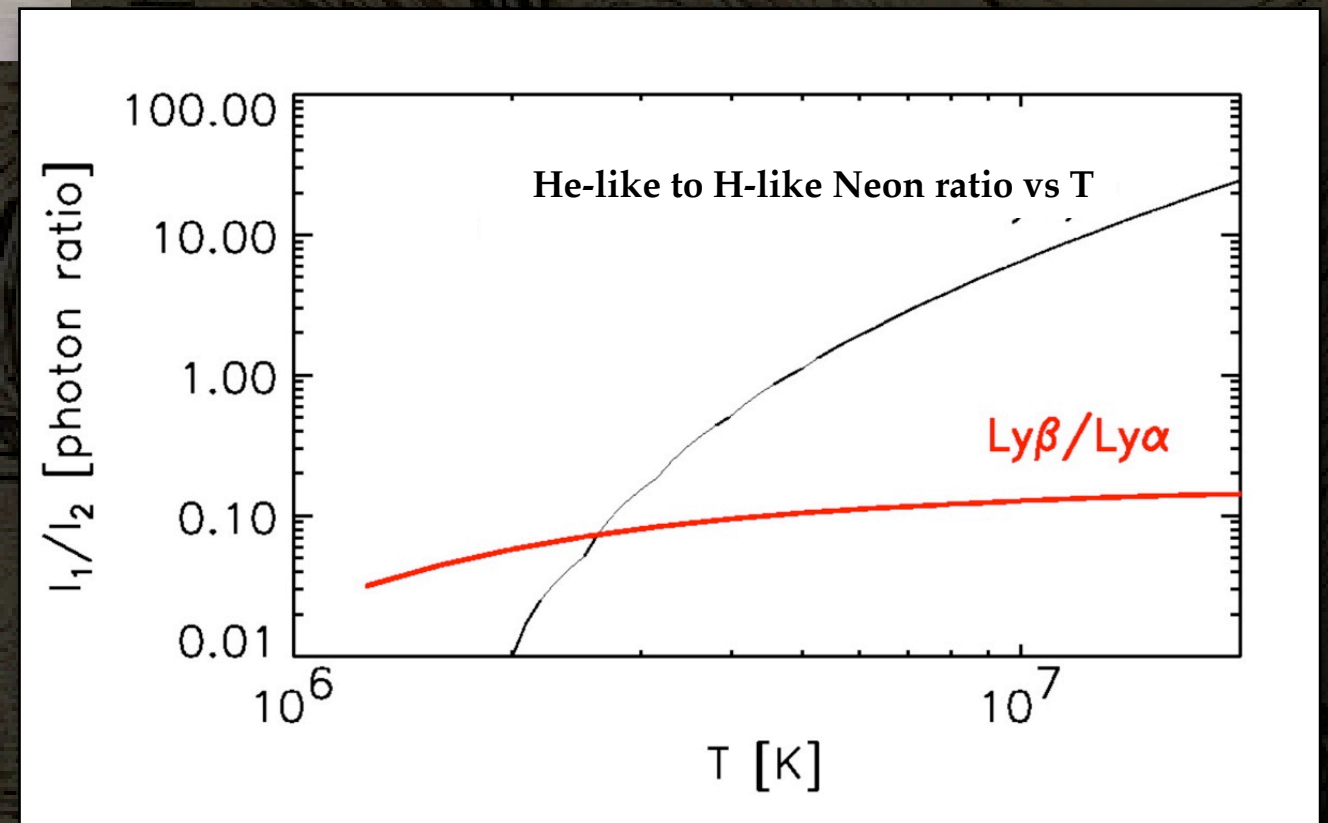
The line flux is strongly dependent on T , as well as *density squared* weighting through the volume emission measure.

Also note that the emission measure and abundance appear in a product.



Line Ratios for Temperature

Usually an isothermal approximation is used, using ratios of two ions of the same element (so abundance cancels):

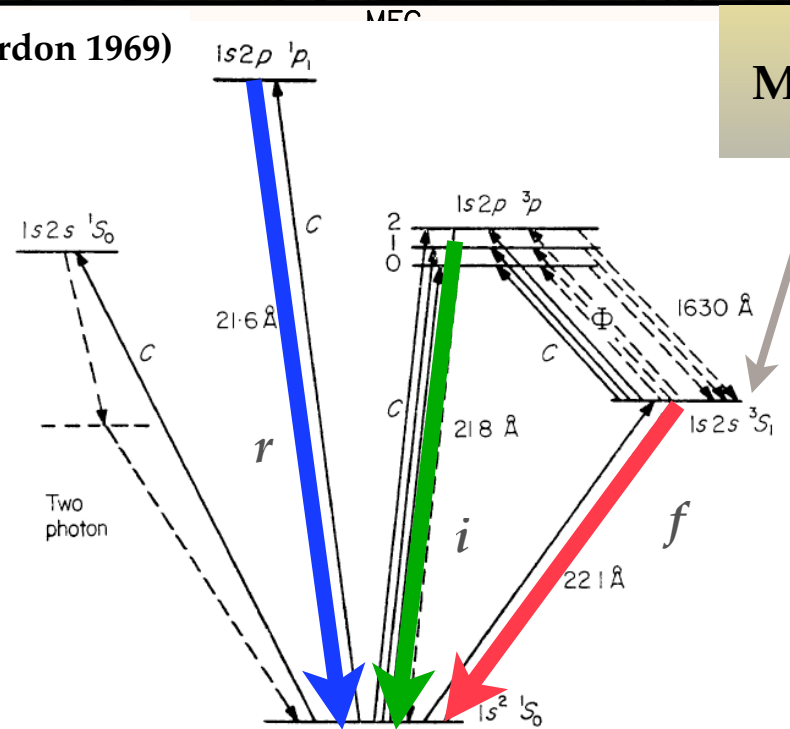


But remember it is really the ratio of two integrals:

$$\frac{f_1}{f_2} = \frac{\int \Lambda_1(T)\xi(T)dT}{\int \Lambda_2(T)\xi(T)dT}$$

He-like Triplets: Line ratios for Density & Temperature

(Gabriel & Jordan 1969)

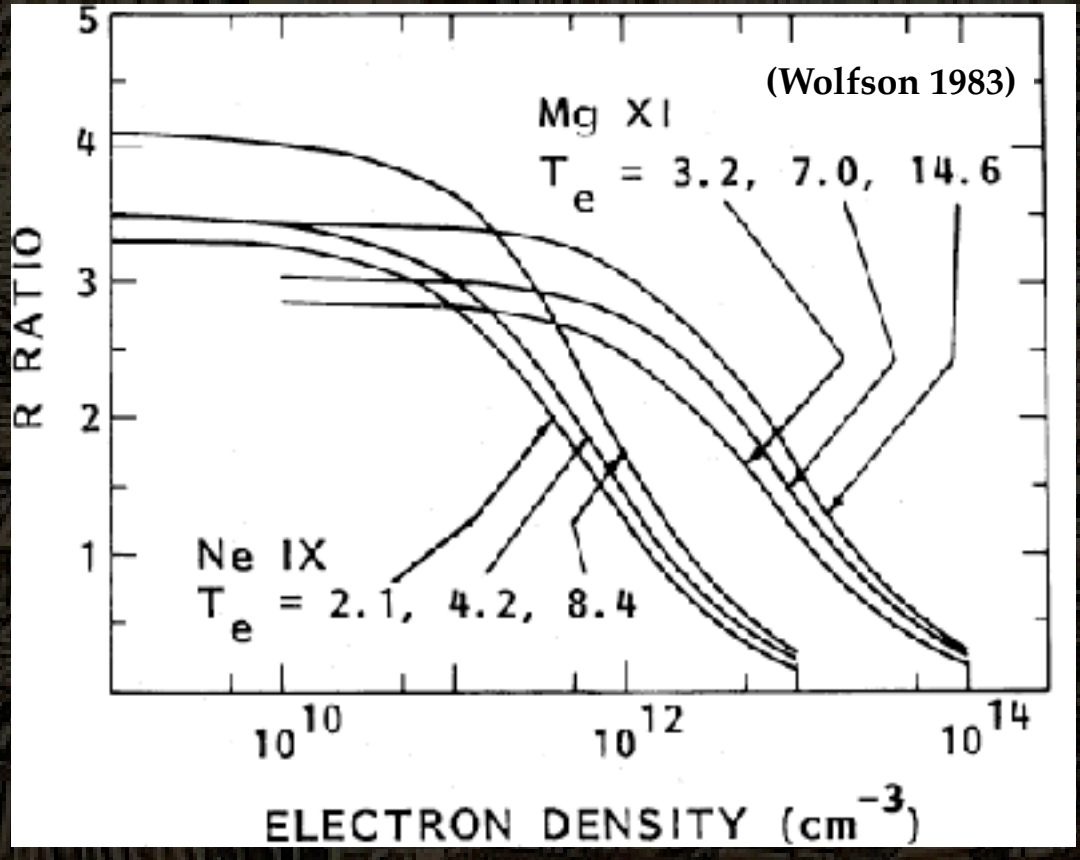
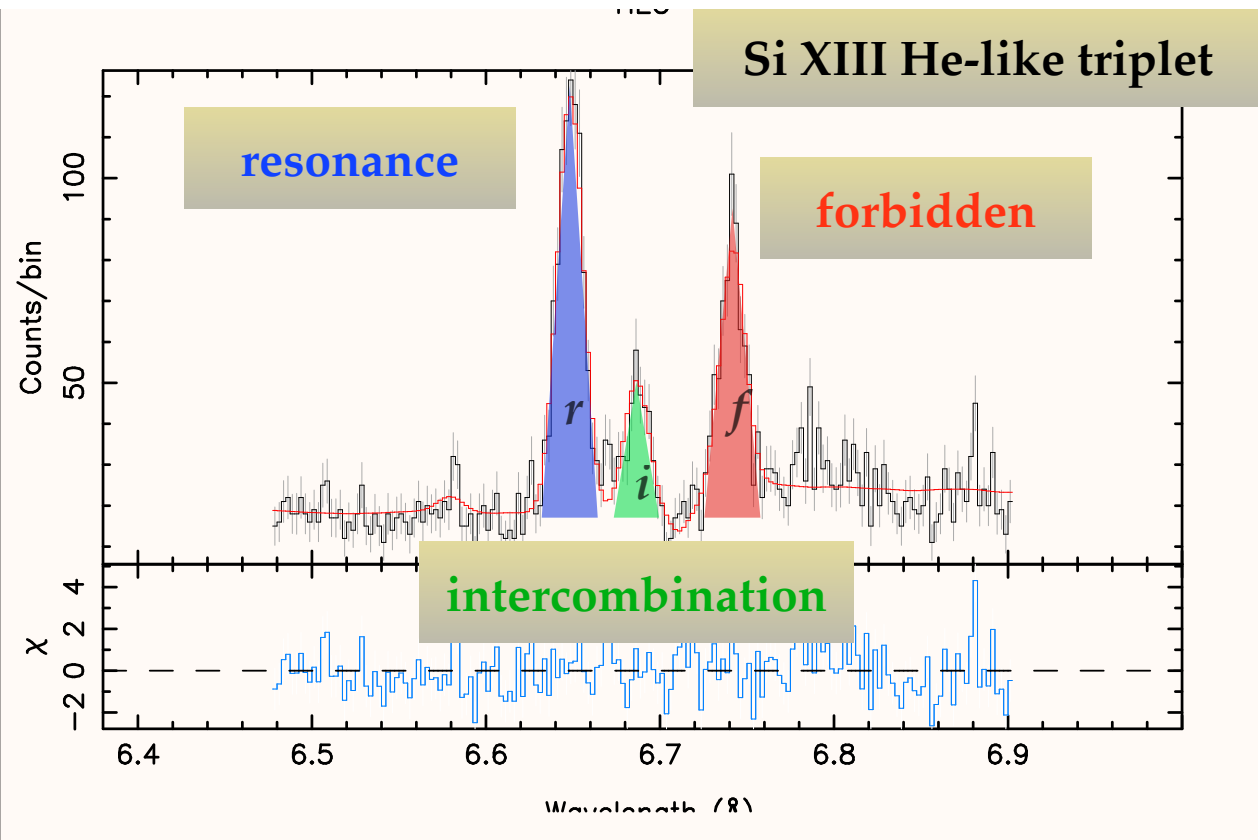


Metastable level, can be de-populated by electron collisions or UV photons.

FIG. 1. The He-like ion, showing those terms and processes involved in the present analysis. The wavelengths indicated apply to the case of oxygen VII.

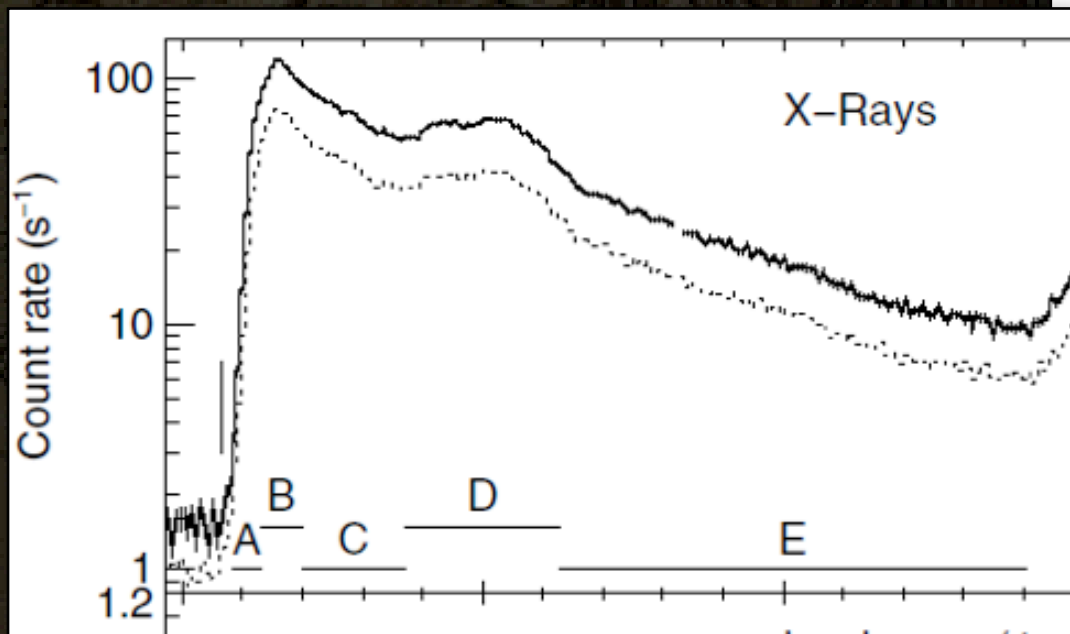
$$(f/i) \equiv R = \frac{R_0}{1 + n/n_c + \phi/\phi_c}$$

$$(f + i)/r \equiv G(T)$$

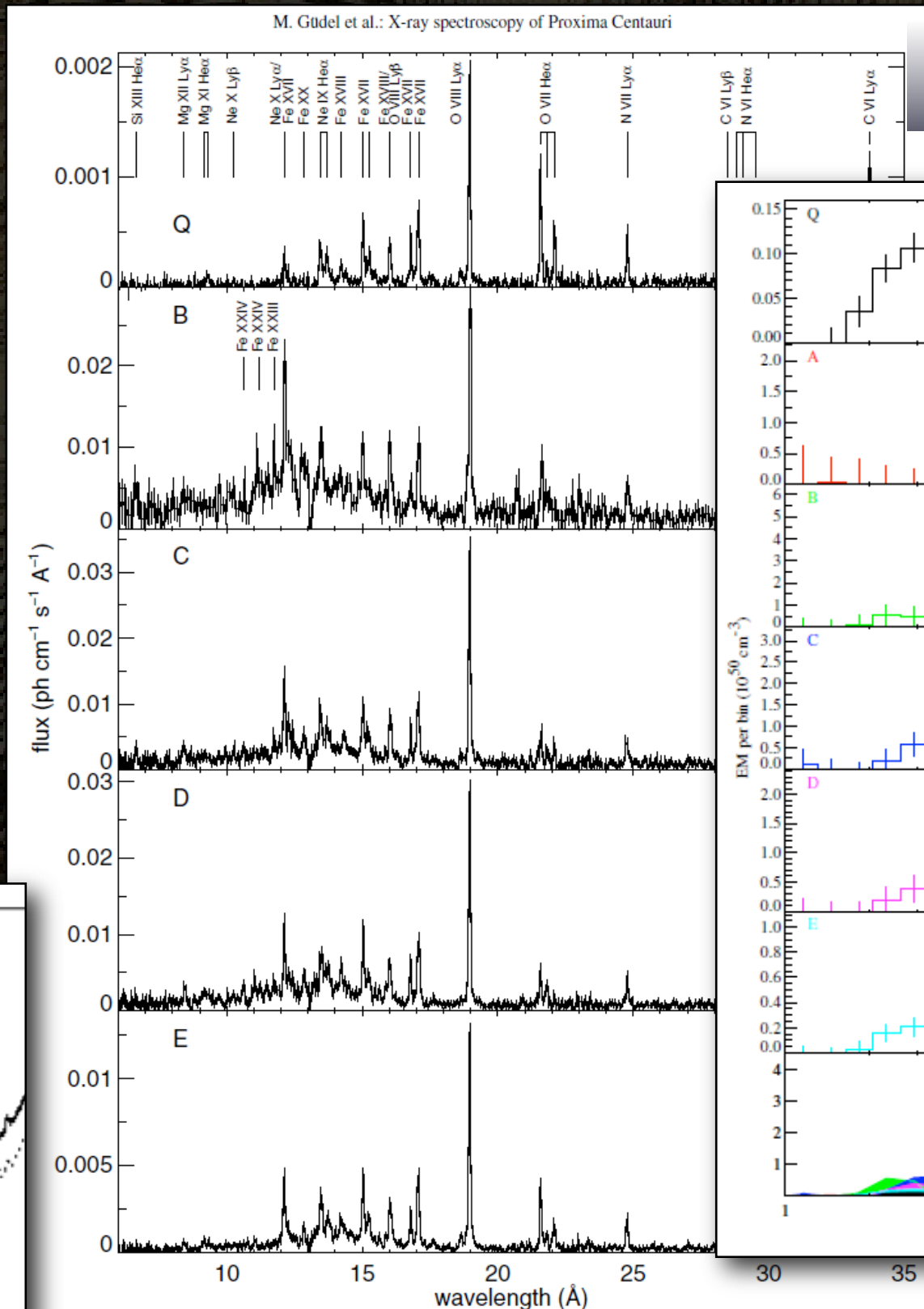


Coronal Questions

What powers a corona? It's related to rotation (dynamo-generated magnetic fields). But an *a priori* theory is lacking. Hence, there are many phenomenological studies to detect, then determine characteristics and trends, using emission-measure reconstruction, mapping via modulation, or flare diagnostics.

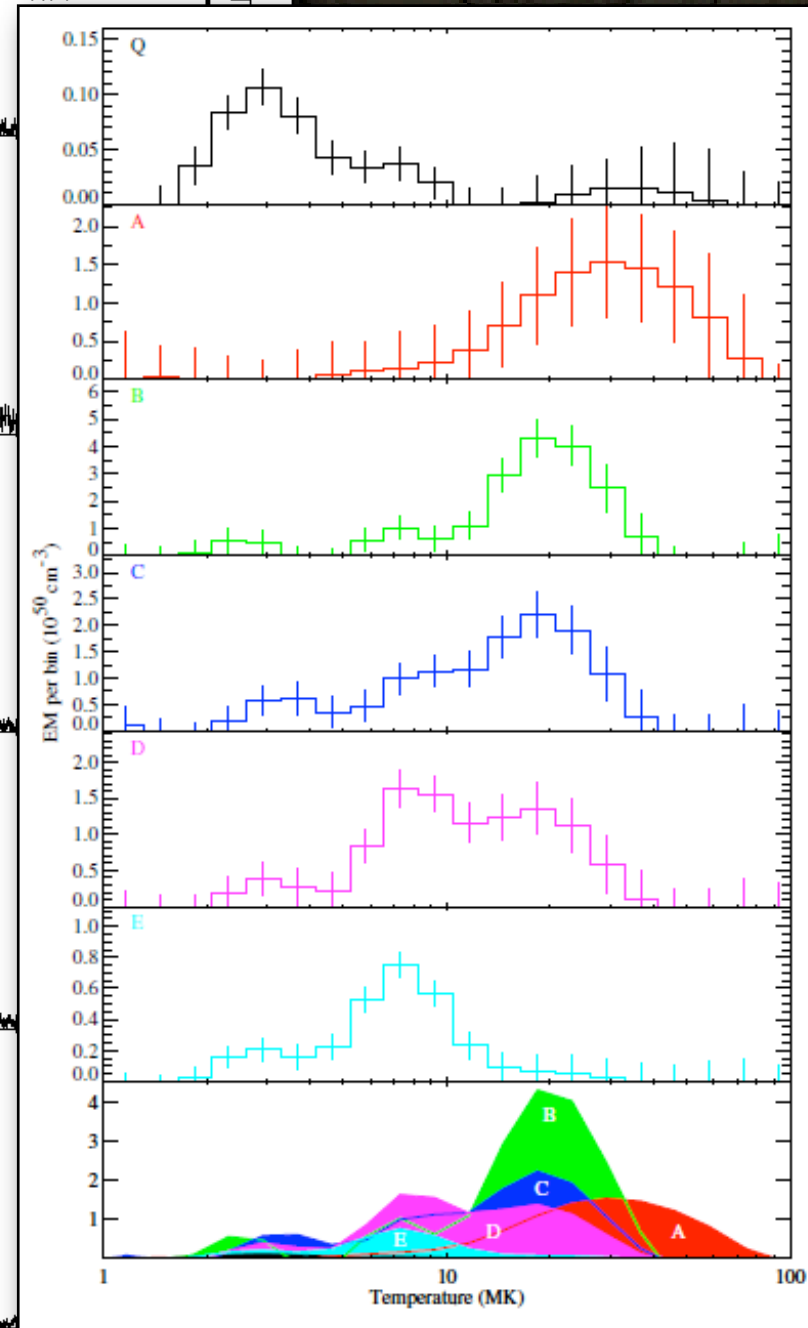


EPIC Light Curve (10 ks)



RGS Spectra in time intervals

Proxima Centauri
(Gudel 2004)

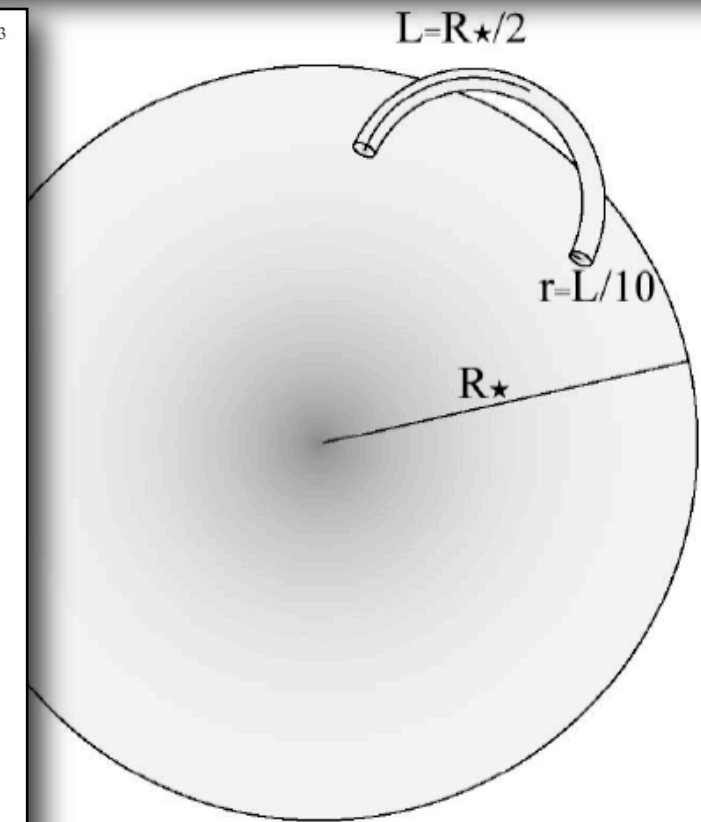
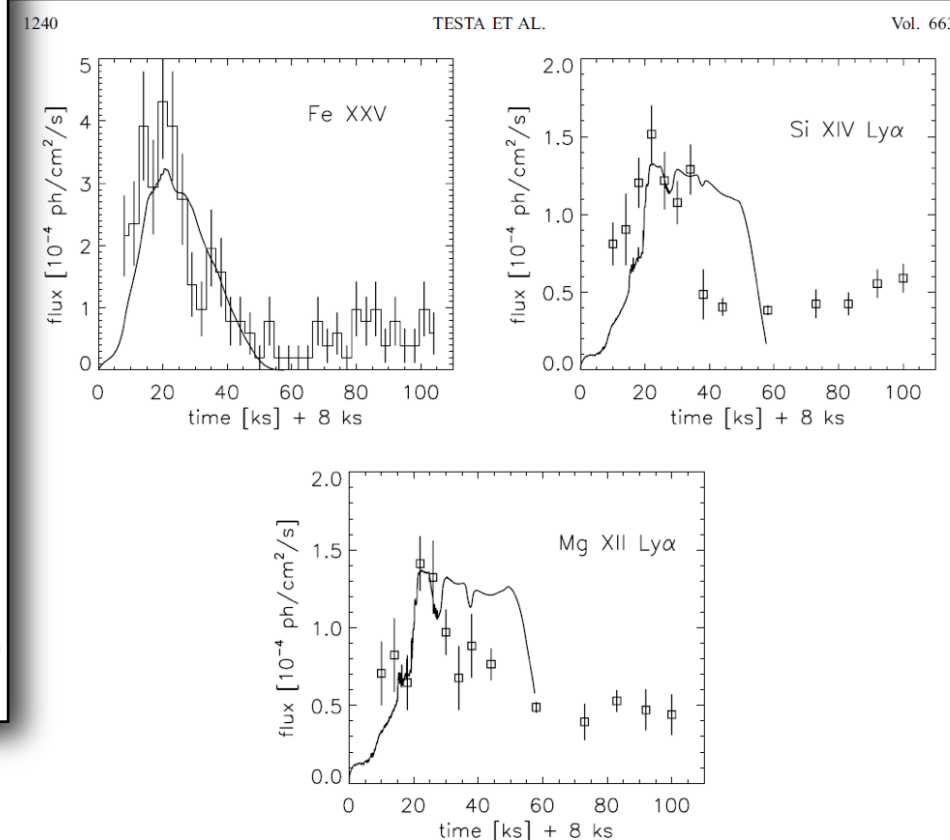
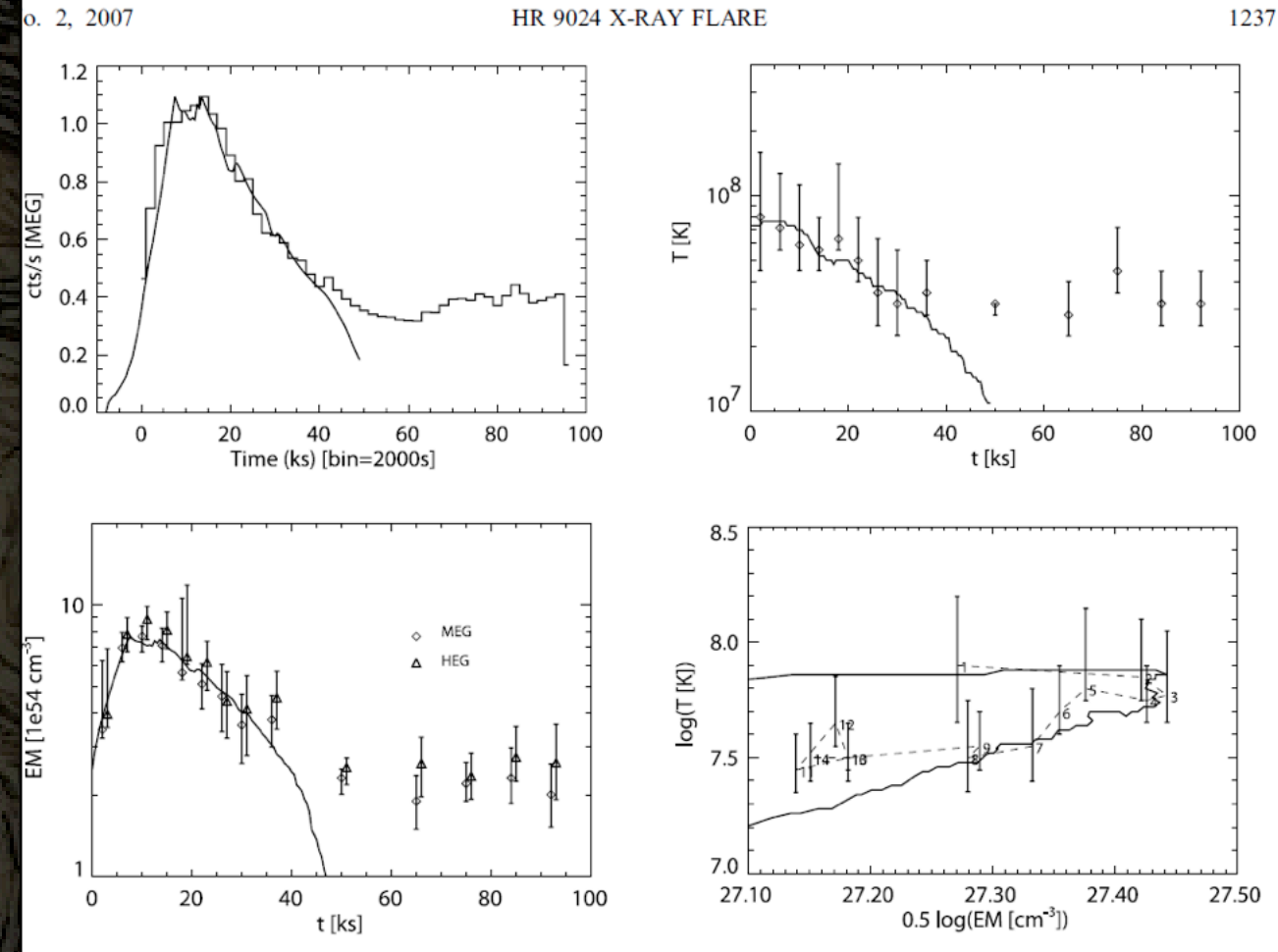
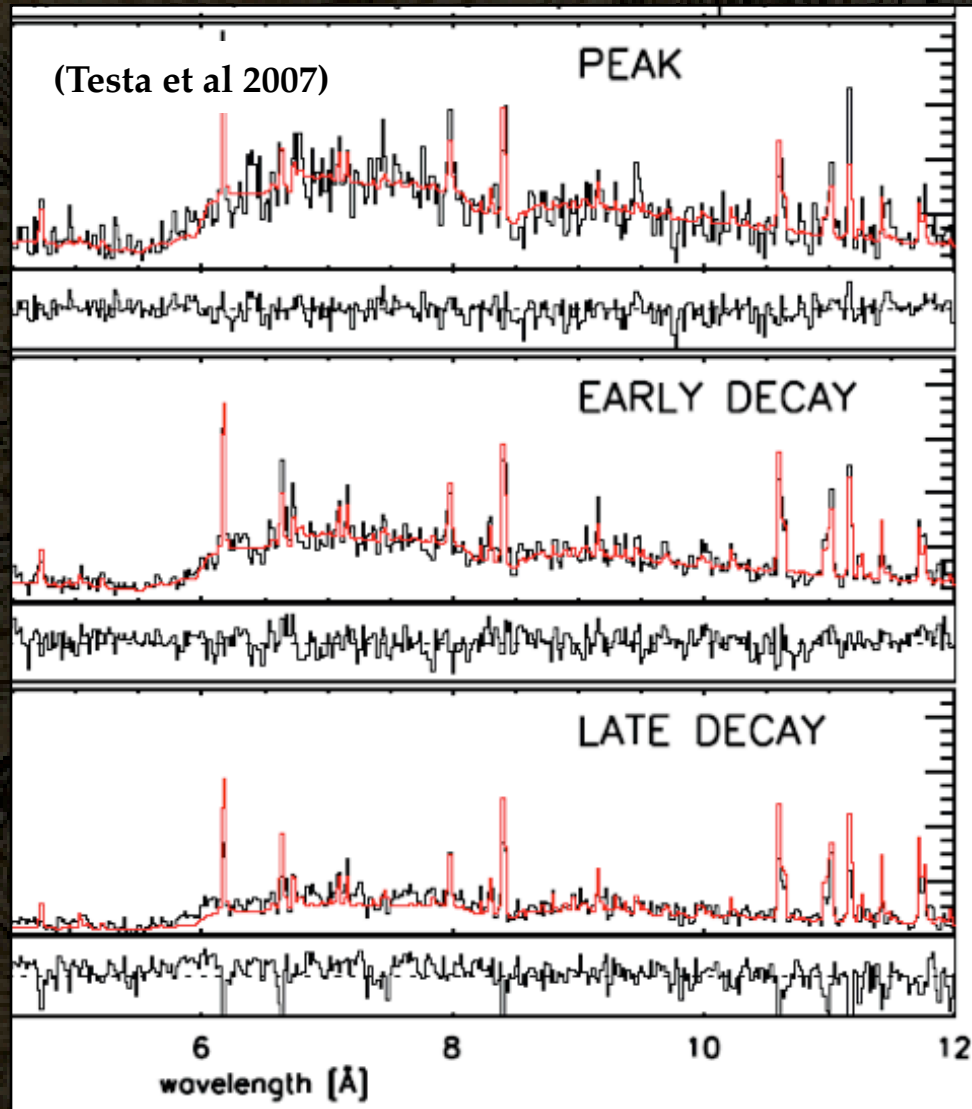


Emission Measures

More Flare Modeling - with hydro ...

Assuming flares occur in loops, and implementing a simple quasi-static hydrodynamical model (Reale 2007), you can derive loop parameters from spectral evolution.

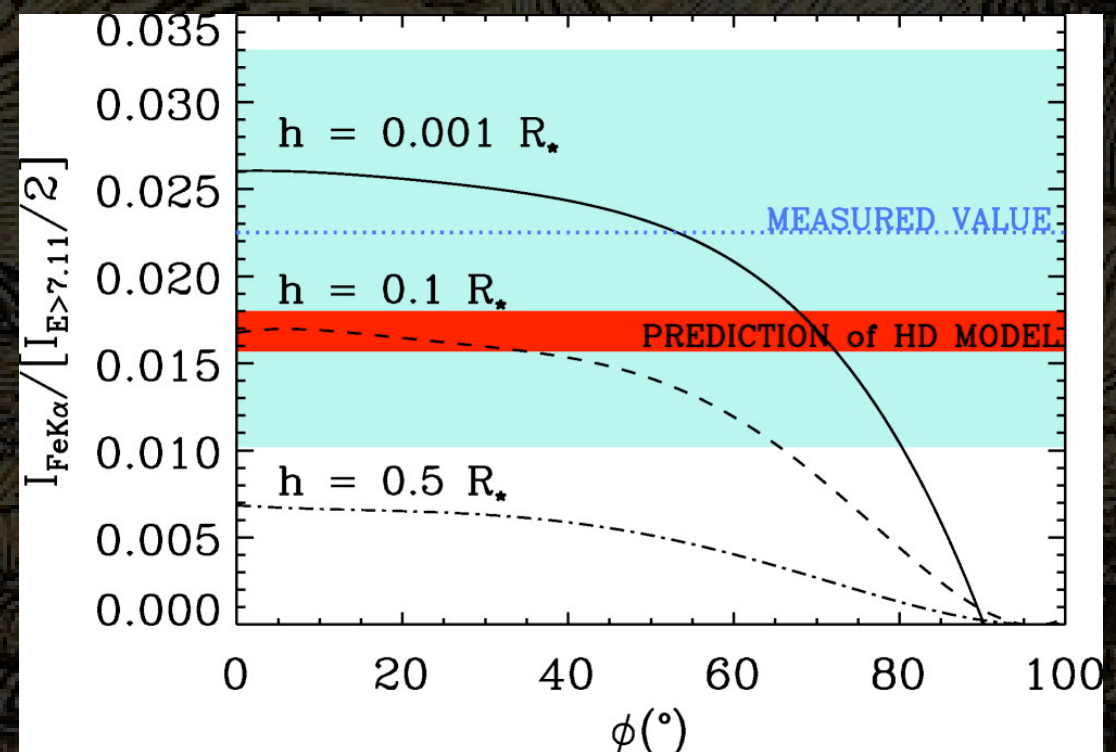
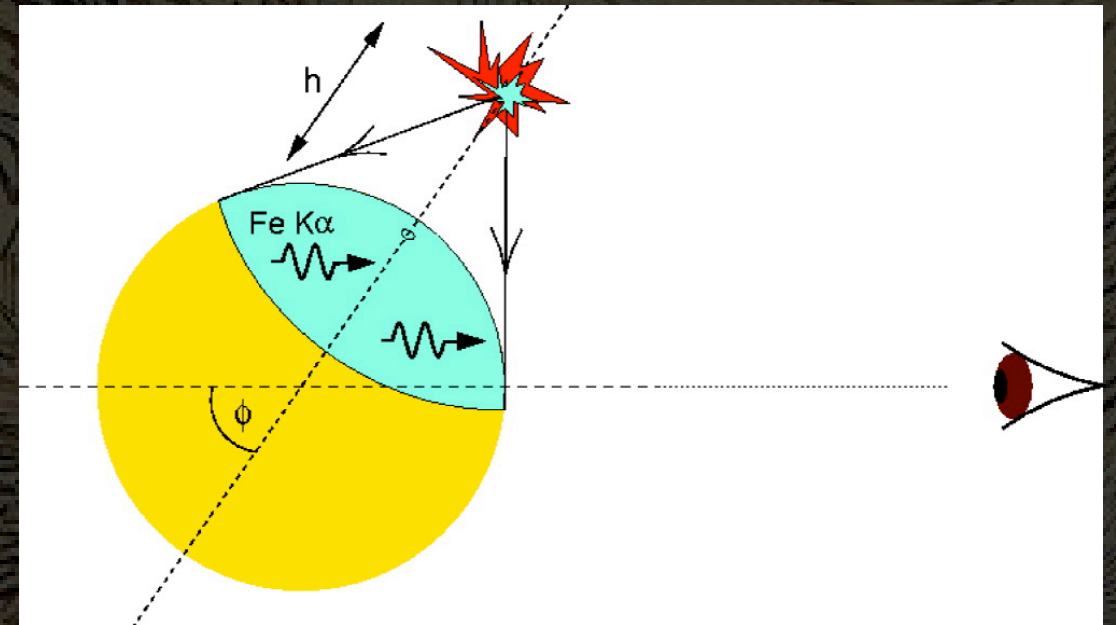
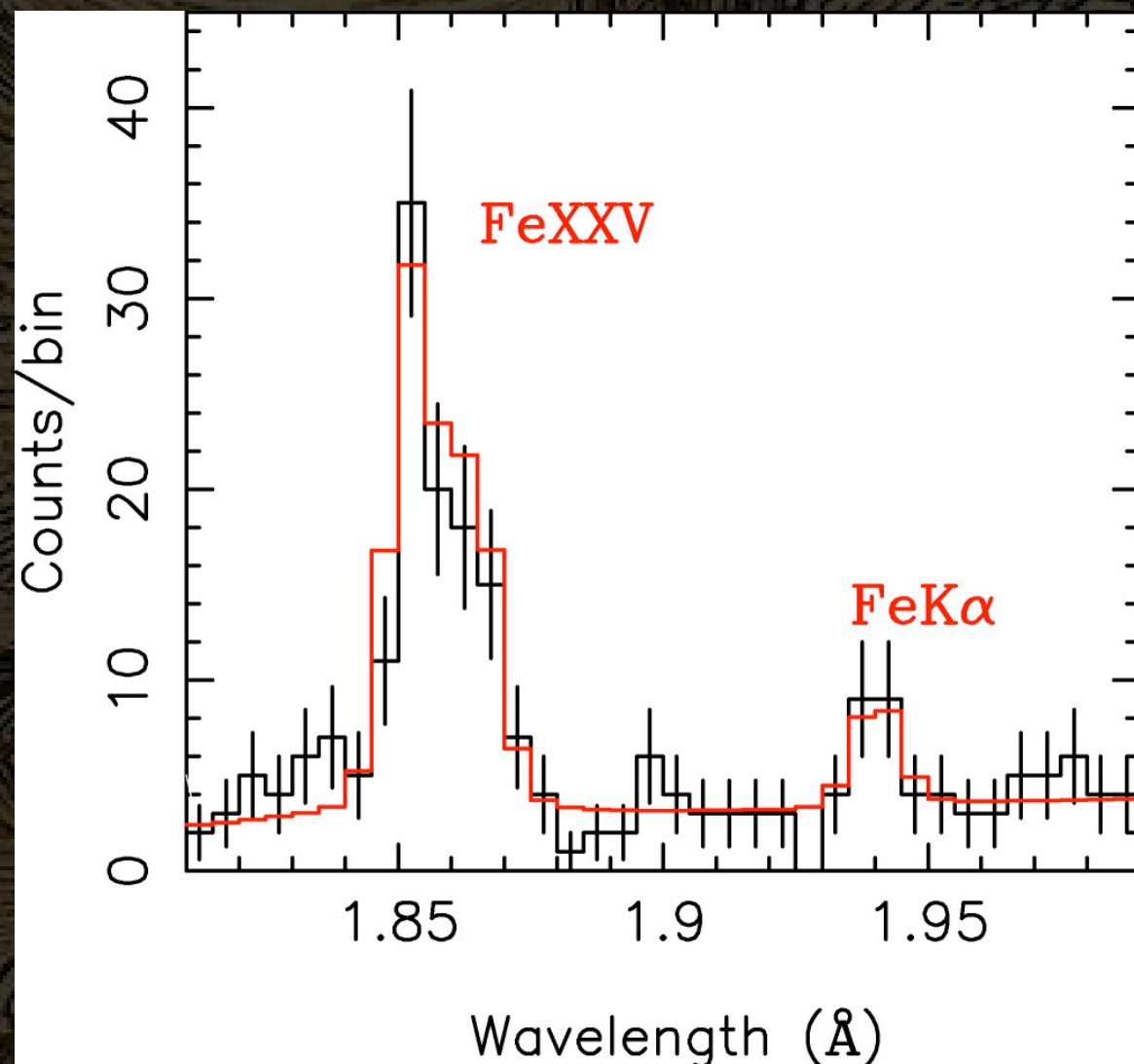
Example: HR 9024 (Testa et al 2007)



Flare Modeling - fluorescence

Hard photons from flares will cause the photosphere to fluoresce. The flux in Fe K α can be used to model the loop height.

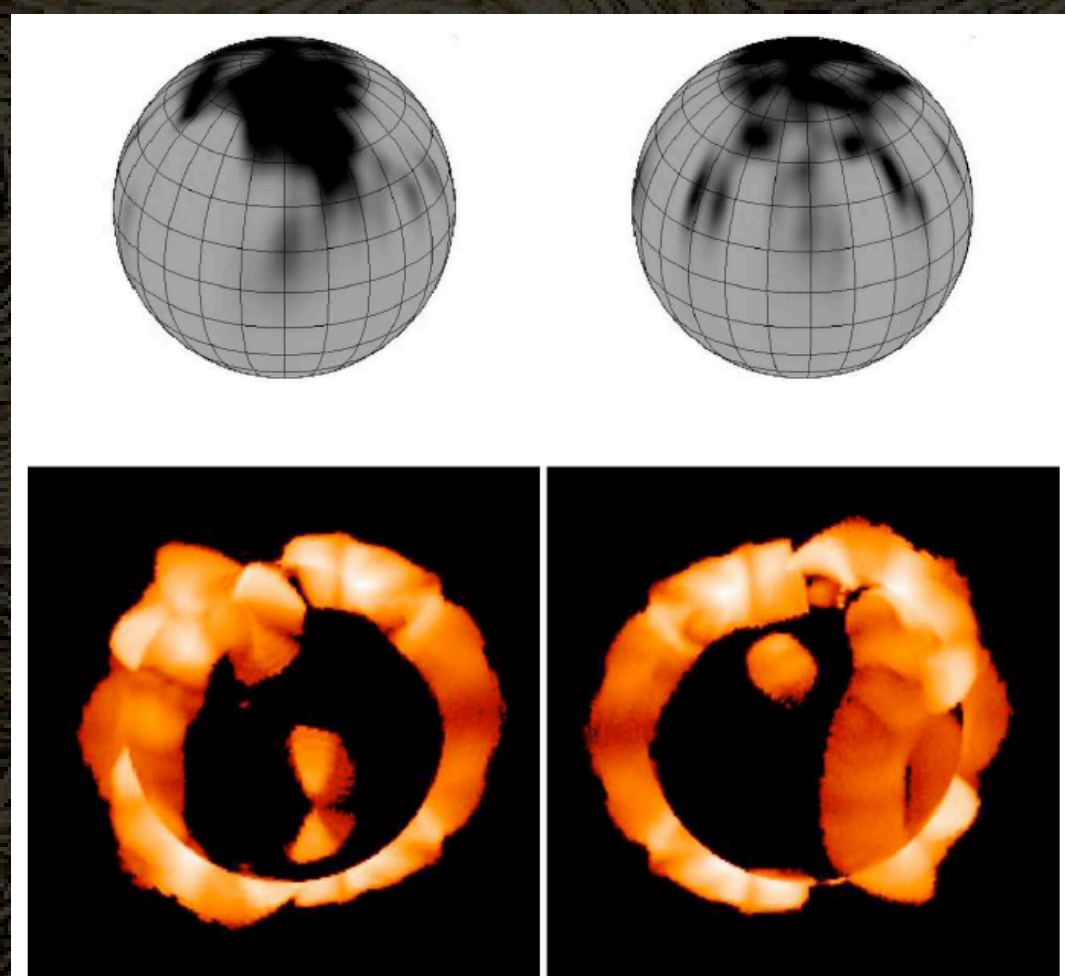
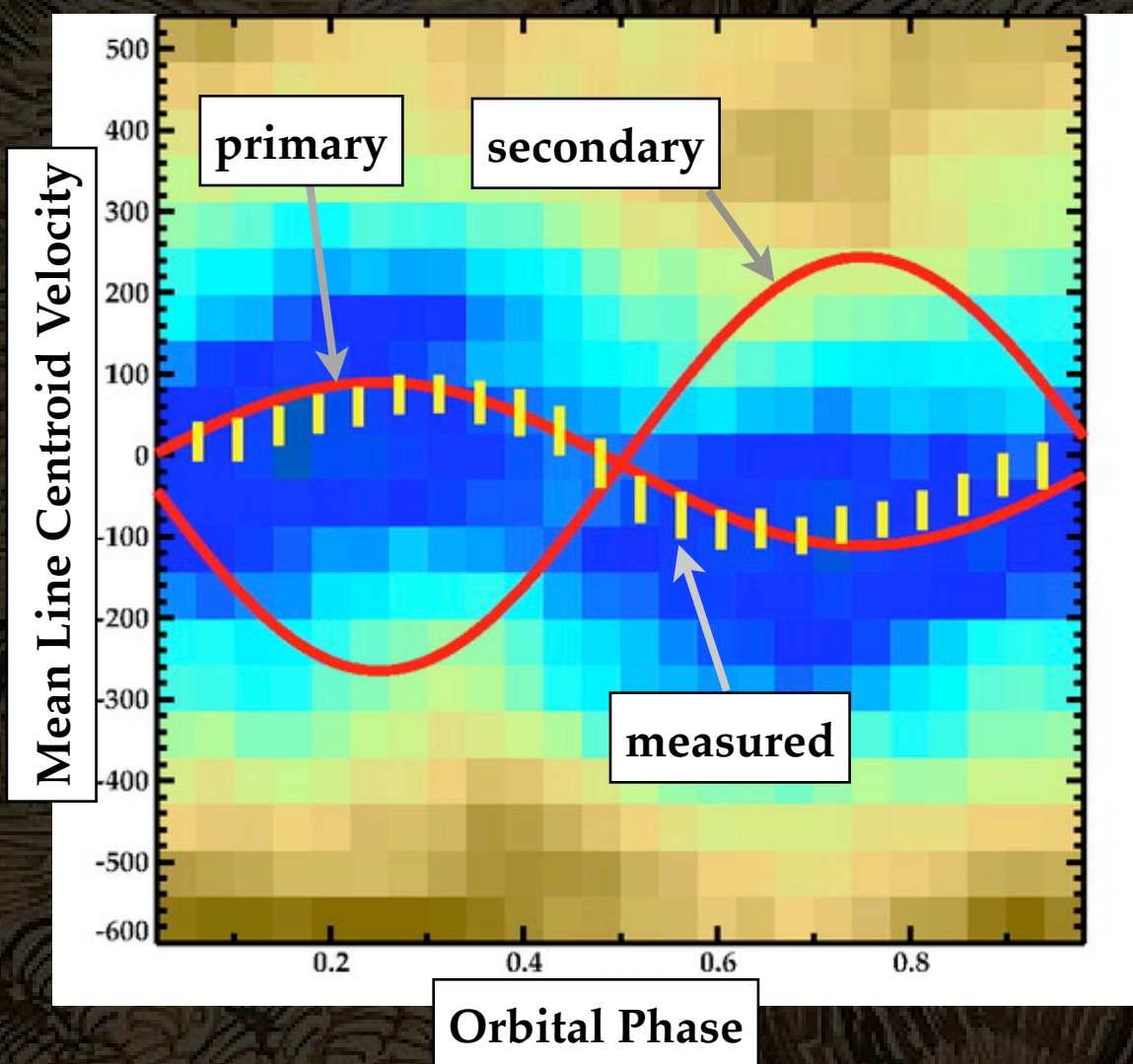
A large flare in HR 9024, measured with HETGS (Testa et al 2008)



Mapping Coronae

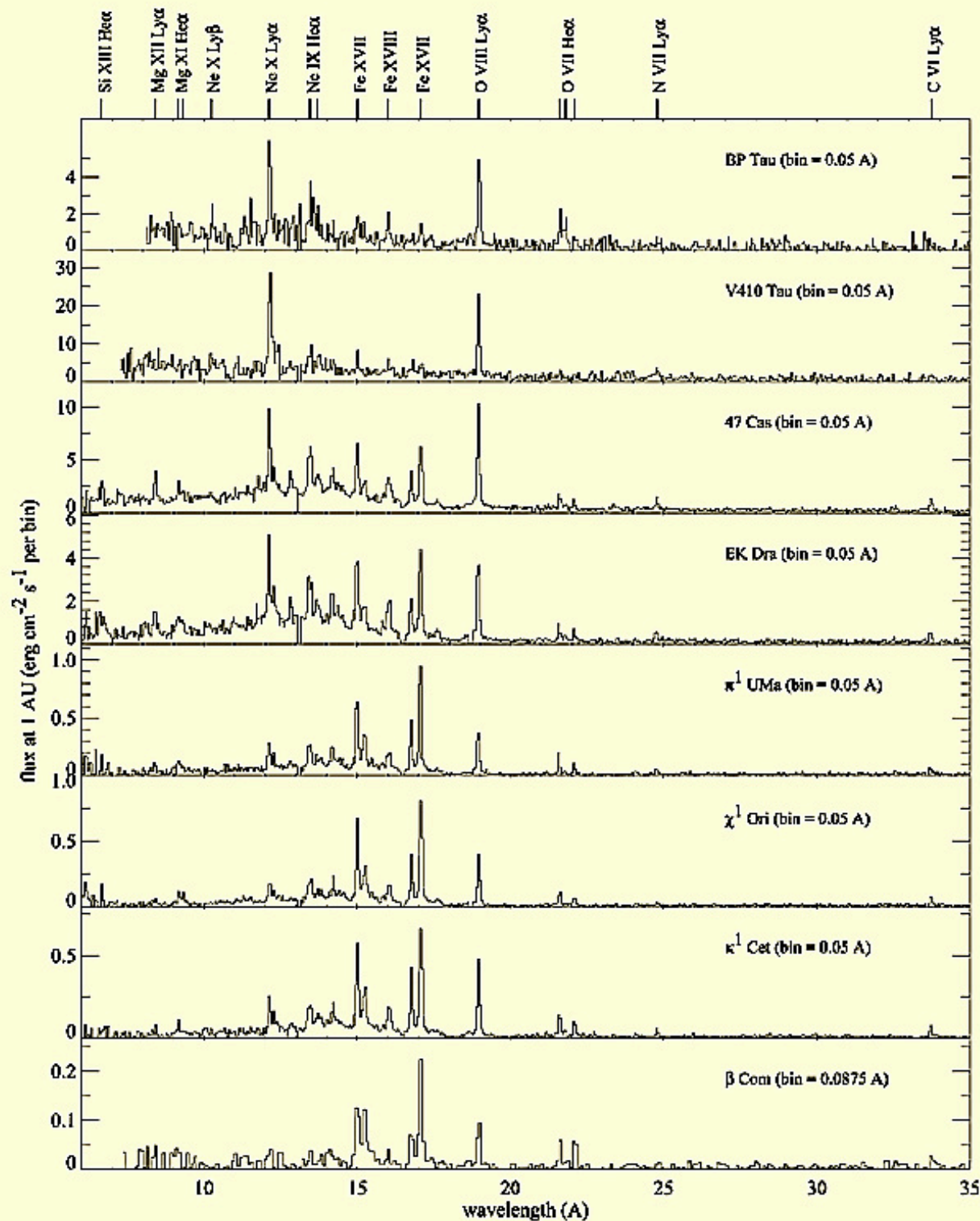
HETGS line centroids in VW Cep, a contact binary, follow the primary star. Lack of eclipses in the light curve locate the coronal material at high latitudes. (Huenemoerder et al 2006)

HETGS line shape and flux modulation in conjunction with optical polarimetric surface magnetic field mapping and extrapolation can provide an “image” of the corona on another star (AB Dor; Hussain et al 2007).

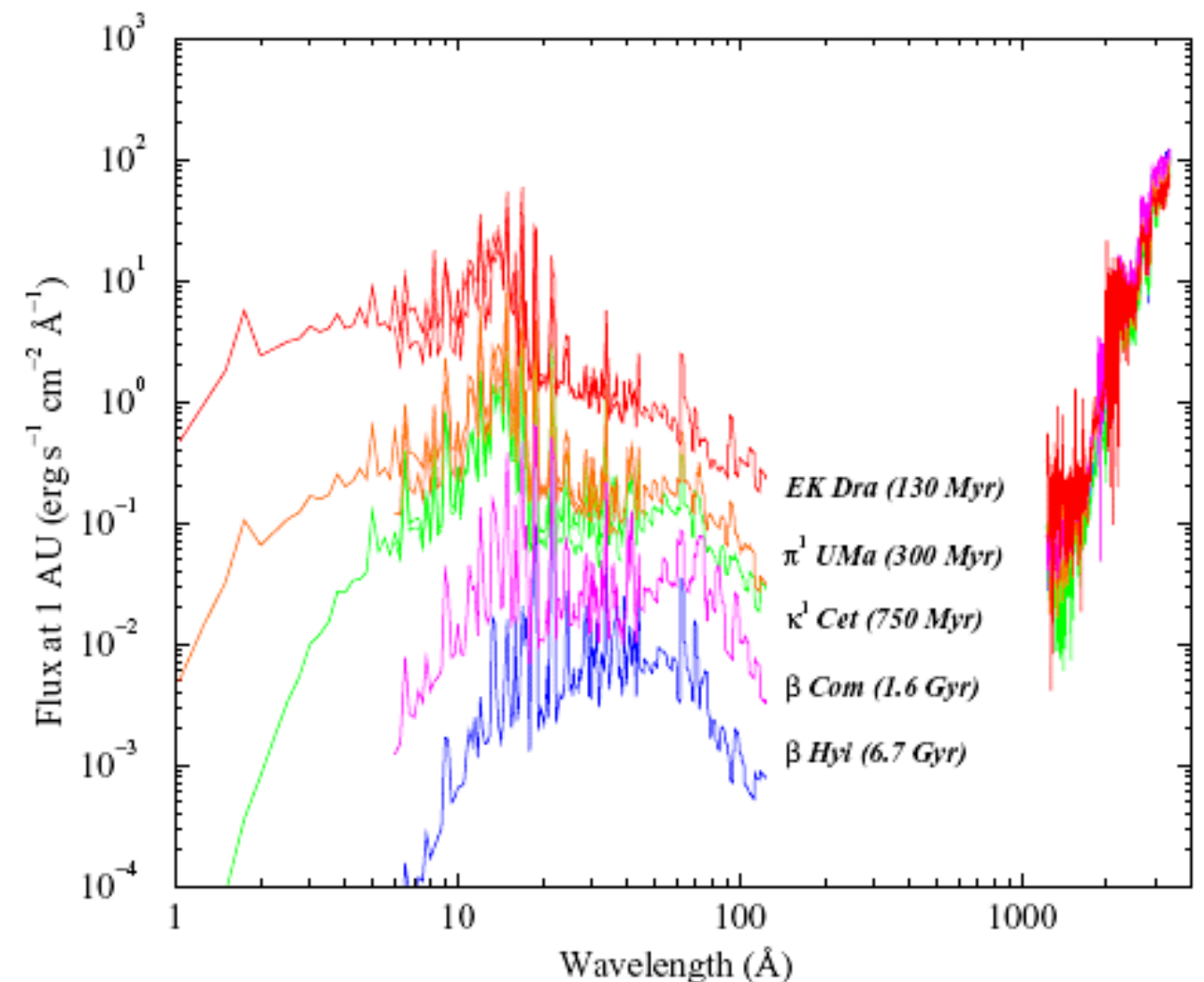


Coronal "Apps": Differential Studies

Solar system history: evolution of X-ray flux, and its influence...
XMM/RGS spectra of Solar analogs vs. age (Guedel 2007):

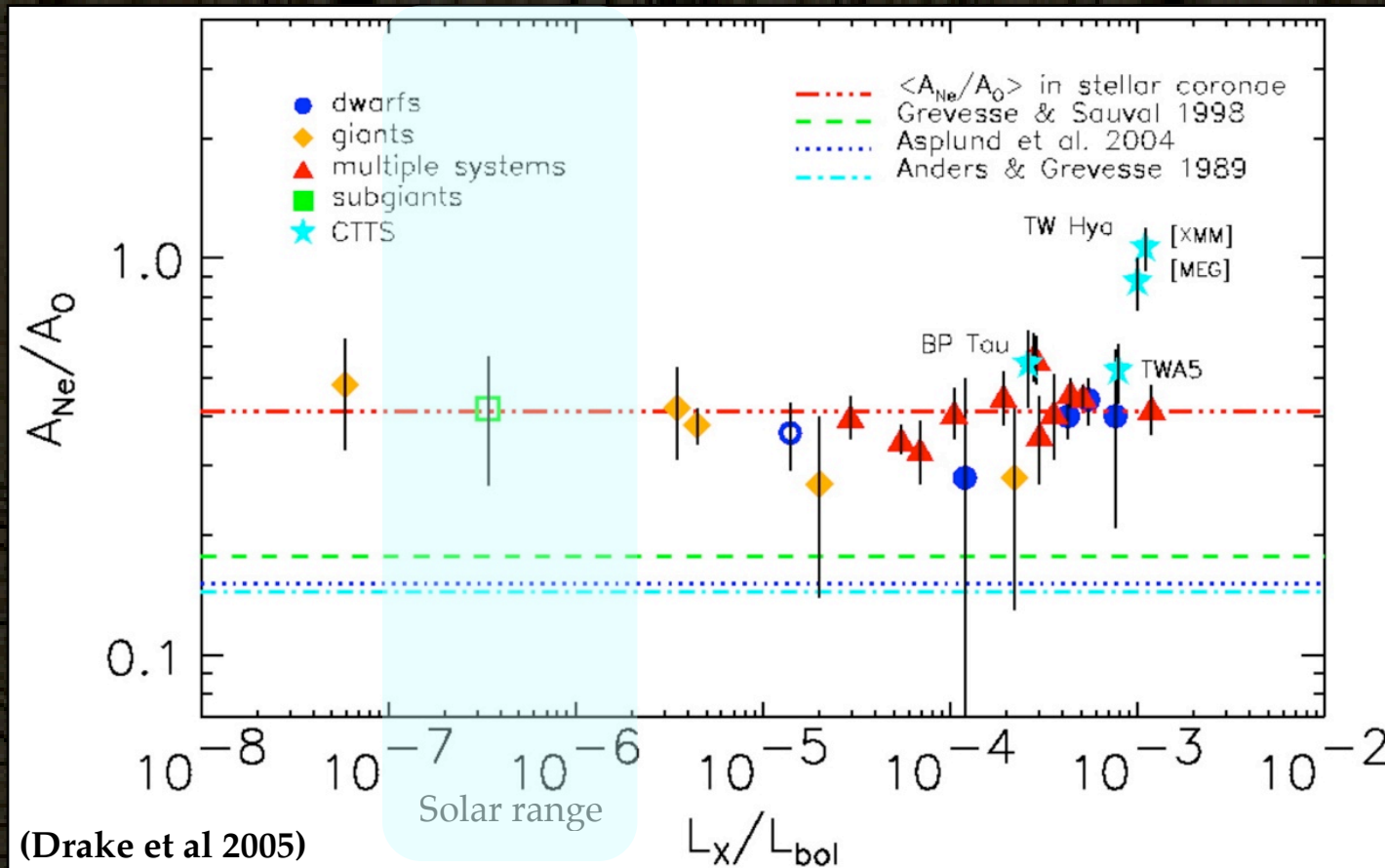


This portion of the spectrum is fundamental to ionization and chemistry in planetary atmospheres:



Coronal “Apps”: Differential Studies

Cosmic abundances and stellar evolution:



The Ne:O ratio is important for both stellar interior models and for disk-depletion models. Neon abundance is difficult to determine --- except in high-resolution X-ray spectra. Left: Ne:O from a sample of stars observed w/ HETG. Are Solar abundances wrong? Are accretion disks depleted in oxygen?

Algol systems undergo mass transfer. Algol B (a K-type star) has a very high N:C ratio, consistent with its evolutionary state, and loss of about half its mass. The K-component of HR 1099 has an approximately normal ratio.

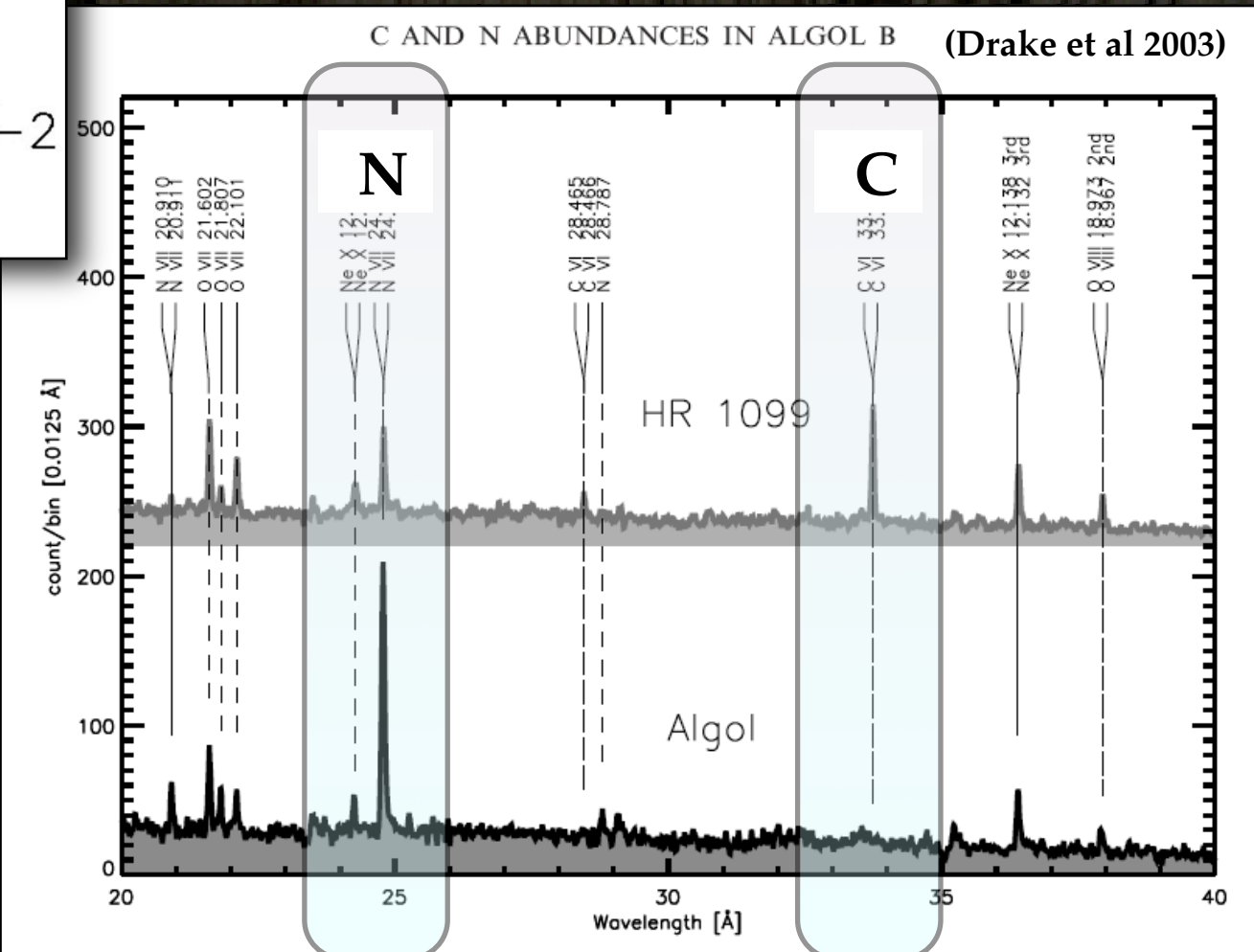
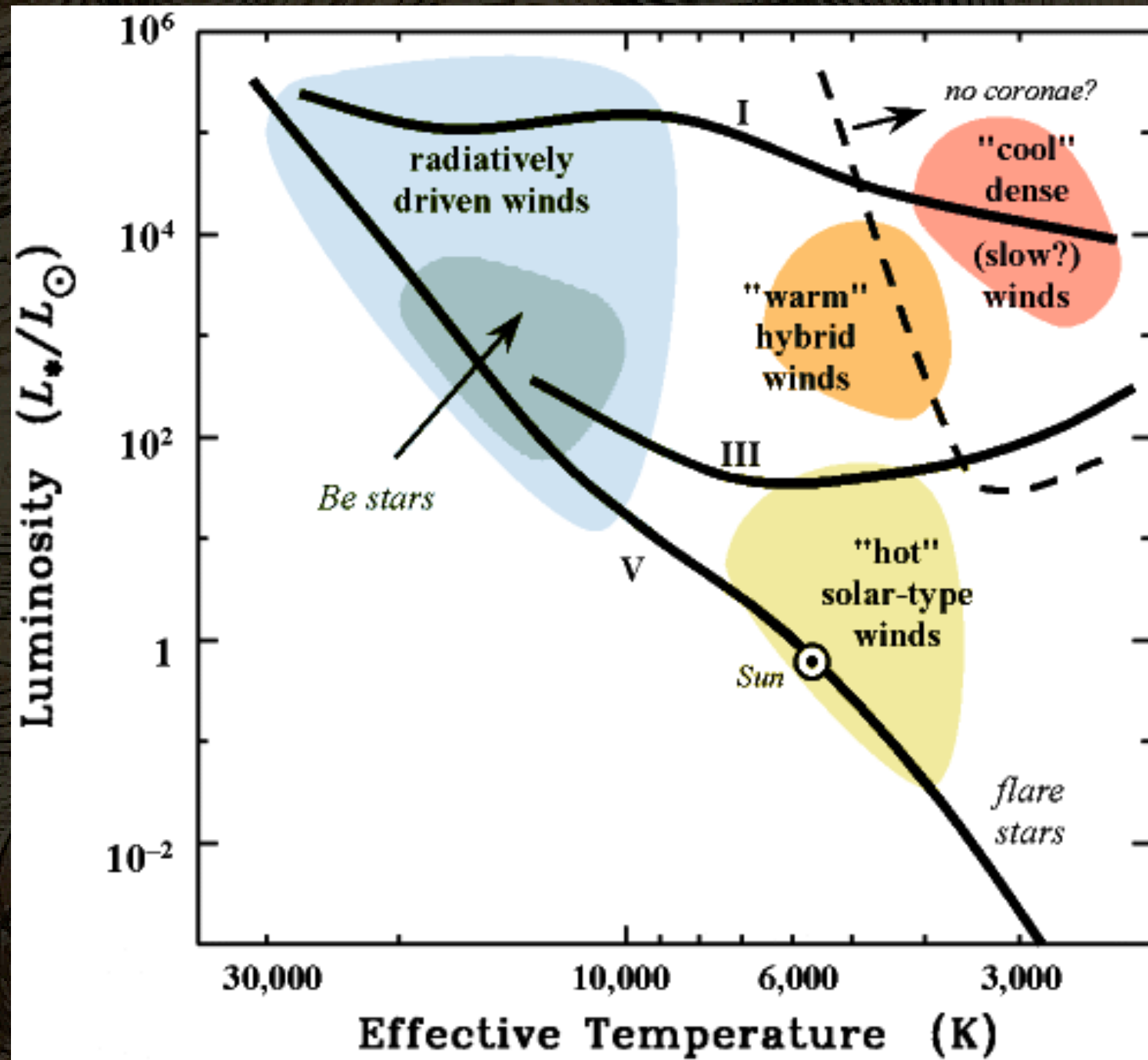


Fig. 2.—Comparison of the 20–35 Å range containing spectral lines from C, N, O, and Ne in Algol and HR 1099 LETG+HRC-S spectra

Stellar Winds Across the H-R Diagram



Massive Stars: wind profiles

Constant velocity

Constant optical depth

Less absorbed

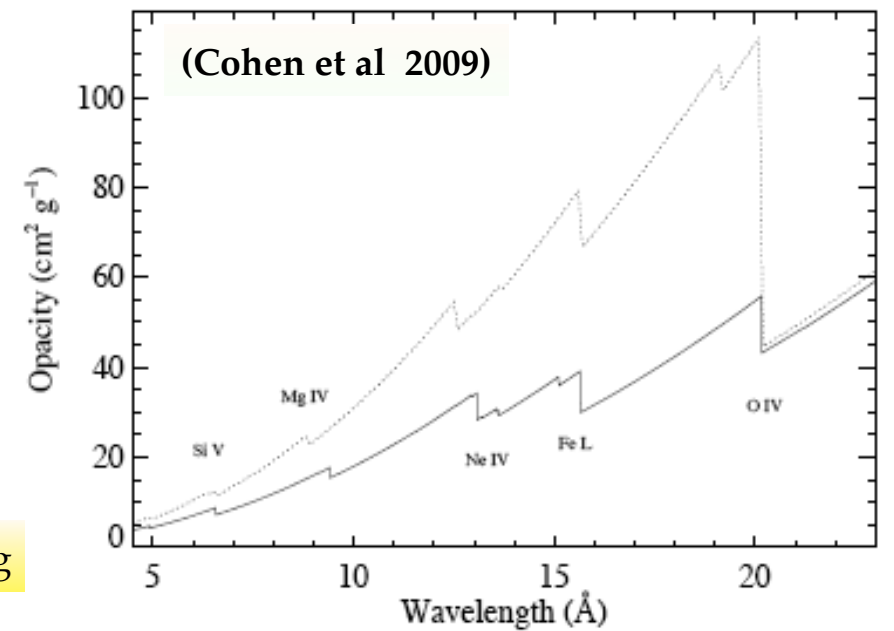
More absorbed

occulted

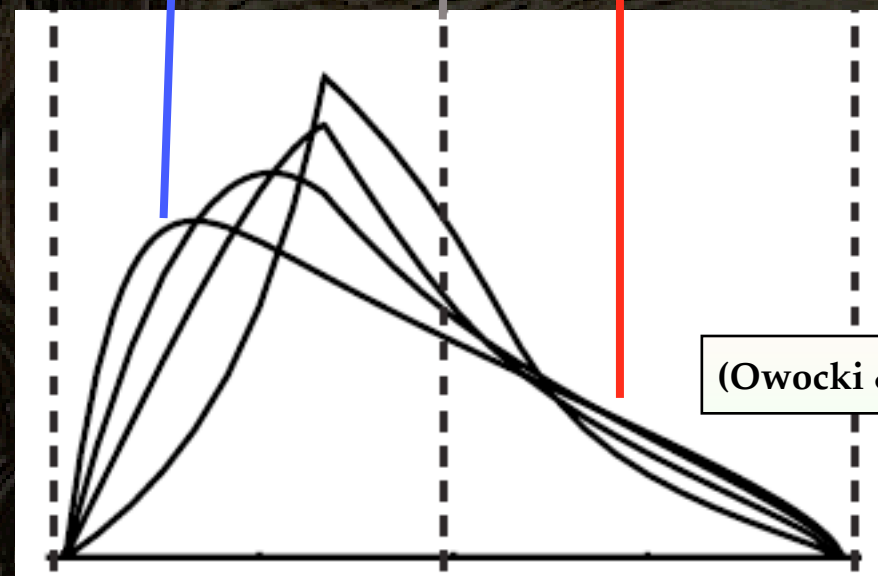
approaching

receding

Continuum absorption



Classical stellar wind: X-ray lines are *blueshifted*, *broad*, and *asymmetric*. The continuum (from shocks) was relatively *cool* (few MK; few tenths keV).



(Owocki & Cohen 2001)

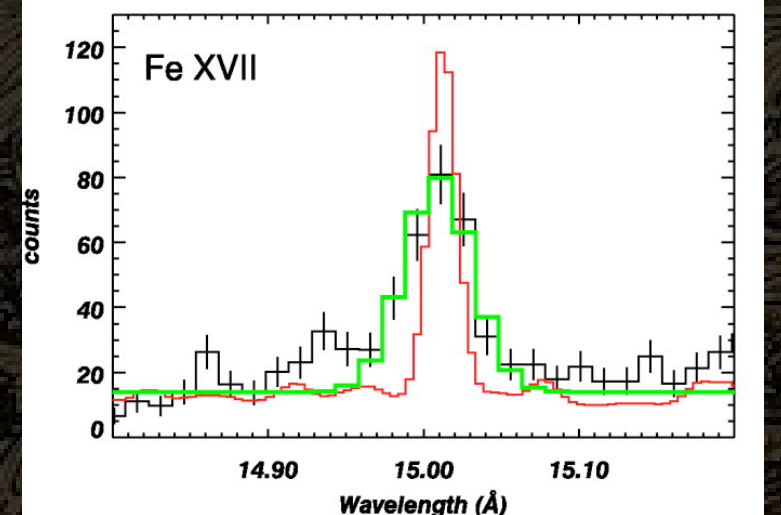
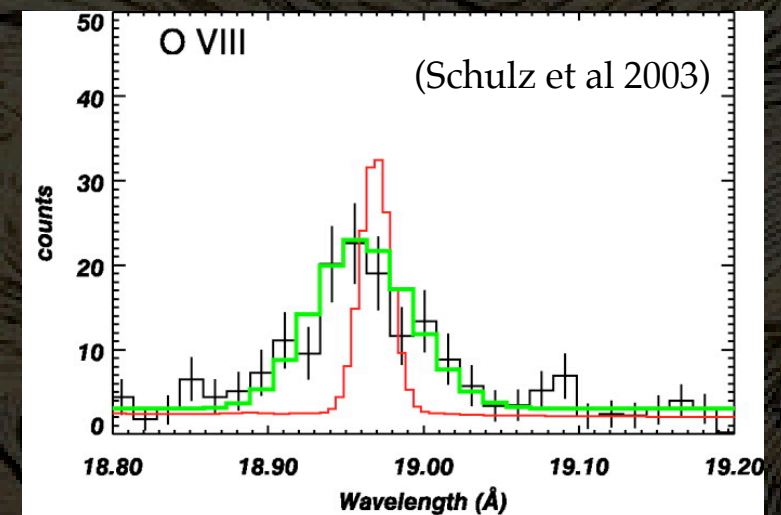
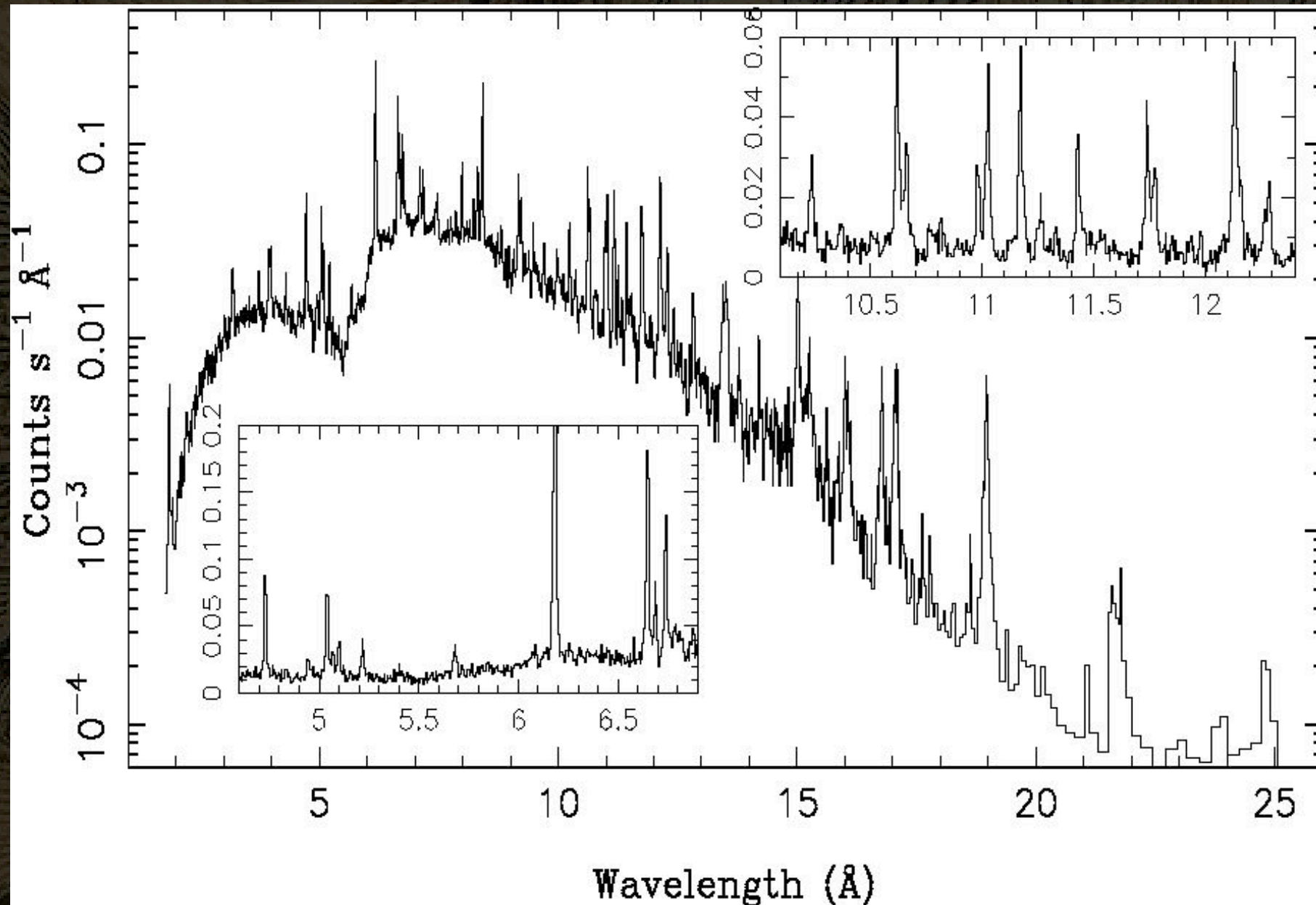
Wavelength offset

Massive Stars: θ^1 Ori C (O5.5V, $35.5M_{\text{sun}}$)...

... destroys the standard model!

In θ^1 Ori C lines were *unshifted, narrow, and symmetric*, and the continuum looked *hot* (tens of MK, a few keV)!

In more detail, short wavelength lines are unresolved, centered; long-wavelength are broadened.



Massive Stars: Magnetically Confined Winds

θ^1 Ori C narrow lines explained by the Magnetically Confined Wind Model (MCWM) (Gagne et al 2005) (and a magnetic field was detected in the star):

Subsequently, some stars were found which conformed to the expected profiles:

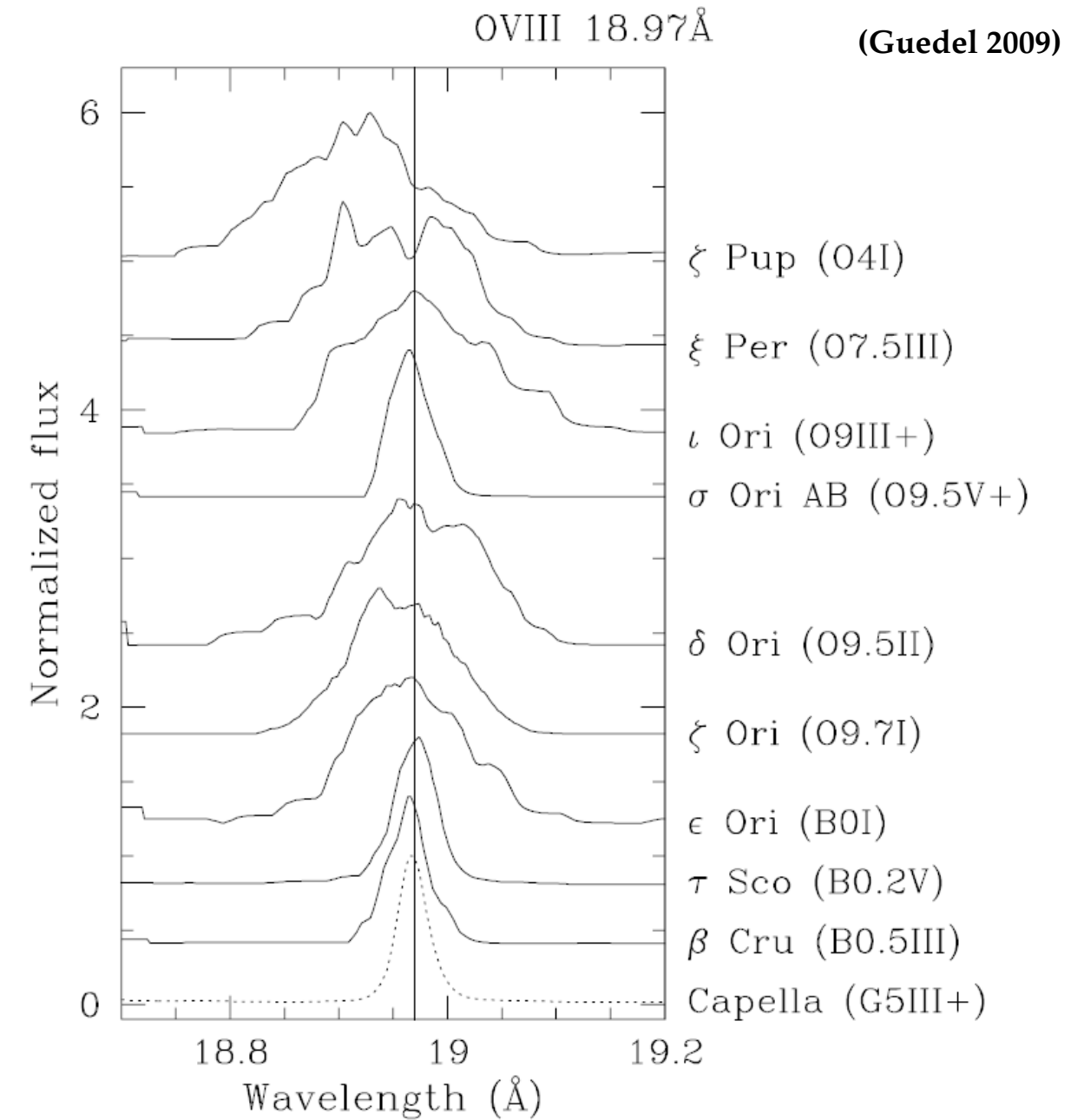
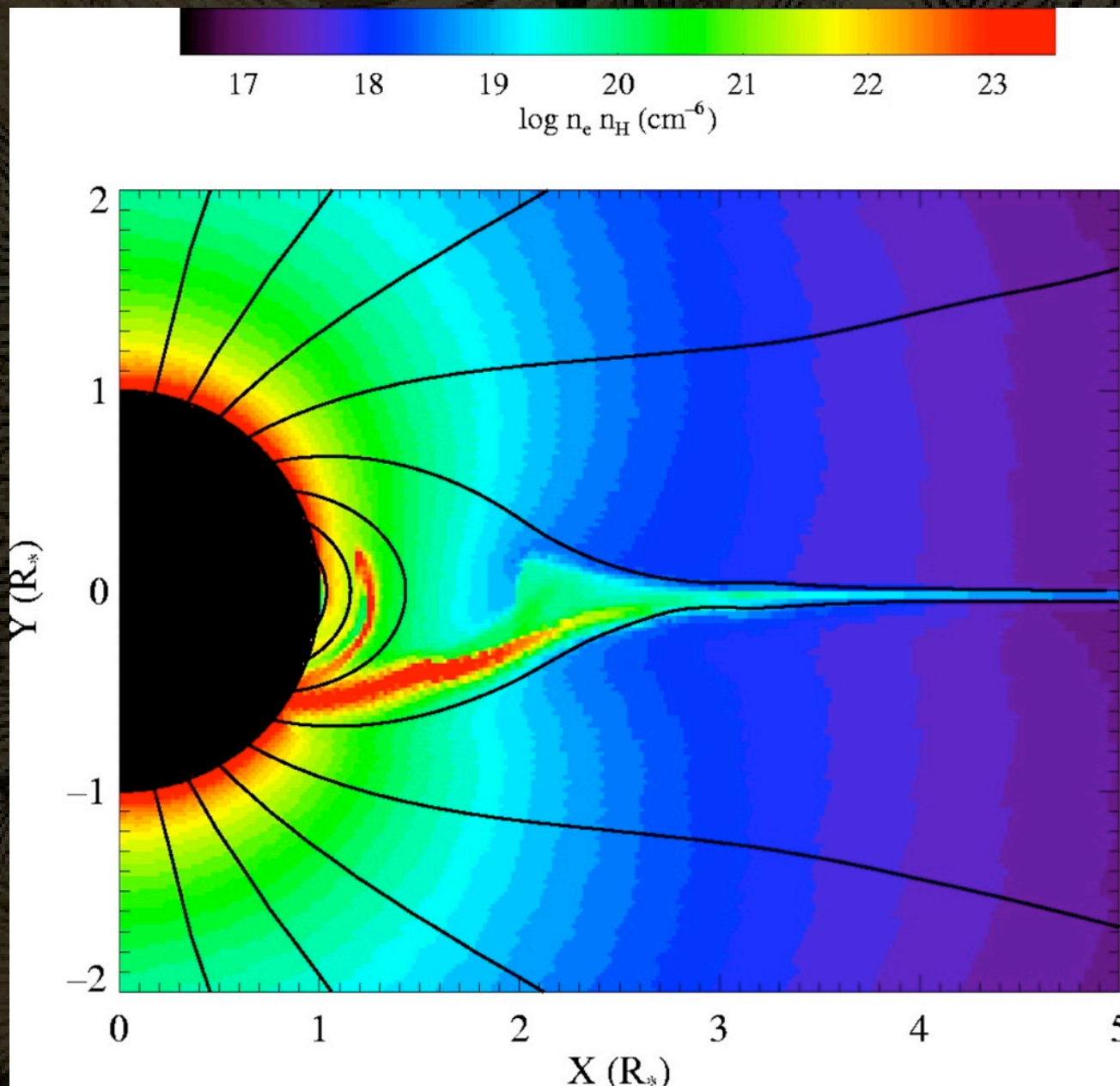
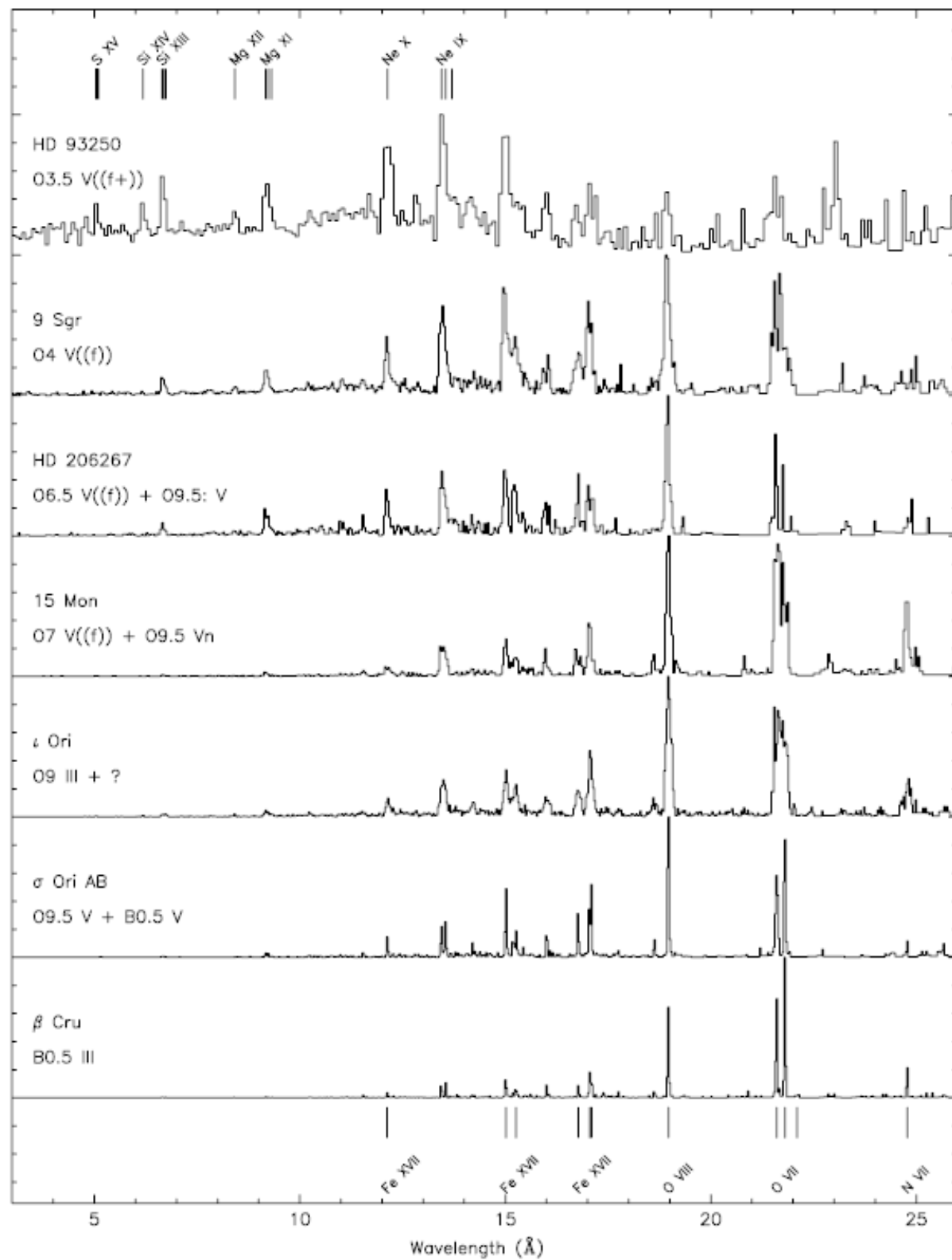


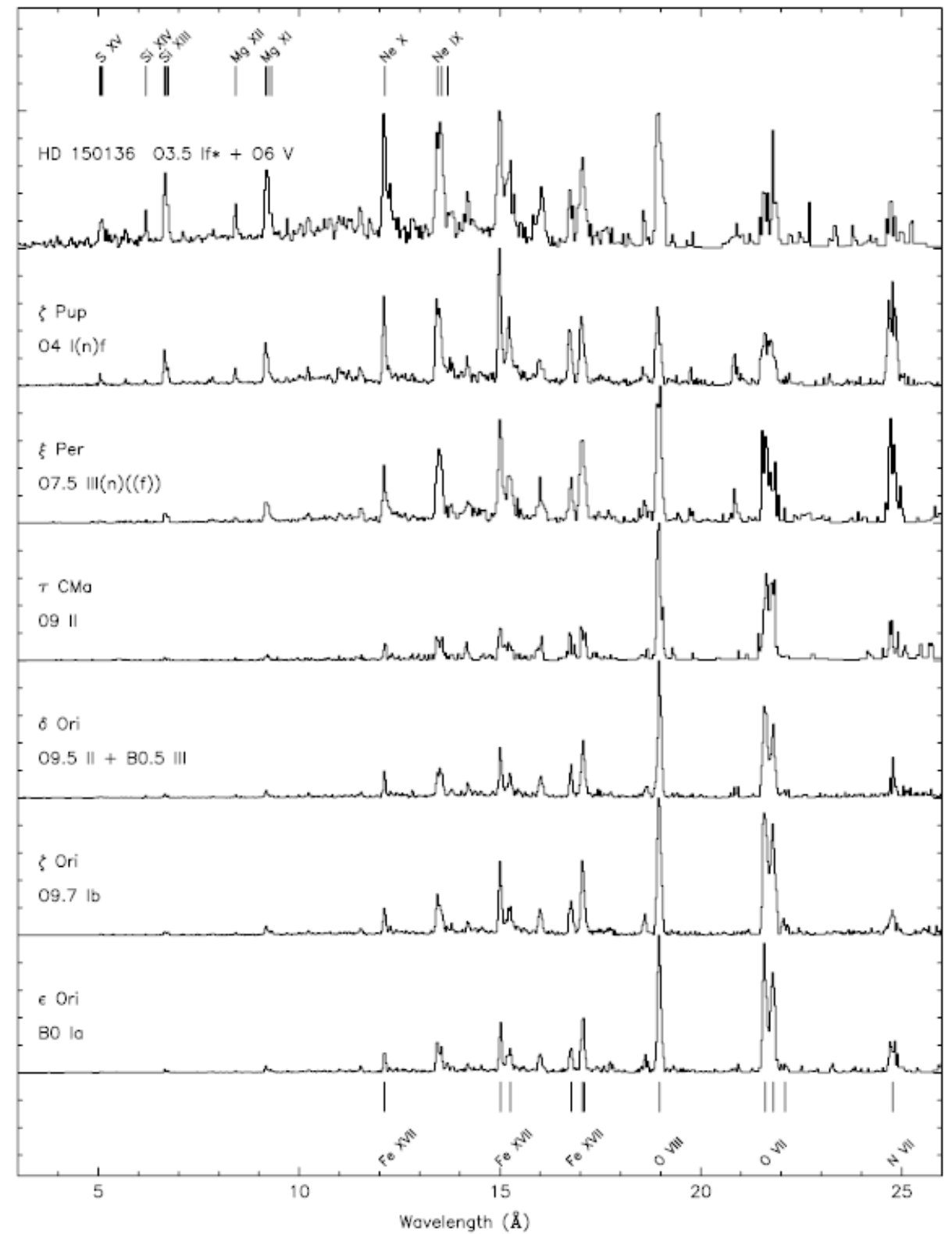
Fig. 25 Observed line profiles for OVIII λ 18.97Å in a sample of bright OB objects and in the coronally active late-type star Capella (where the line width is mostly instrumental). The vertical line corresponds to the rest wavelength of the line; the normalized profiles have been shifted upwards by an arbitrary amount for clarity (data taken from the Xatlas database and smoothed by a box of 4 pixels half width).

Massive Stars: X-ray trends

CORRELATION BETWEEN X-RAY LINE IONIZATION AND OPTICAL SPECTRAL TYPES

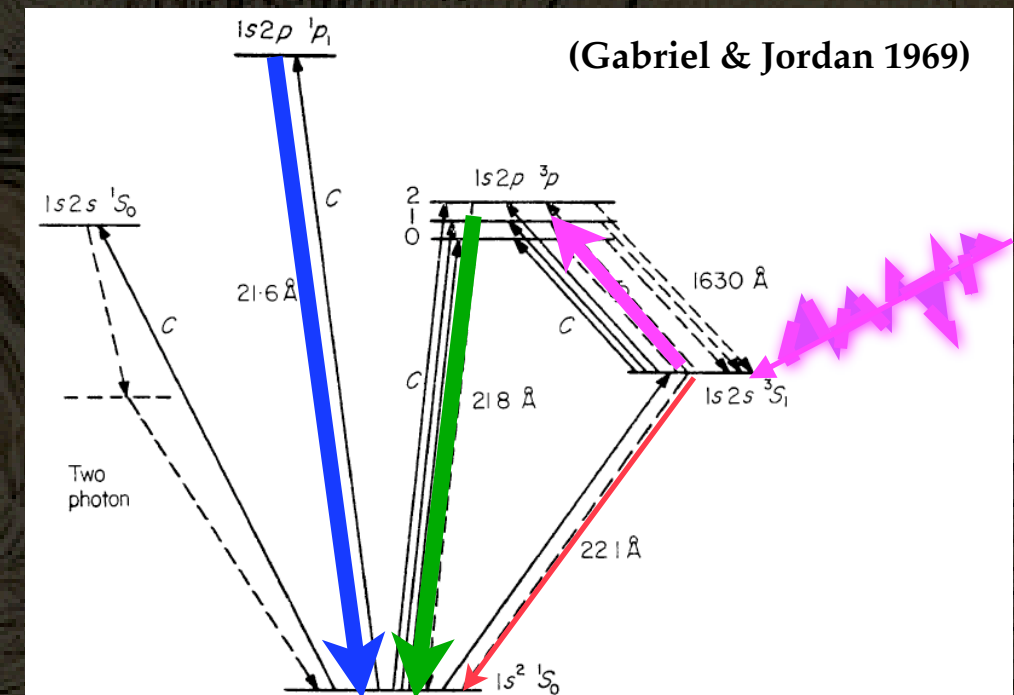


WALBORN, NICHOLS, & WALDRON (2009)

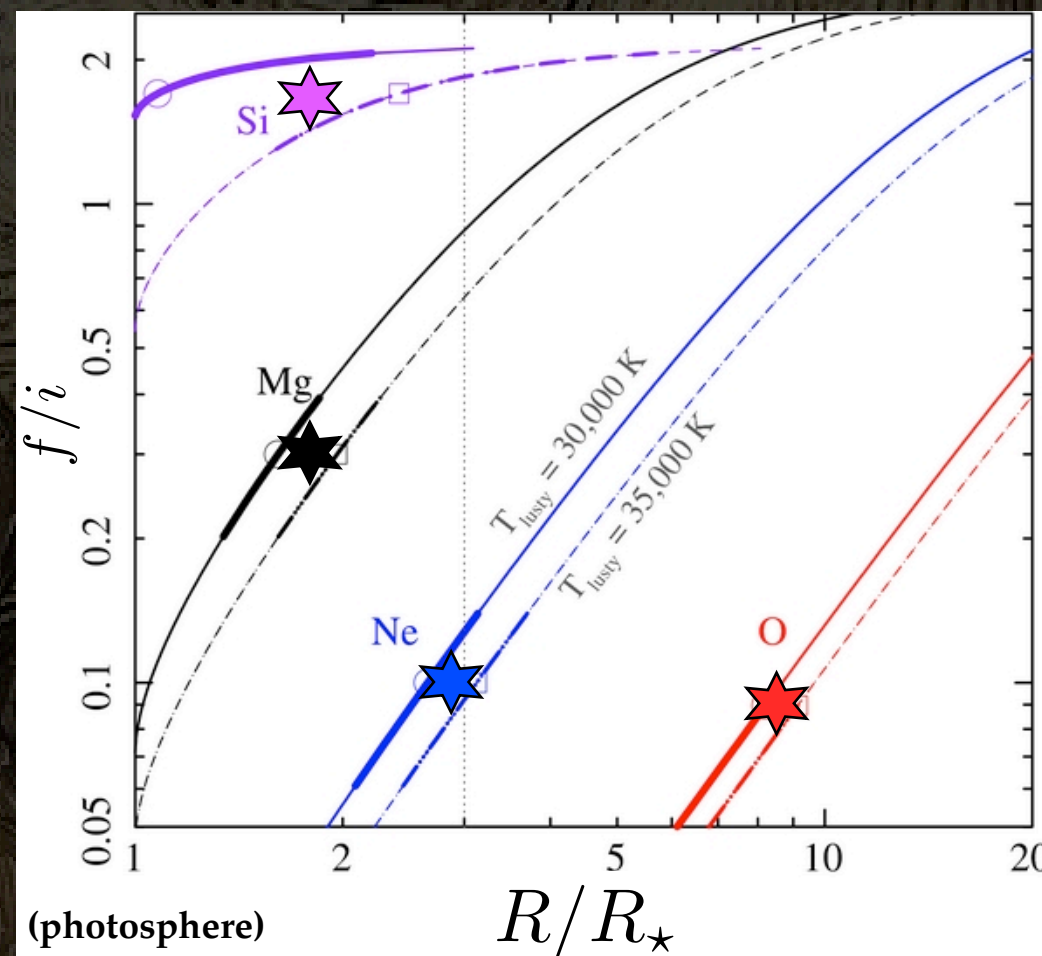
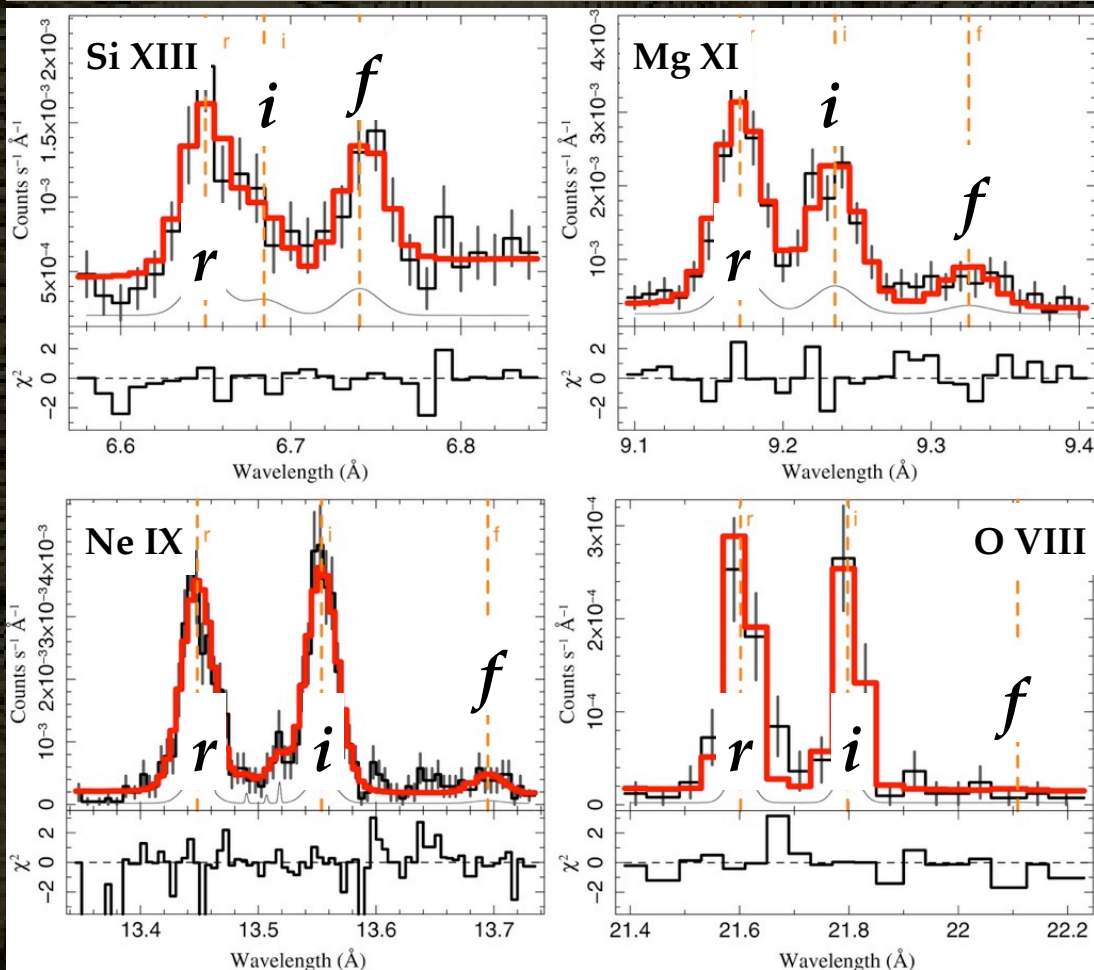


Where Does a Wind's X-ray Emission Originate?

We use the photoexcitation dependence of the He-like triplets' **forbidden / intercombination** ratio as a diagnostic of distance from the O-star's strong UV field. **UV photons** de-populate the upper level of the forbidden line and weaken it while enhancing the intercombination line.



Triplets in θ^2 Ori A form very close to the stellar photosphere!
(Mitschang et al 2011)

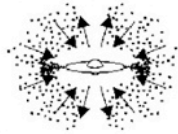
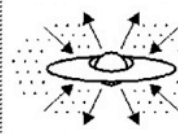
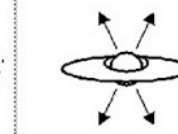
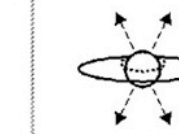
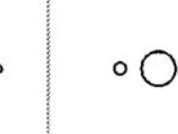


Pre-(Lower)-Main Sequence Stars

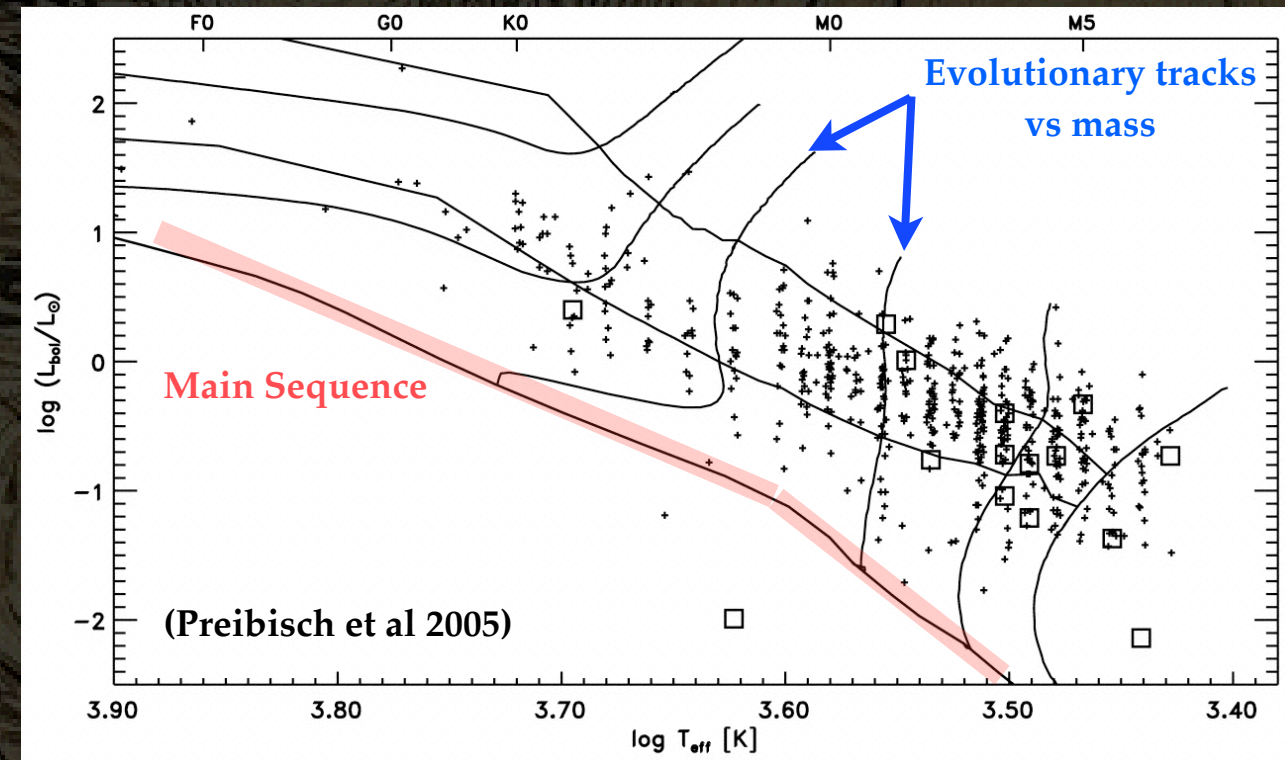
T Tauri Stars (TTS) come in two main flavors:

- Classical (CTTS), and
- Weak-lined (WTTS) (the line being H α).

Further subdivision has been define by Class:

PROPERTIES	Infalling Protostar	Evolved Protostar	Classical T Tauri Star	Weak-lined T Tauri Star	Main Sequence Star
SKETCH					
AGE (YEARS)	10^4	10^5	$10^6 - 10^7$	$10^6 - 10^7$	$> 10^7$
mm/INFRARED CLASS	Class 0	Class I	Class II	Class III	(Class III)
DISK	Yes	Thick	Thick	Thin or Non-existent	Possible Planetary System
X-RAY	?	Yes	Strong	Strong	Weak
THERMAL RADIO	Yes	Yes	Yes	No	No
NON-THERMAL RADIO	No	Yes	No ?	Yes	Yes

(Feigelson & Montmerle 1999)

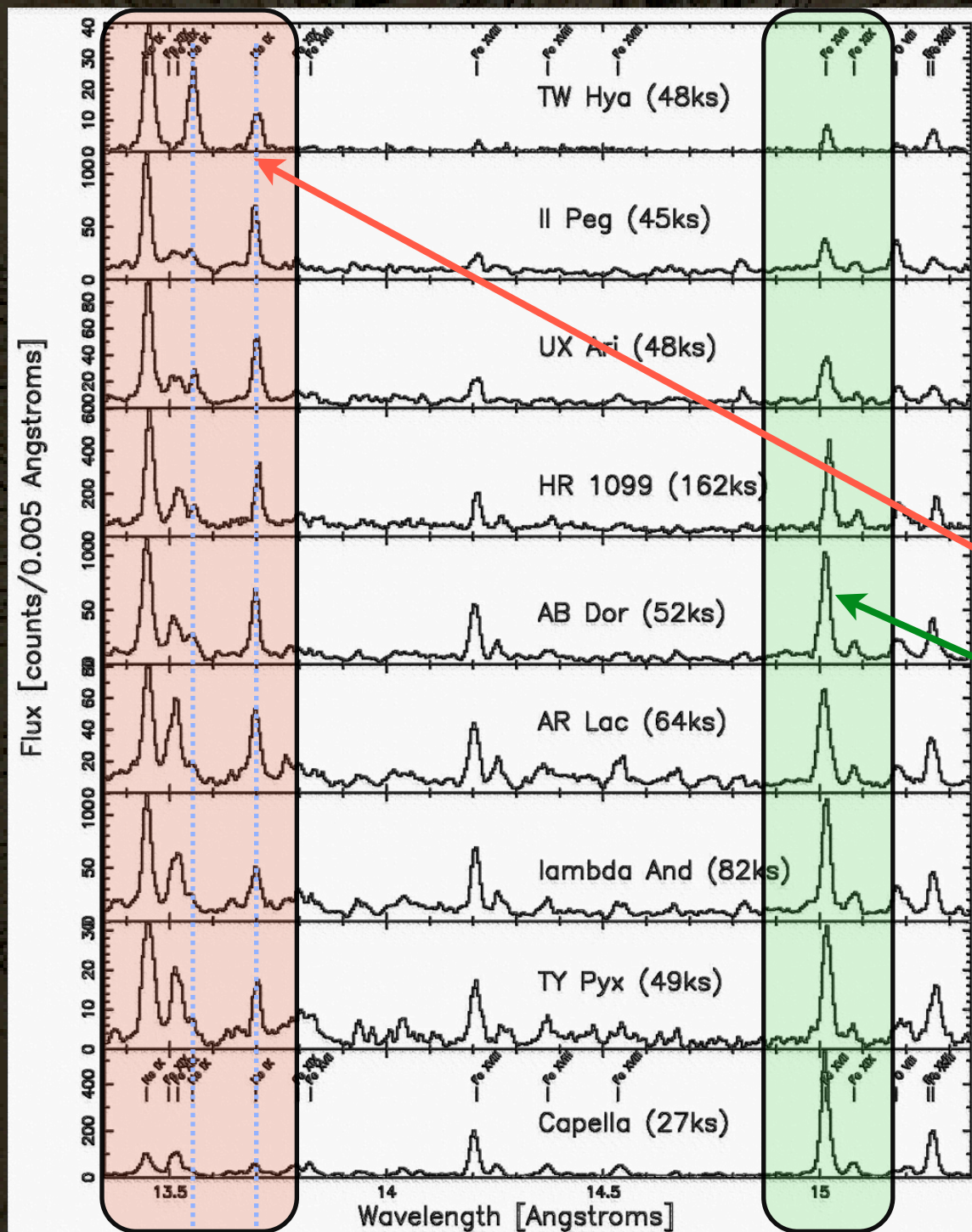


TTS are easily detected and characterized in X-rays; for example, the Orion Nebular Cluster in the infrared (left; VLT) and X-rays (right; Chandra ACIS).



PMS Plasma Density

A very early Chandra/HETGS spectrum of TW Hya showed the signature of high density in the triplet lines ($\sim 10^{13} \text{ cm}^{-3}$) and a very cool plasma (3 MK) (Kastner et al 2002):

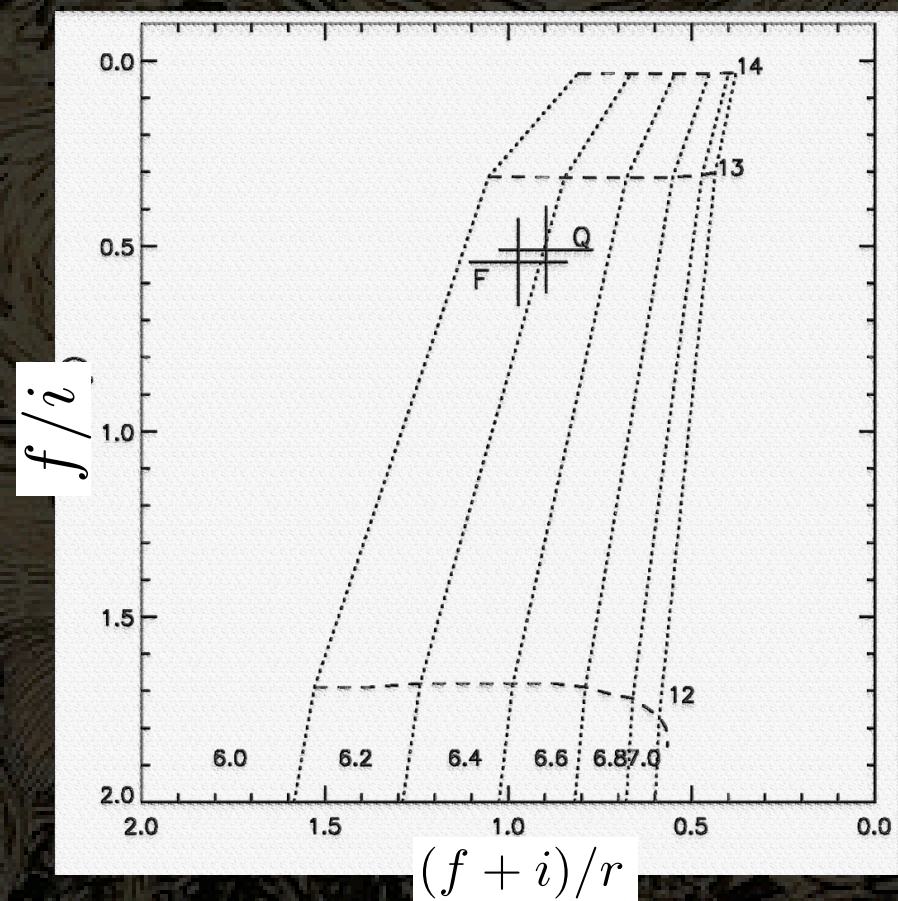


TW Hya

A gallery of coronally active stars (which show very different spectra):

Ne IX He-like Triplet

Fe XVII

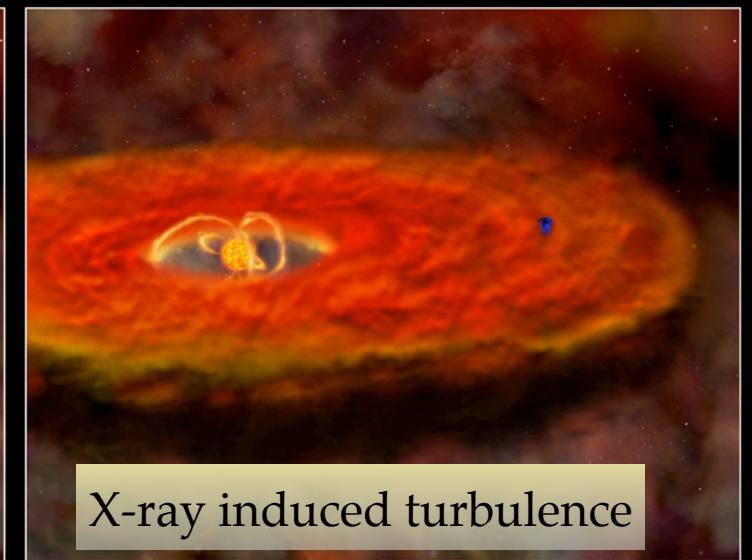
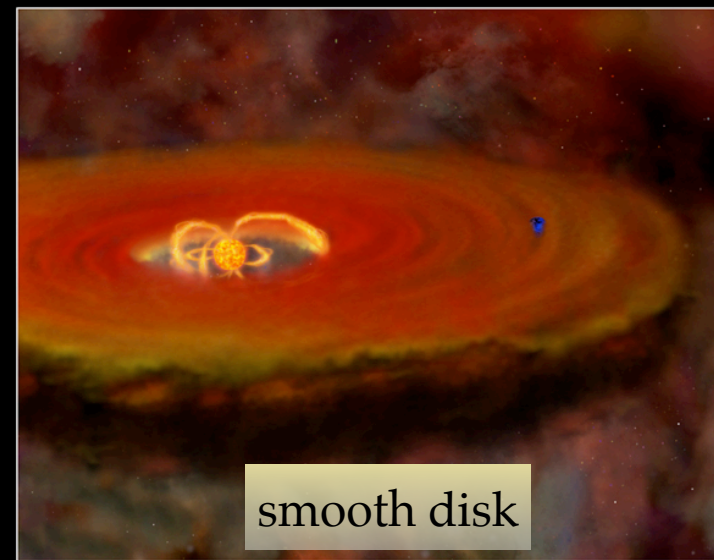


Low Mass Stars: Star-Disk Interactions

It is probable that there are interactions between accretion disks and central stars:

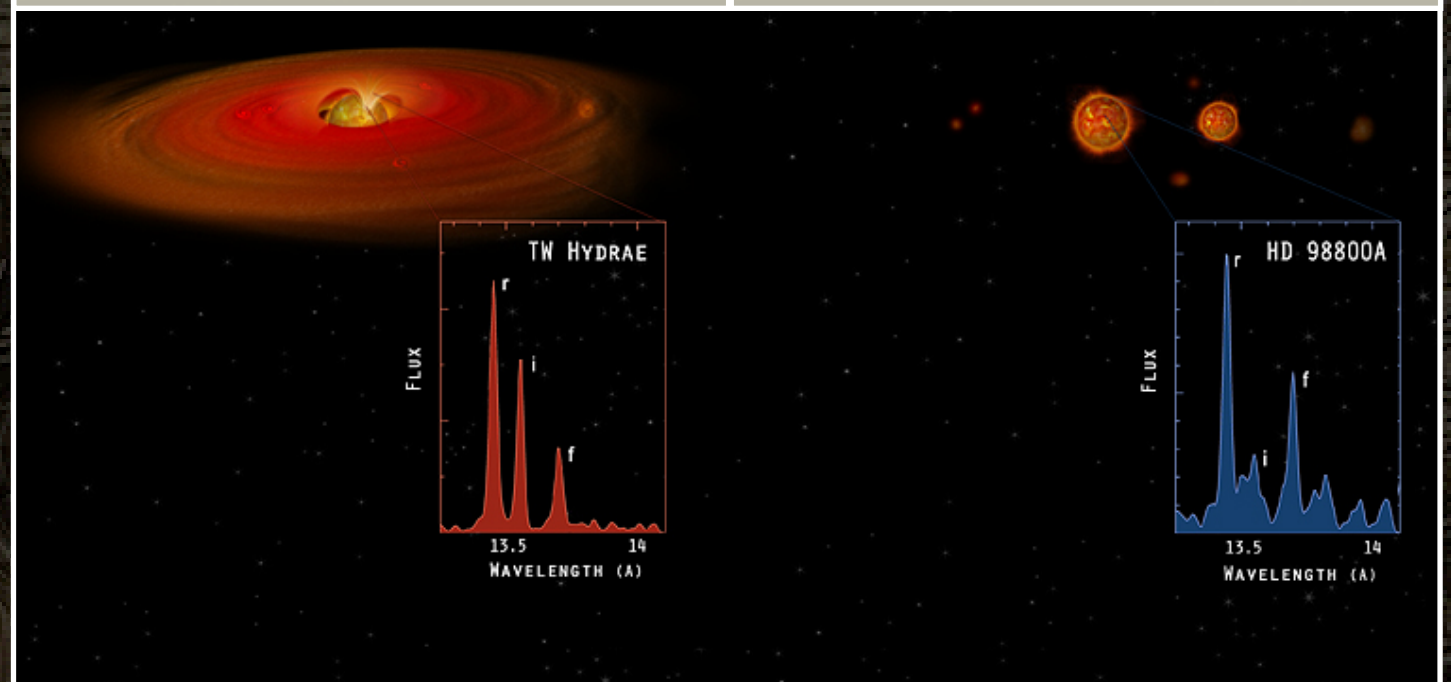
- accretion streams, funneled by magnetic fields
- magnetic loop reconnections, between star and disk
- X-ray induced opacity / turbulence

TW Hya, BP Tau, MP Mus, V4046 Sgr (all CTTS) show evidence for accretion in X-ray spectra: very cool (shocks) and high-density (via He-like triplets).



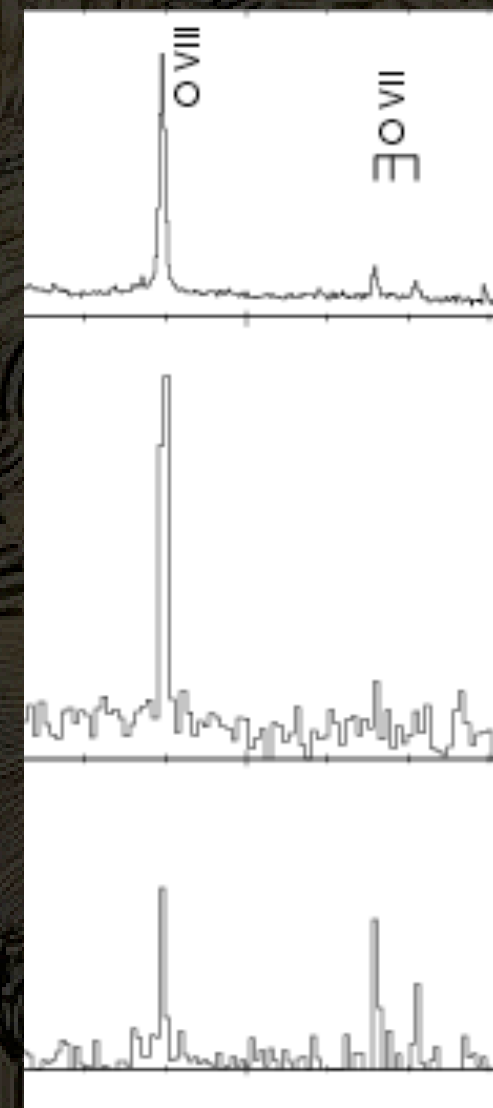
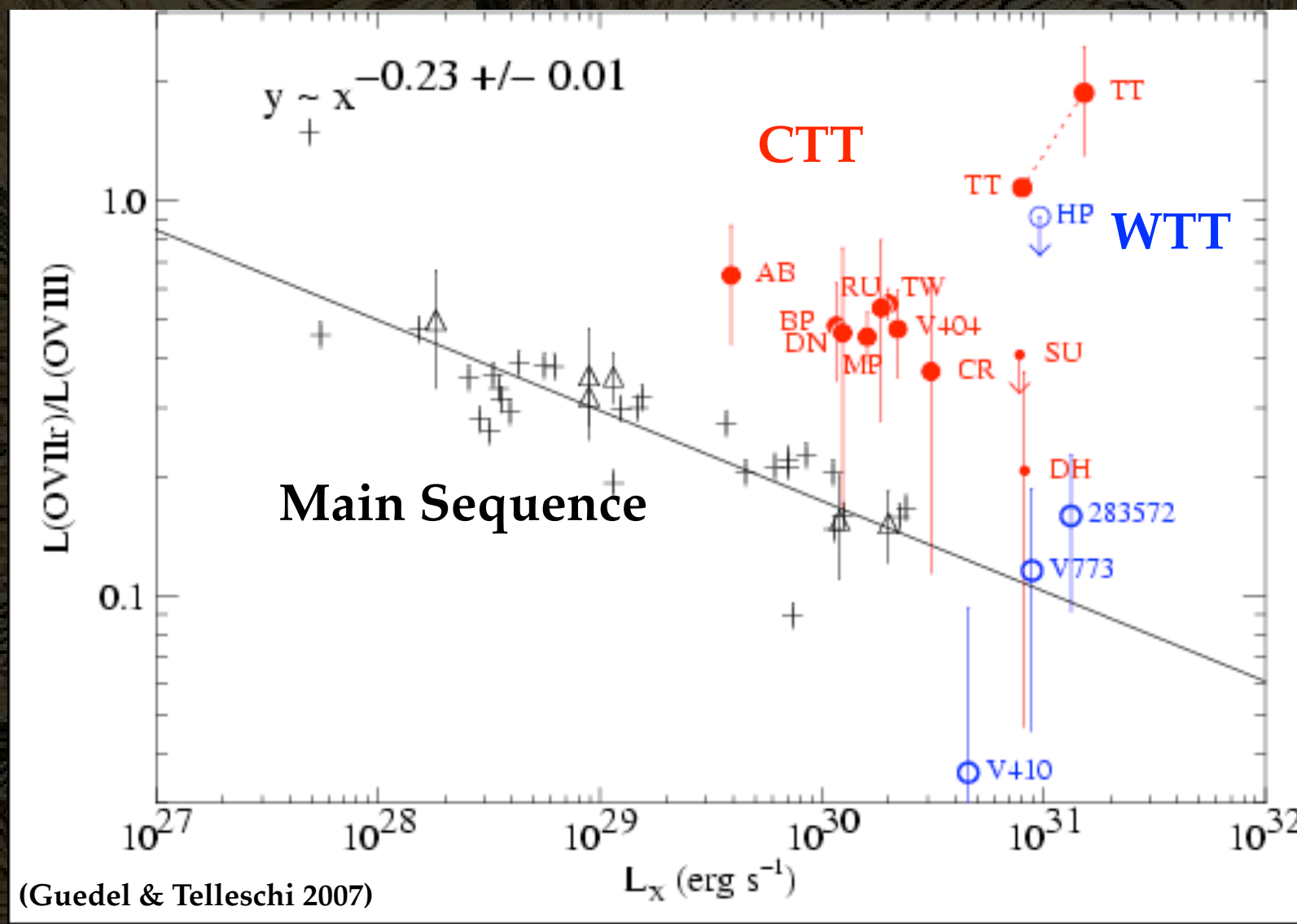
evidence for high-density accretion in CTT TW Hya ...

... is absent in WTT HD 98800.



Spectral Survey of CTTS & WTTS

O VII has an excess relative to O VIII in Classical T Tauri stars. This is interpreted as an excess in cool plasma from an accretion shock



Coronal

WTTS

CTTS

Accretion Modeling

Observational and theoretical efforts continue to determine the nature of the accretion and disk interactions.

Inferences from line profiles in a 500 ks HETGS exposure of TW Hya

3D MHD, time-dependent simulations:

(Bouvier et al 2007)

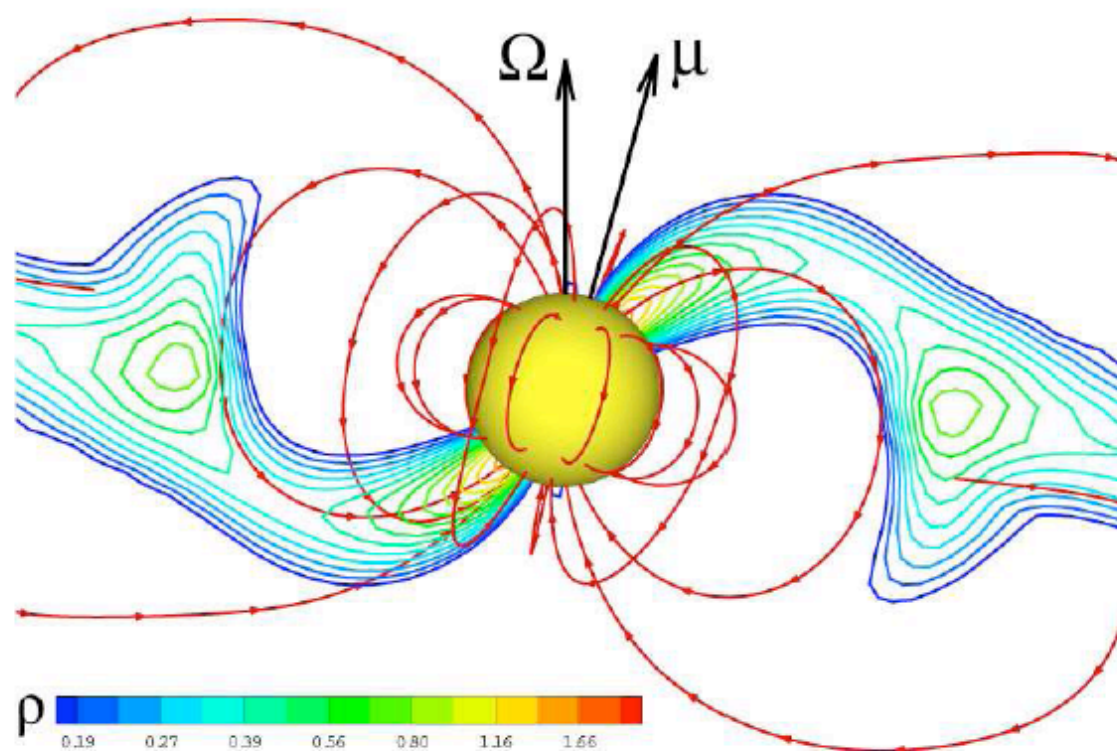


Fig. 8.— A slice of the funnel stream obtained in 3D simulations for an inclined dipole ($\Theta = 15^\circ$). The contour lines show density levels, from the minimum (dark) to the maximum (light). The corona above the disk has a low-density but is not shown. The thick lines depict magnetic field lines (from Romanova et al., 2004a).

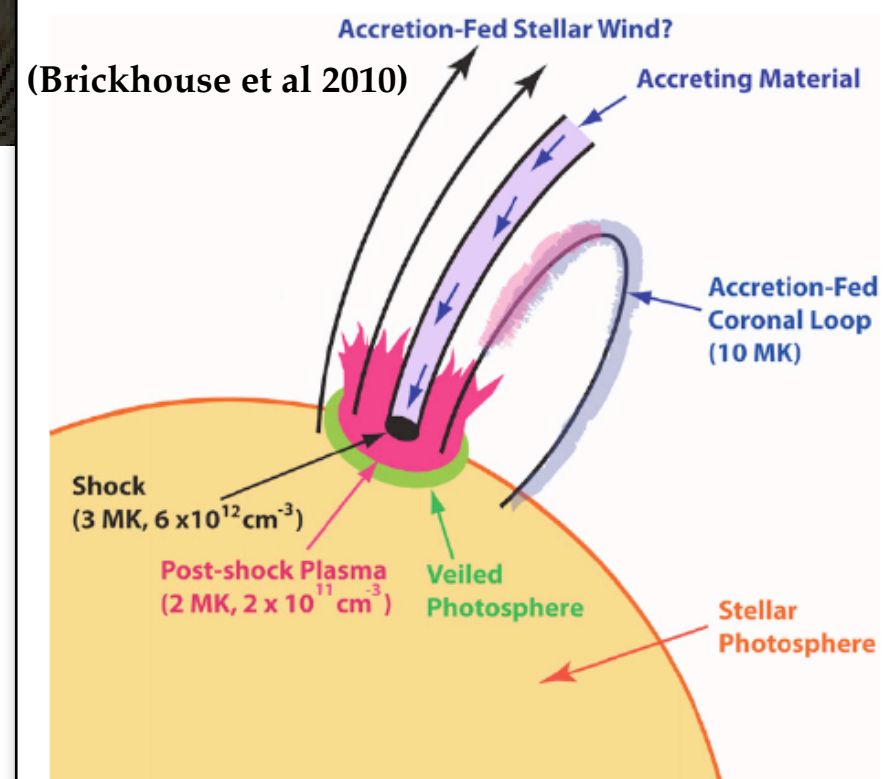
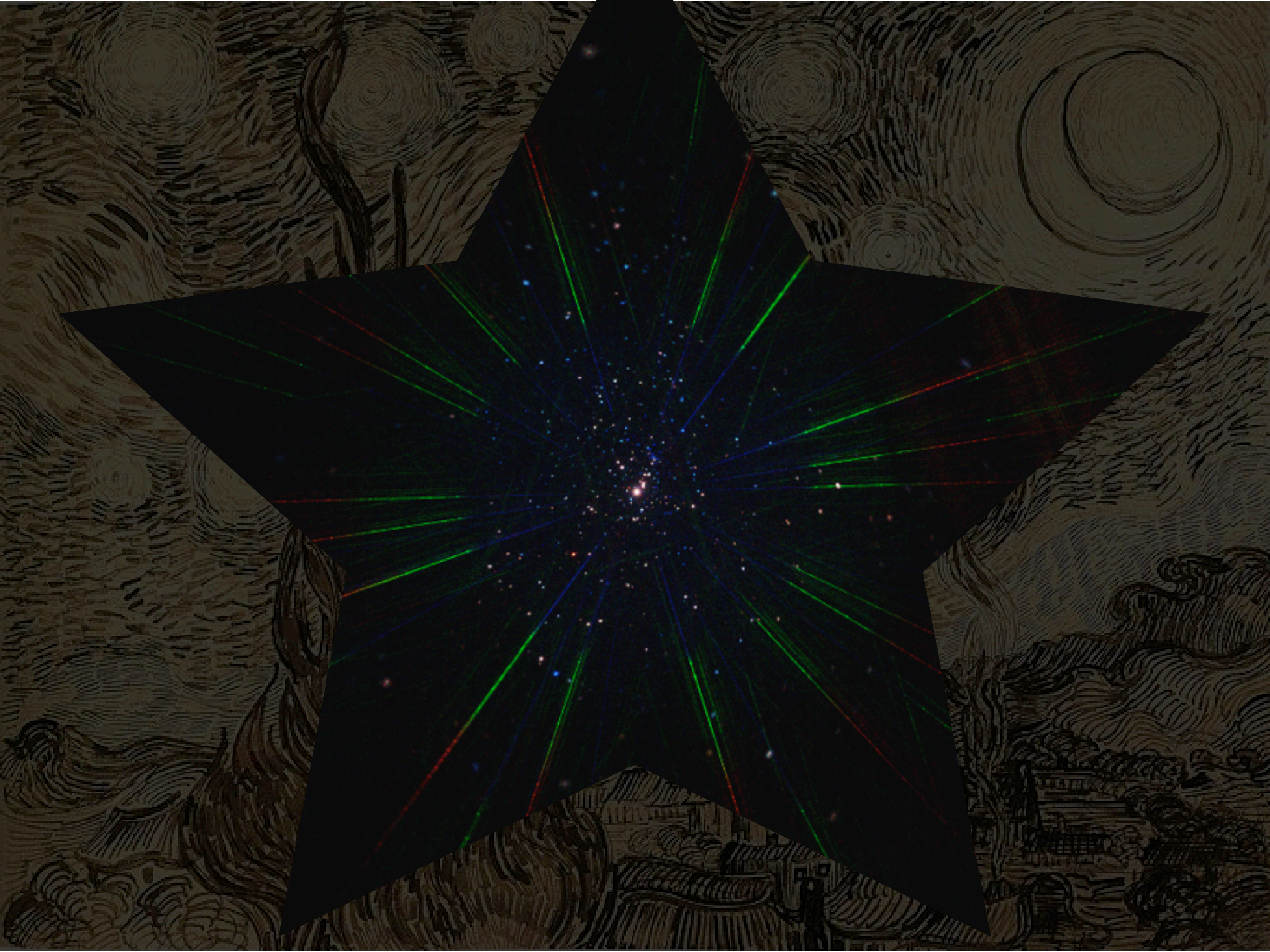


Figure 10. Illustration of the shock and its surrounding environment. Region 1 in the text corresponds to the shock and region 2 to the postshock plasma. Figure courtesy of A. Szentgyorgyi.



Extras; Wolf-Rayet Stars

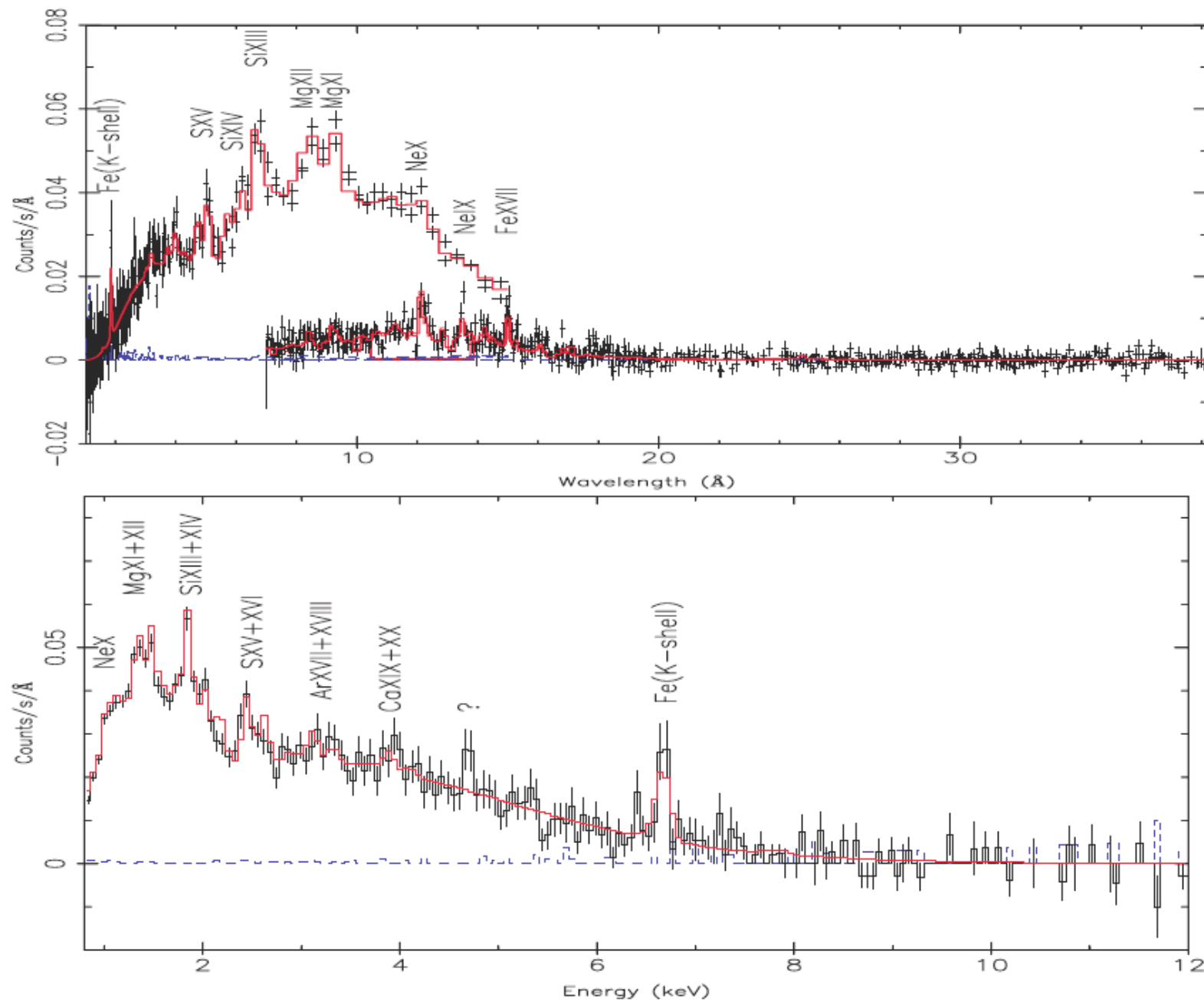


Fig. 2. *Top:* first-order background-subtracted spectra of WR 25 of rev. 284 and 285, observed by *XMM-RGS* (5–38 Å) and *XMM-EPIC-MOS* (1–15 Å). The spectra are not corrected for the effective areas of the instruments, in order to show the different efficiencies. Several prominent lines are labelled with the emitting ions. Note the small error bars. The red line shows the best-fit model and the blue line the subtracted background. Due to the higher resolution the lines above 10 Å are more prominent in the *RGS* spectrum. The oxygen edge at 23 Å is invisible due to lack of flux for $\lambda \gtrsim 20$ Å. *Bottom:* the *XMM-EPIC-MOS* spectrum of rev. 284. The question mark indicates an unknown emission, which happens to be located at the position of Ti K-shell lines. The cosmic Ti-abundance, however, is low and no other confirmations for the presence of Ti have been found in the spectrum.

Extras; Wolf-Rayet Stars, colliding winds

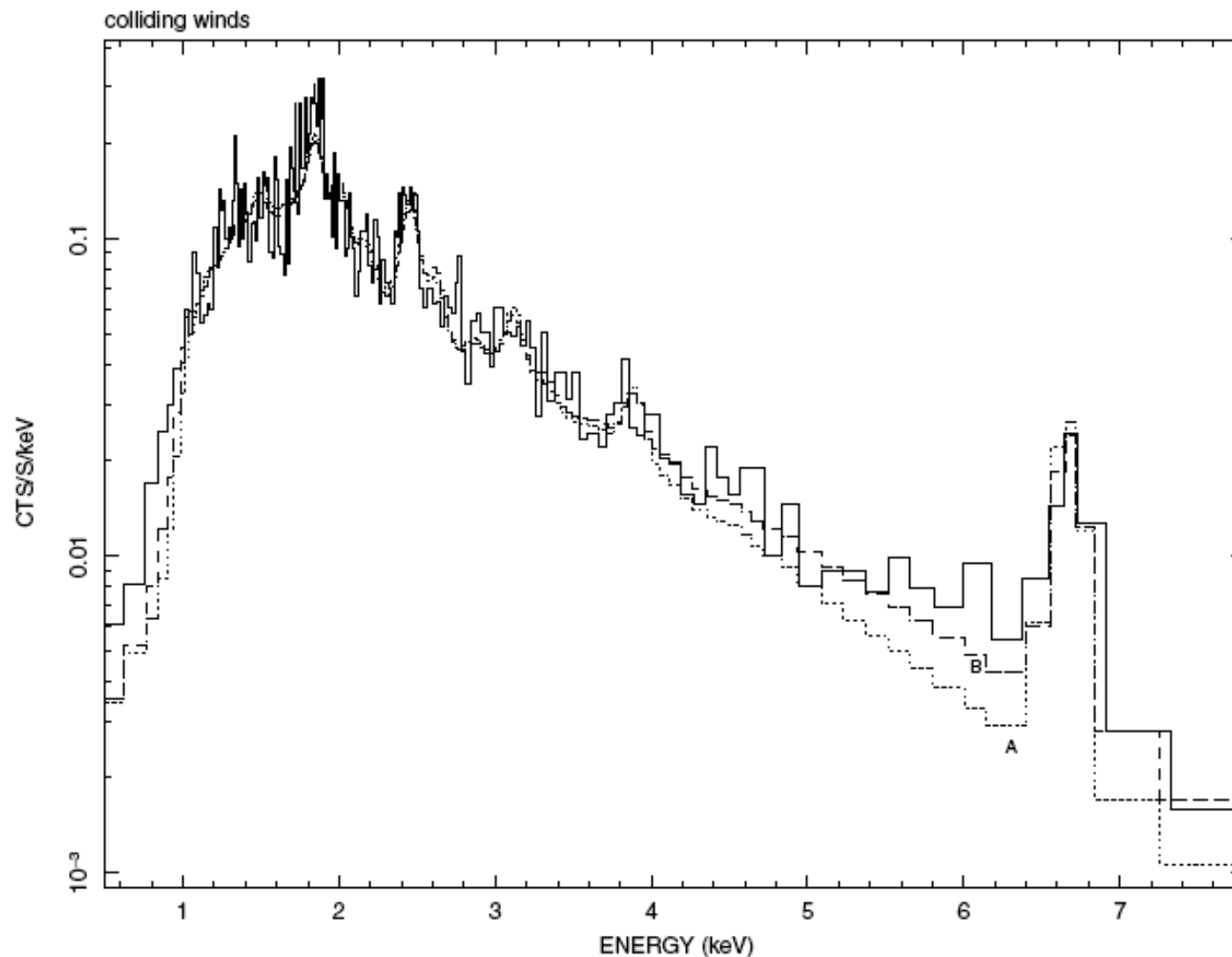
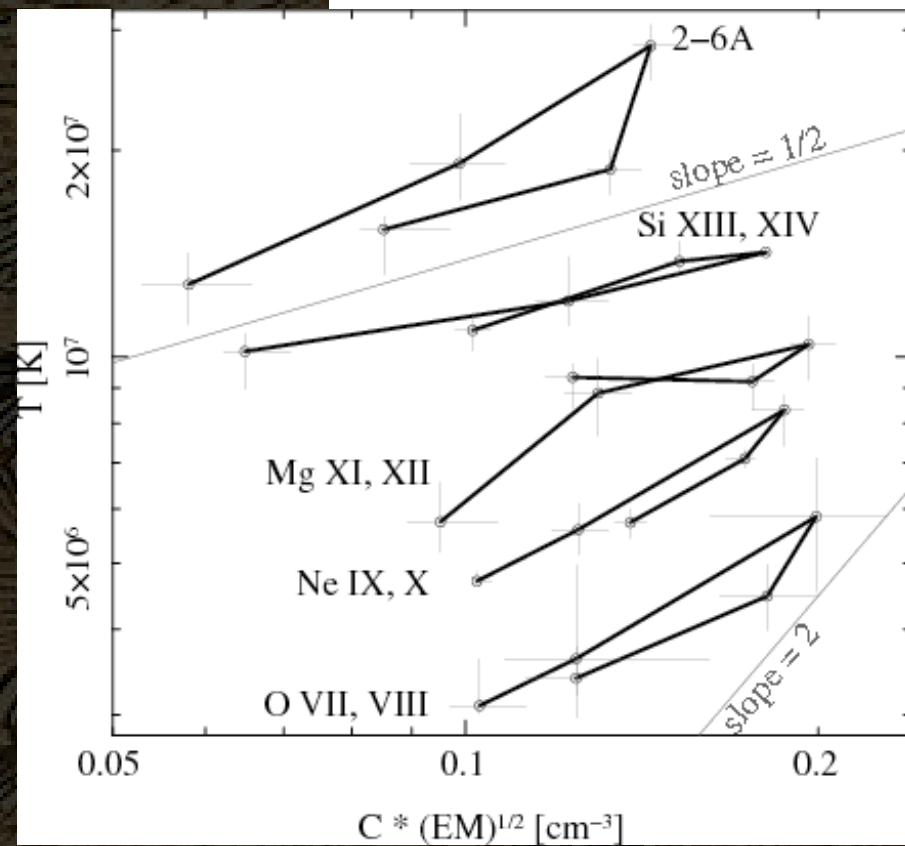
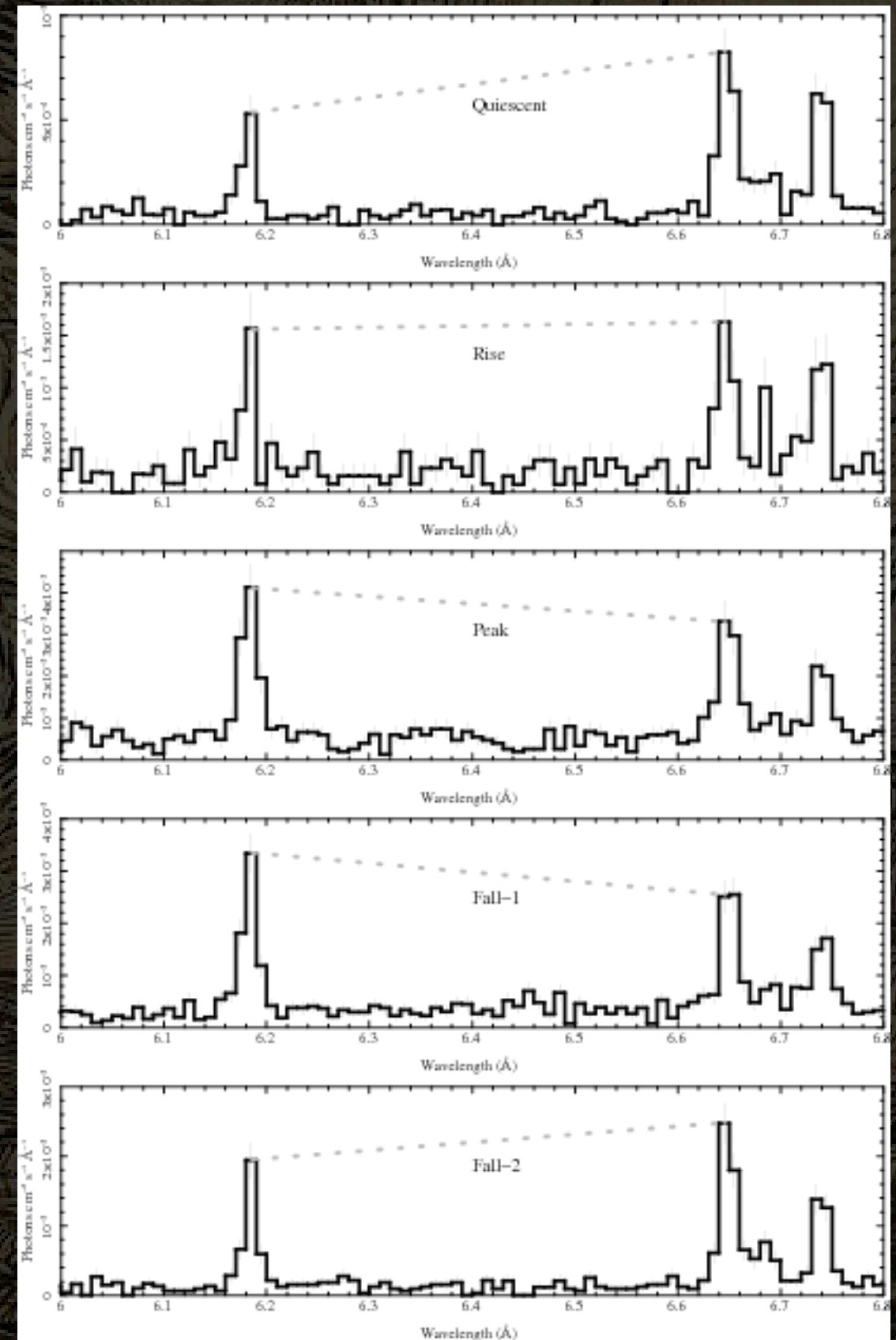
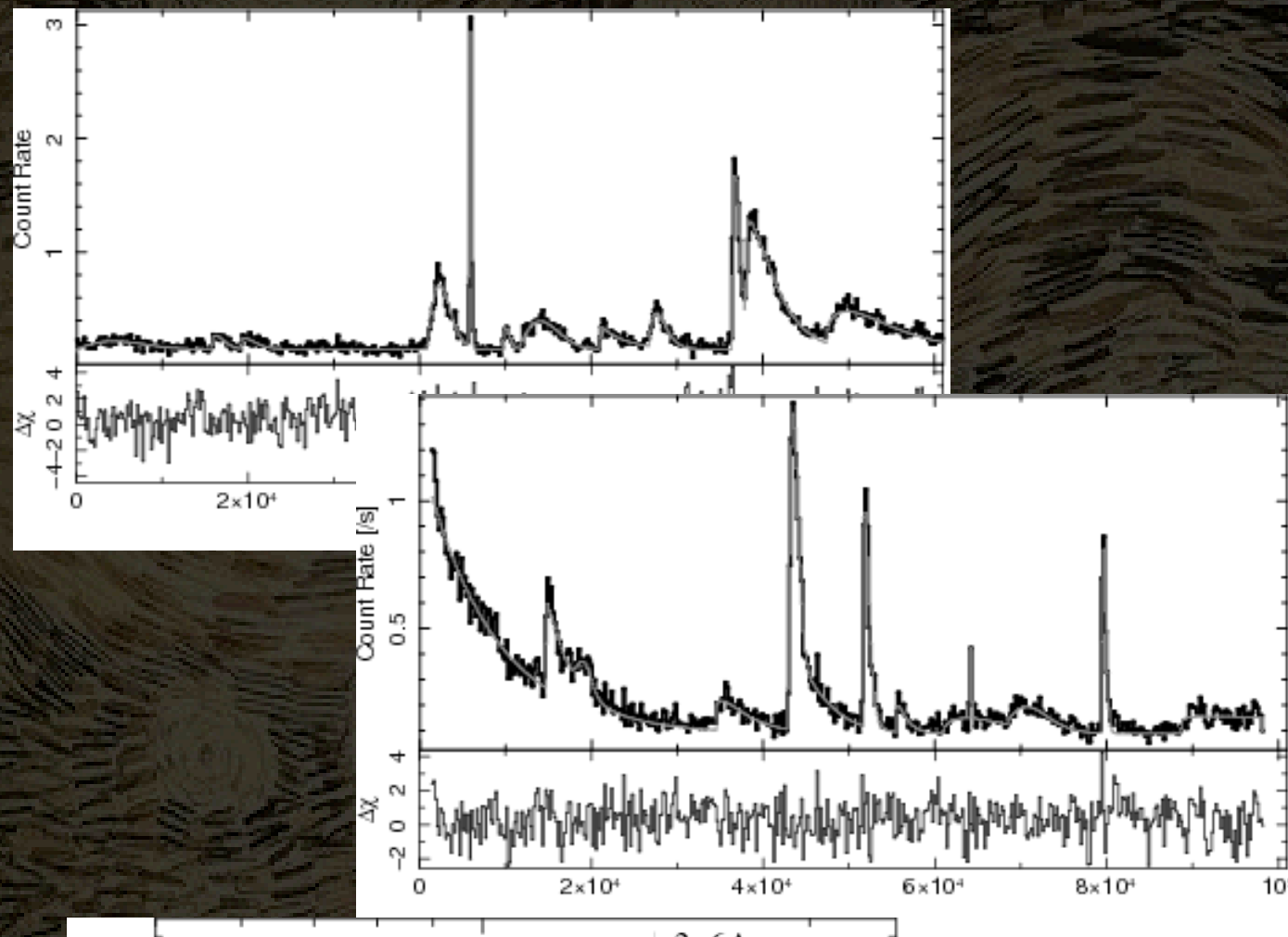


Figure 7. Colliding wind shock models overlaid on the pn spectrum of WR 147 (solid line). The dotted line (A) uses the nominal mass-loss parameters given in Section 4.2 and a wind momentum ratio $\eta = 0.028$. The dashed line (B) assumes 30 per cent higher wind velocities with values $v_{\infty}(\text{WR}) = 1235 \text{ km s}^{-1}$ and $v_{\infty}(\text{OB}) = 2080 \text{ km s}^{-1}$ and leaves the wind momentum ratio unchanged. Error bars have been omitted for clarity and the X-axis scale is linear to accentuate the high-energy portion of the spectrum.

Extras; EV Lac flares



Extras; more flares

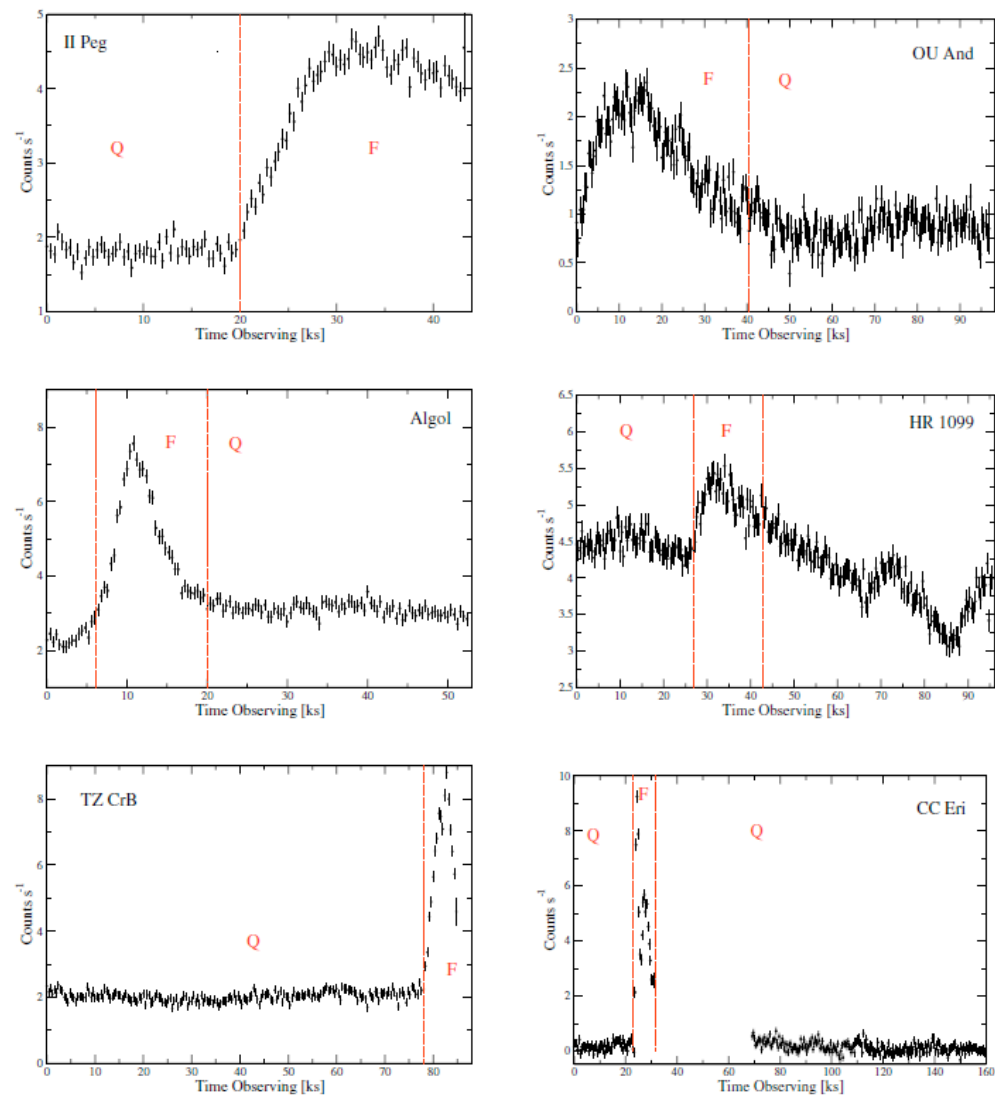


Fig. 1. Light curves of the observations using 400 s bins. All orders of diffraction are included and background is subtracted. The vertical dashed lines indicate the segments considered as flaring or quiescence and marked with letters F and Q respectively. The CC Eri observation consists of two nearly continuous observations.

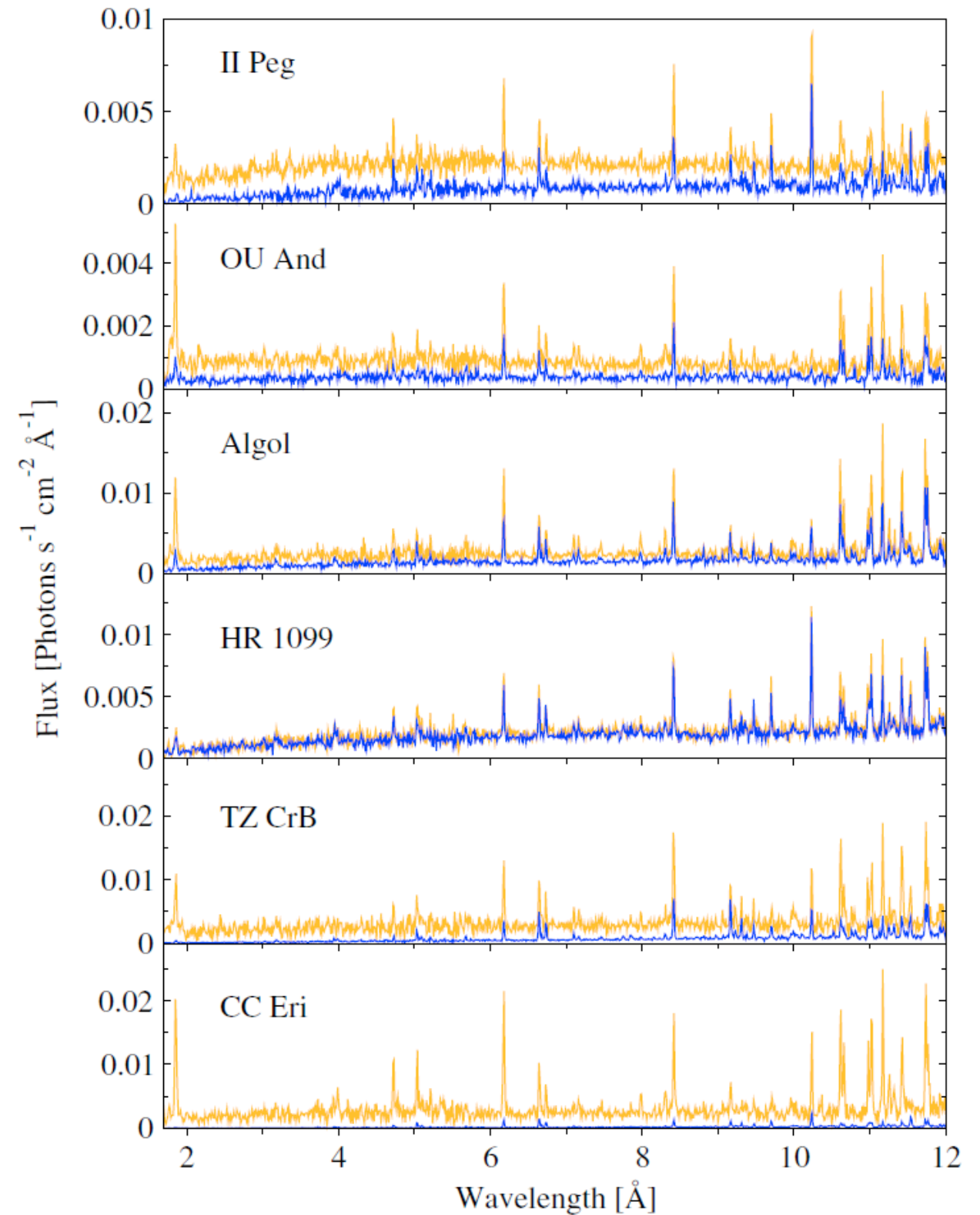


Fig. 2. Time averaged flare and quiescence spectra of the 6 targets in the 1.7–12 Å range. HEG and MEG gratings 1st orders are combined at MEG resolution and 0.01 Å bins. Orange is flare and blue is quiescence.

Extras; Capella radial velocity

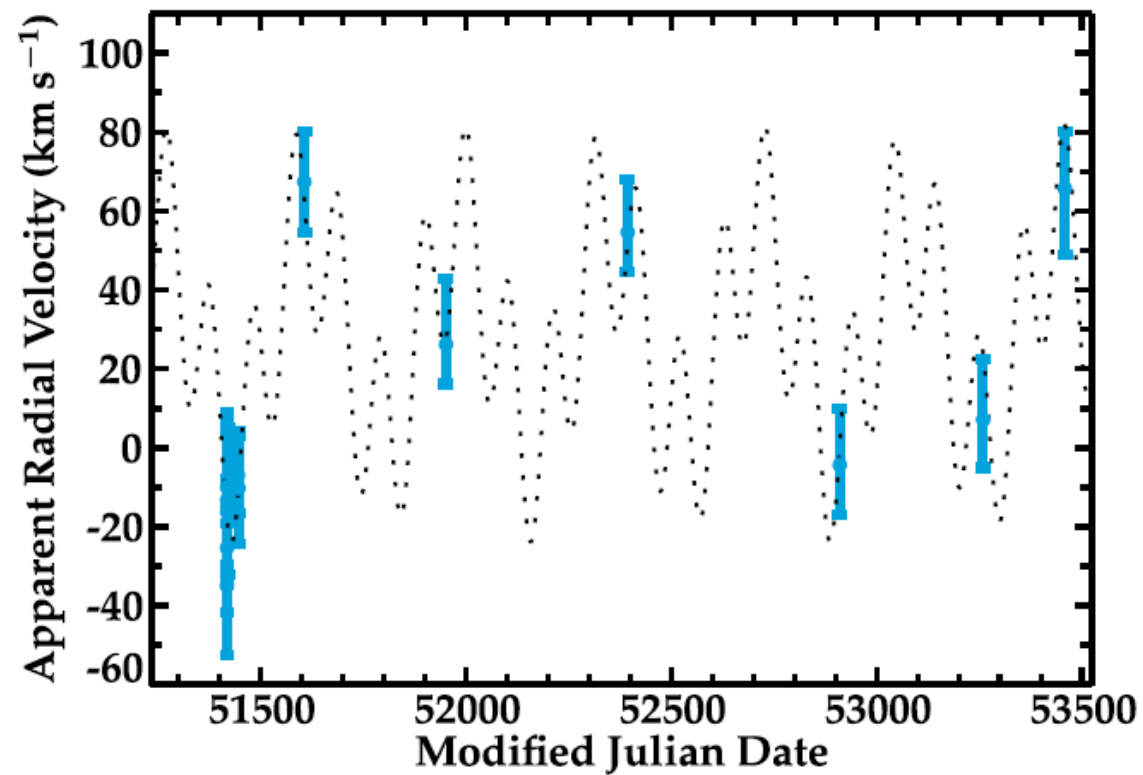


FIG. 1.—Apparent radial velocities of Capella measured with the *Chandra* HETGS. The dotted line shows the calculated apparent radial motion of Capella Aa viewed from Earth (including the barycentric, orbital, and systemic motion of Capella Aa); 3 σ error bars are shown in the plot.

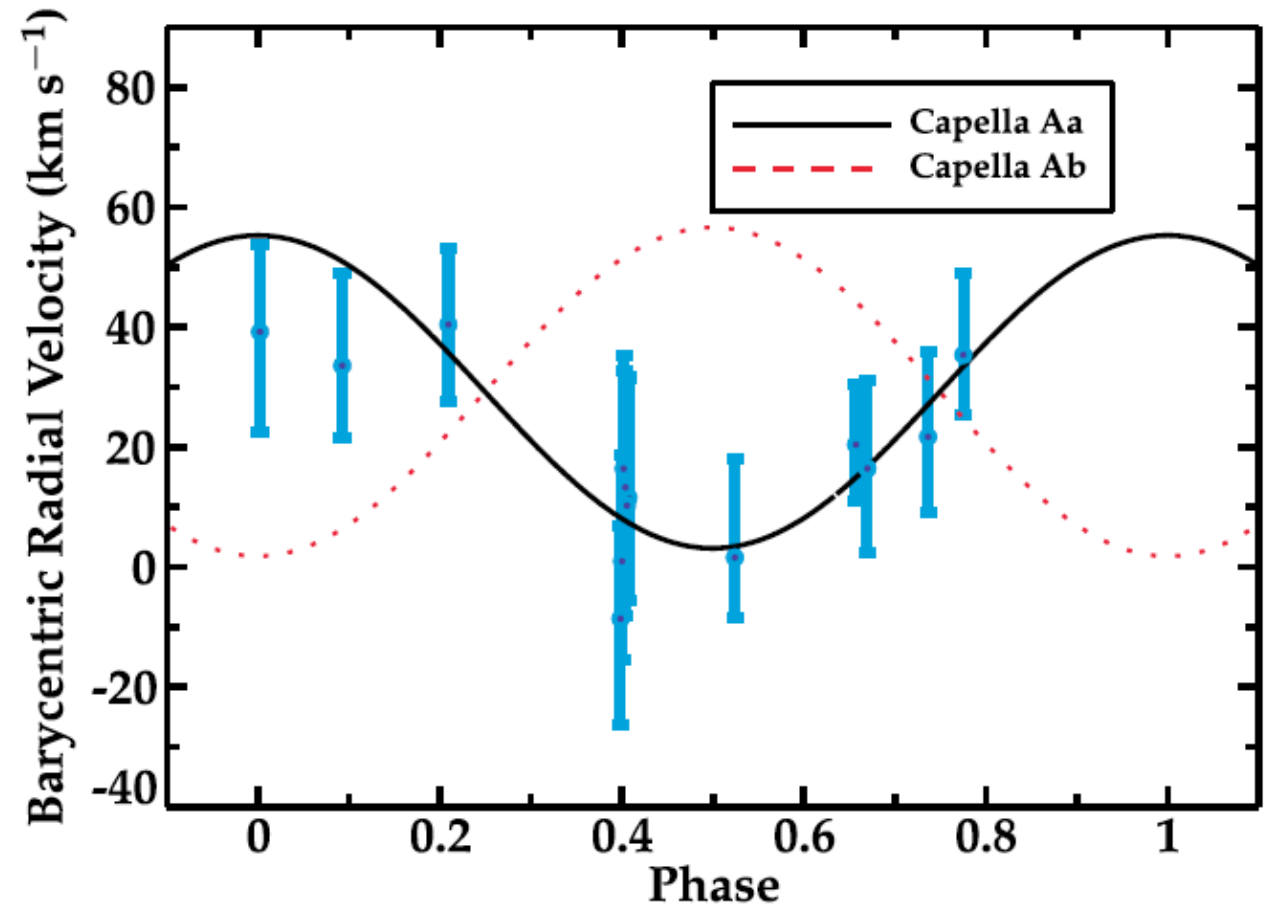
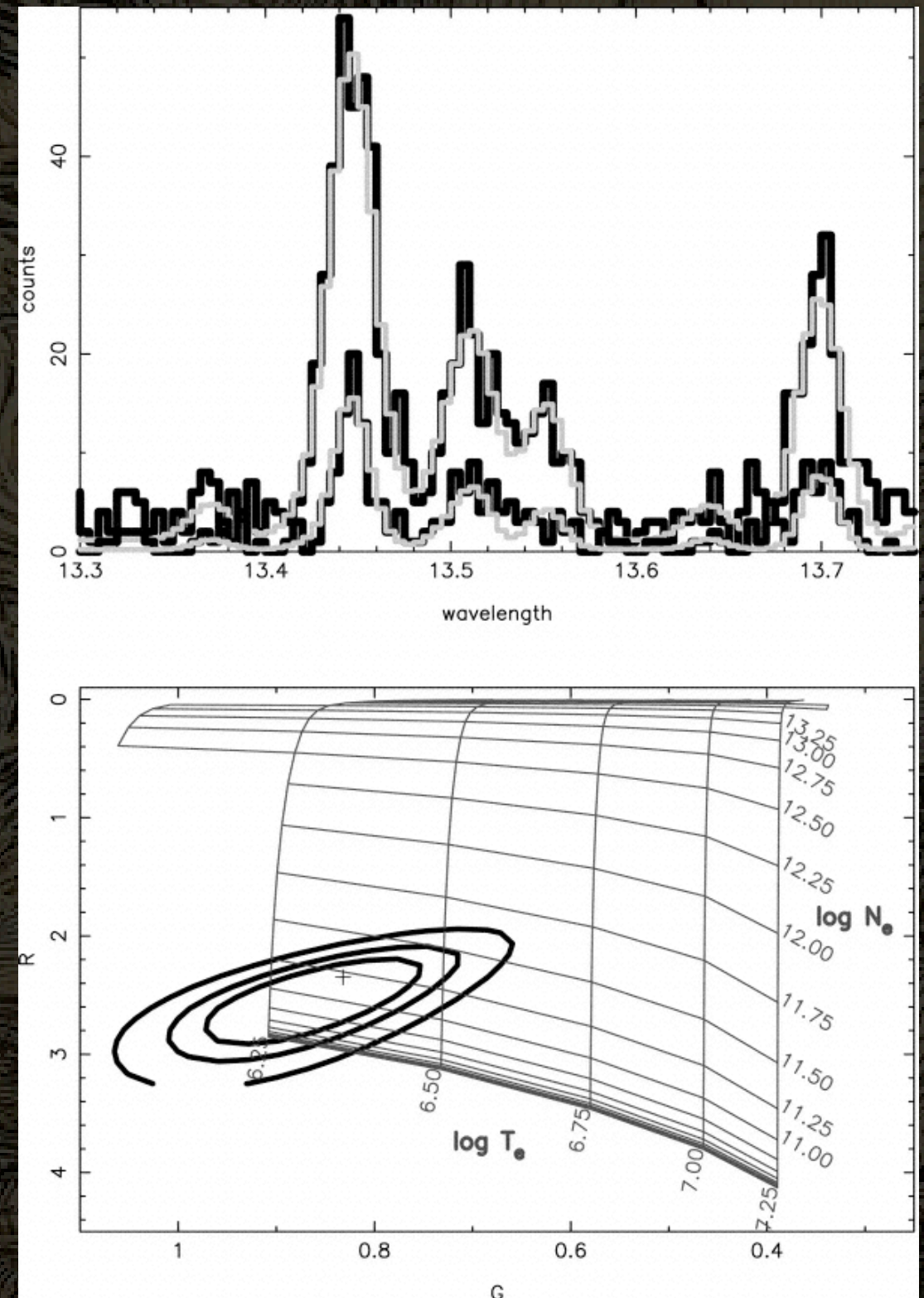
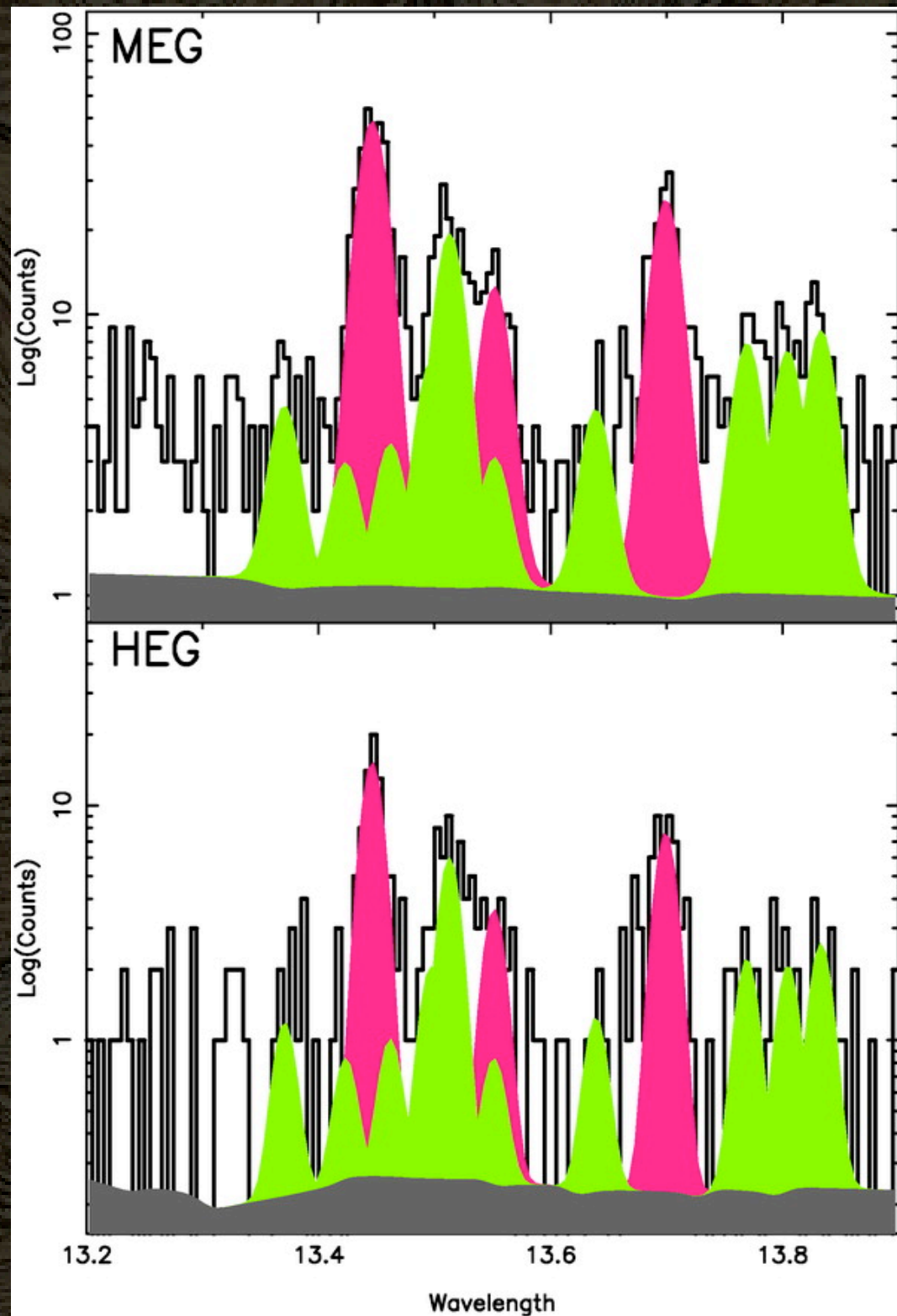
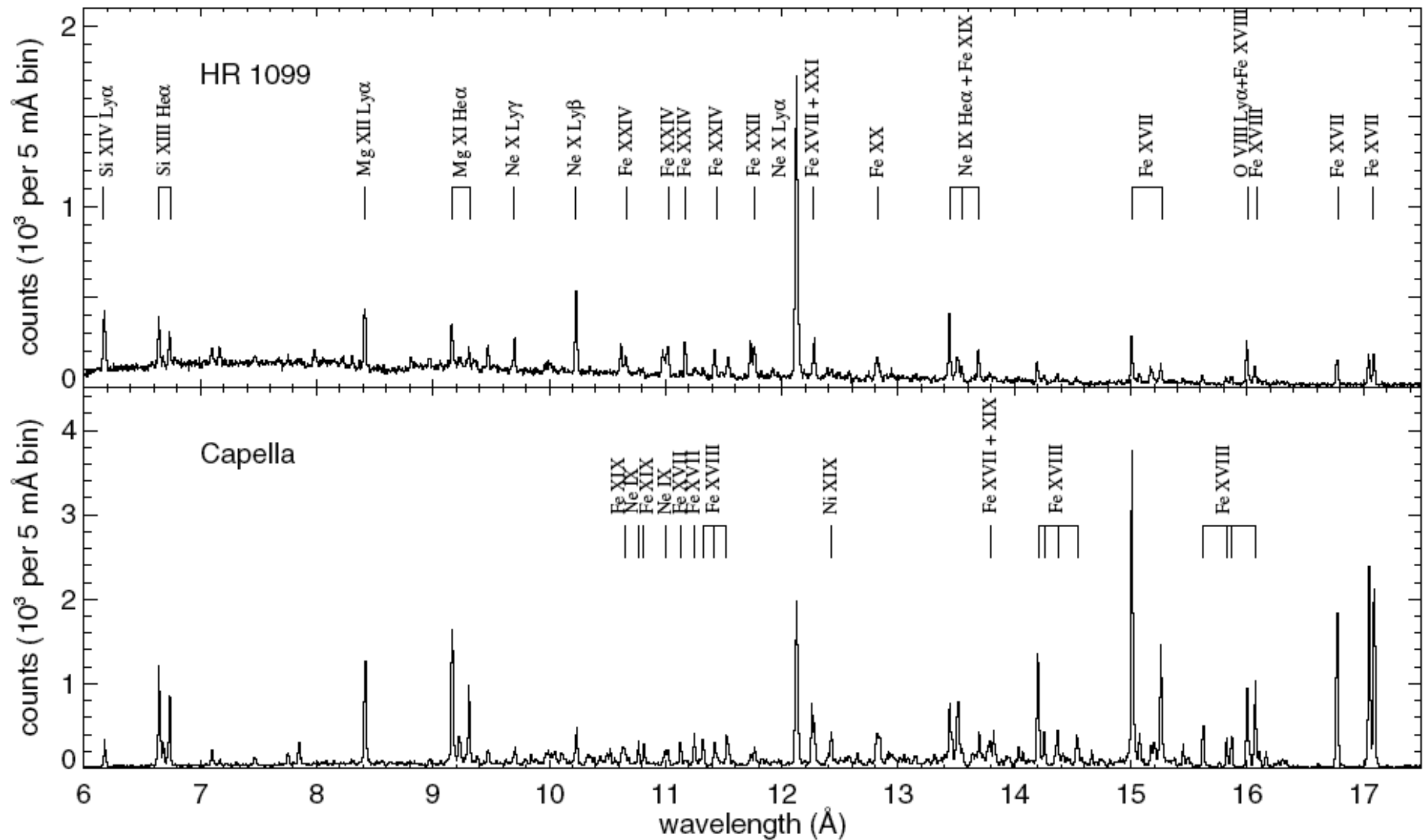


FIG. 2.—Observed radial motion of Capella vs. orbital phase after barycentric correction (see the seventh column in Table 1). The measured radial velocity clearly follows the trend of Capella Aa (primary); 3 σ error bars are shown in the plot.

Extras; triplet modeling



Extras; more spectra



Extras; more spectra

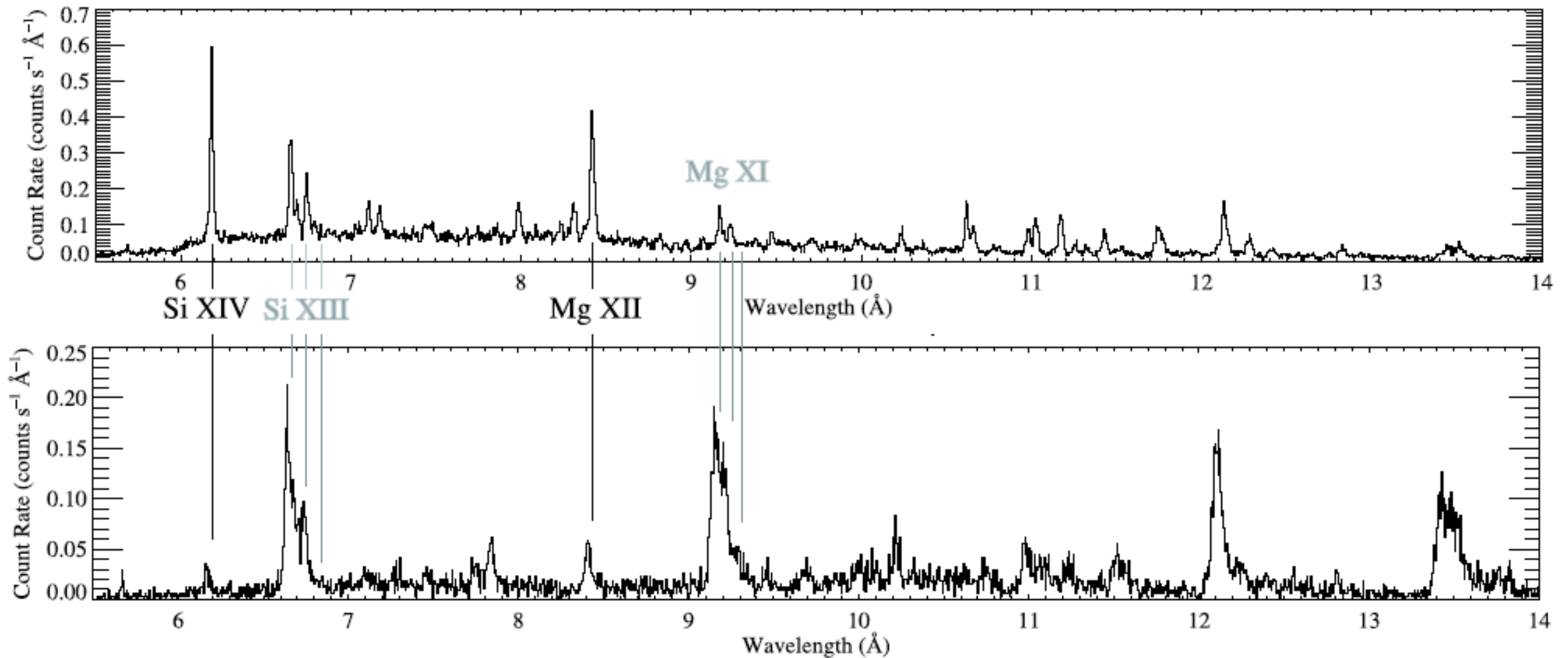


Figure 1. *Chandra* MEG spectra of θ^1 Ori C (top) and ζ Pup (bottom). The hydrogen-like Lyman alpha lines of Si and Mg are indicated in black, while the helium-like resonance-intercombination-forbidden complexes of the same elements are indicated in gray.

Extras; spectra of giants

No. 1, 2007

FIRST CROSSING GIANTS

309

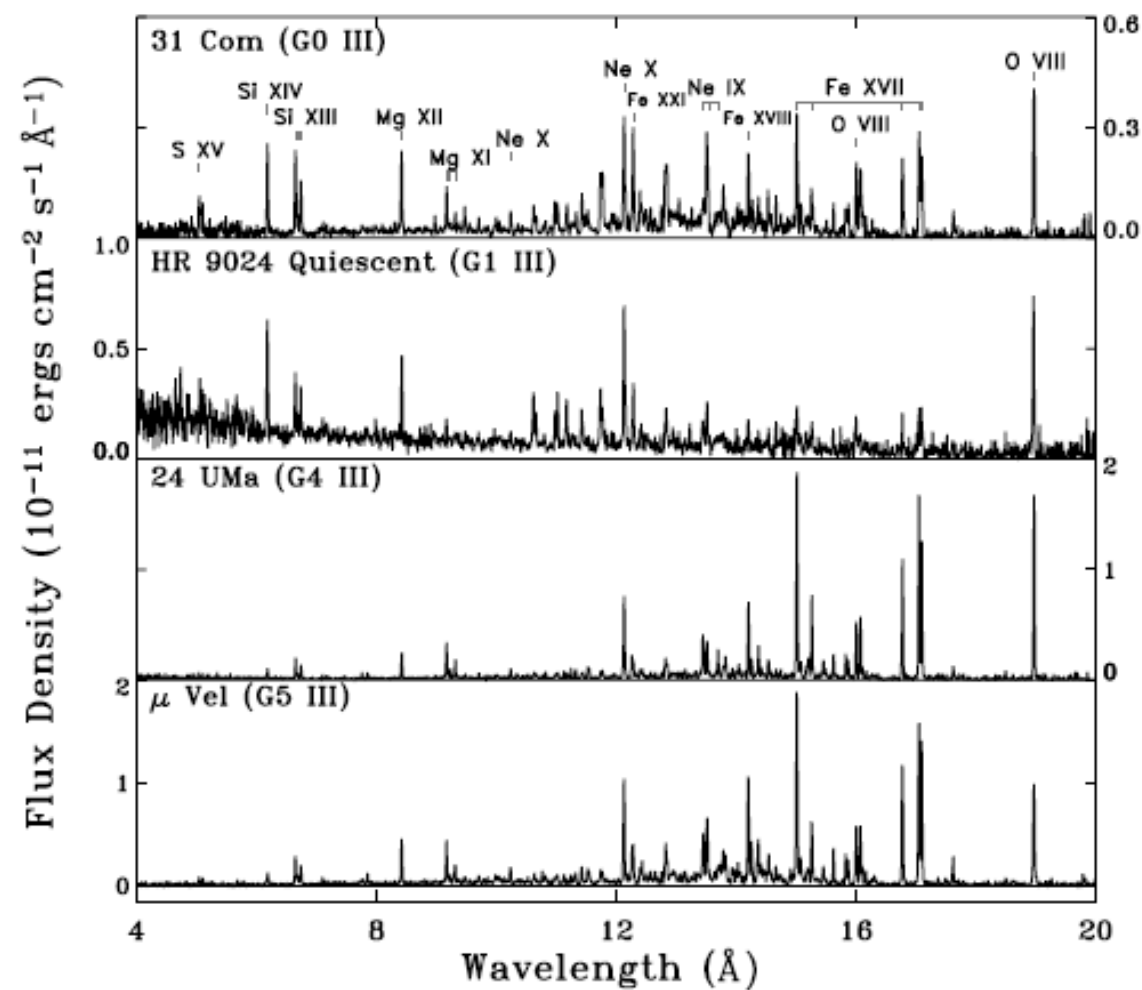


FIG. 4a

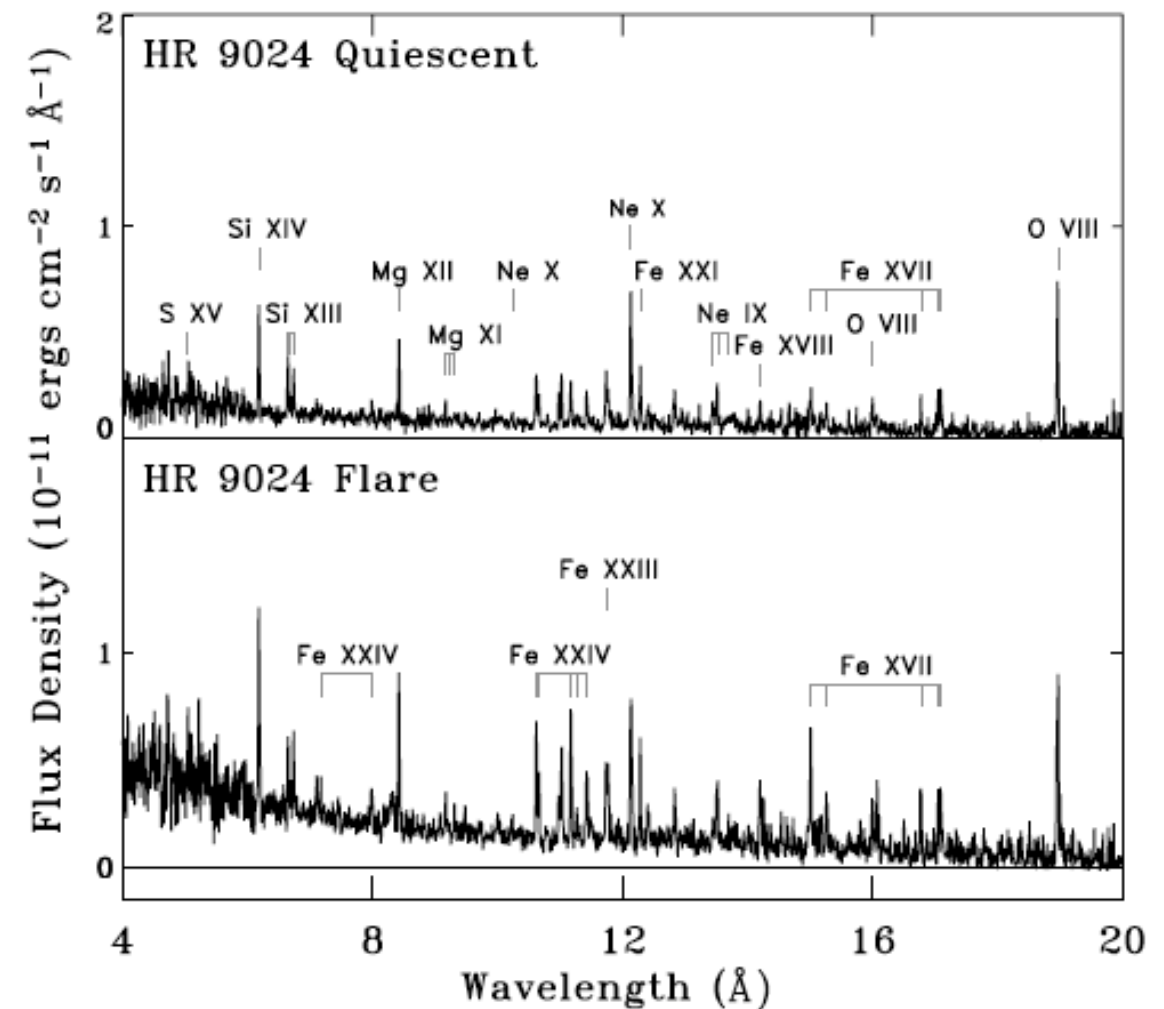


FIG. 4b

FIG. 4.—(a) Calibrated MEG first-order spectra with selected strong lines identified. 24 UMa and μ Vel are co-additions of two or more pointings. Note the different ordinate scales. (b) MEG first-order spectra of HR 9024, separated into “quiescent” and “flare” intervals.

